UNIVERSITY OF CAPE TOWN

Probing the Cosmological Dynamics of a Logarithmic $f(R)$ Theory of Gravity

Author:
Sheref Nasereldin Aboelhassan

Supervisor:
Prof. Peter.K.S.Dunsby

A dissertation submitted in partial fulfilment of the requirements for the degree M.Sc.in the Department of Mathematics and Applied Mathematics, as part of the National Astrophysics and Space Science Programme
UNIVERSITY OF CAPE TOWN

February 2015

Declaration of Authorship

I, Sheref Nasereldin Aboelhassan, know the meaning of plagiarism and declare that all of the work in the document, save for that which is properly acknowledged, is my own.

Signed: _____

Date: _____

UNIVERSITY OF CAPE TOWN

Science Faculty
Department of Mathematics and Applied Mathematics

Master of Science

Probing the Cosmological Dynamics of a Logarithmic $f(R)$ Theory of Gravity

by Sheref Nasereldin Aboelhassan

Abstract

In this thesis we make a contribution in the area of Extended Theories of Gravity (ETG) by studying the dynamics of the $R\ln R$ model. We draw attention to the importance of introducing complete alternative theories of gravity and studying the possible geometrical origin of Dark Energy (unknown form of energy), which is commonly thought to be responsible for the present epoch of accelerated expansion that our universe undergoes. The first chapter of the thesis is an introduction to one of the most successful models in the realm of cosmology i.e. the ΛCDM model. At the end of the first chapter we give a brief discussion on the ground breaking news from the BICEP2 experiment. However, part of the community argues that the BICEP2 results cannot be ascribed to a primordial gravitational waves. In fact, the recent dust map was released by Planck's team lowered the chances that the signal detected by BICEP2 team can be due to primordial gravitational waves. The second chapter introduces a review of the motivations that stimulated researchers to pursue new theories of gravity. Moreover, we revisit the mathematical basis of the $f(R)$ theory of gravity and explain how a viable model of $f(R)$ can account for the most bizarre phenomenon in the universe, namely Dark Energy. The third chapter is dedicated to the basis and the techniques of the theory of dynamical systems. The fifth chapter includes some original work on the $R\ln R$ model dynamics in two different versions (compact and non-compact phase space). In this thesis, we show that the $R\ln R$ model cannot be considered as a viable model since it has serious flaws. These flaws will be addressed, in detail, in chapter5.

Acknowledgements

Over the past two years, there were great persons played very important role in my life through encouraging me and pushing me forward to finish my masters degree. I am greatly thankful to my supervisor Prof. Peter Dunsby, whose patience and careful guidance were the best help to me. Next, my admiration and deep gratitude go to my family (my father, my mother, Ghada, Ashraf, Amera, Karam and Aya). I would like to take the chance to thank all my friends here in South Africa and in Egypt. Especially, my gratitude to Ibraheem Abdellah who probably has spent some nights out of bed editing some chapters of the first script of this thesis. I am also thankful to Mahmmoud Wahba and Khaled Saeed who cheered me up over the past few months through our outgoings for Hiking and swimming. It is a pleasure to thank my colleagues Mohammed Elshazely and Anthony for the fruitful discussions. Indeed, this thesis would not be finished without the appreciated editing of Pier De jagger and Salmaan Alfredo Moronell and Stephen Rae. I am also thankful to Dr.Hyung Won Lee from Republic of Korea for the fruitful discussions on one of his recent papers. I am also thankful to Nicky Walker for always being there whenever I needed admin-related help, and Siphelo Funani for timely help when I ever had a computer-related problems.

Contents

List of Figures

List of Tables

Symbols

Total derivative	$\frac{df}{dt} \equiv \dot{f}$
Partial derivative	$\frac{\partial f}{\partial t} = \partial_t f = f_{,t}$
Covariant derivative	$\nabla_\mu f \equiv f_{;\mu}$
Laplace operator	$\triangle f \equiv \nabla^2 f \equiv \sum_i \frac{d^2 f}{dx_i^2}$
D'Alembert operator	$\Box f \equiv \nabla_\mu \nabla^\mu f$

Chapter 1

The concordance model of cosmology

Cosmology may be defined simply as the branch of science that searches for understanding of the universe as a whole - its history, its present, its future - on the largest scales. It attempts to find answers to the oldest questions of mankind: How has the universe evolved? What is the universe made of? What is the fate of the universe? In this thesis we study a class of Extended Theories of Gravity (ETG) namely metric $f(R)$ gravity, and its role in revealing the possible geometrical nature underlying the accelerated expansion which our universe is currently experiencing.

1.1 Historical Background

It was the Greek philosophers, Aristarchus of Samos (310 BC - 230 BC), Aristotle (384 BC – 322 BC) and Ptolemy (90 AD -168 AD) who proposed the first theories to explain how the heavens work or "Celestial Mechanics". In particular, the "geocentric" Ptolemaic system with it's "perfect circles" and small "epicycles" was the accepted theory to explain the motion of the heavenly bodies. In the 16th century, Copernicus, Kepler and Galileo proposed a "heliocentric" system as an alternative to the Greek philosophers' theories. With Isaac Newton's 1687 publication of "Principia Mathematica", the problem of the motion of the heavenly bodies was solved. Furthermore, Newton provided a physical mechanism for Kepler's laws of planetary motion. Newton's laws of universal gravitation demystified the anomalies in the previous systems - geocentric and heliocentric- caused by gravitational interaction between the planets. Two centuries later, Albert Einstein formulated General Relativity theory which accounts for the implications of Newton's theory on the cosmological large scale.

Scientific cosmology really began in 1917, when Albert Einstein published the final modification to his theory of gravity [8]. This research paper stimulated early cosmologists such as Willem de Sitter, Karl Schwarzschild and Arthur Eddington to explore the astronomical consequences of the general theory of relativity. Einstein inserted a term called the cosmological constant (Λ) into the field equations to prevent the universe from collapsing. In other words, Einstein assumed the universe to be static and unchanging. When it became clear that the universe was not actually static, but it expands; Einstein abandoned the constant term (Λ), calling it the "biggest blunder" of his career [9].
Lately Einstein's cosmological constant (Λ) has been revived to explain a mysterious force called Dark Energy that seems to be counteracting gravity: causing the universe to expand at an accelerating pace.

1.2 The Expanding Universe

The recent observations of distant supernovae type Ia (SNIa) [10, 11] ruled out the possibility that our universe is an Einstein-de Sitter universe and suggested that the universe experiences an accelerated expansion epoch. These results have raised a more crucial question: What could be the nature of the energy needed to cause this accelerated expansion? One of the proposed explanations is a negative pressure cosmic fluid, dubbed **dark energy**. Dark energy is believed to cause cosmic speed-up, despite the known gravitational attractive properties of the matter components of the universe. The acceleration could also be due to the cosmological constant (Λ) term in Einstein field equations. However, a positive and sufficiently large (Λ) would overcome the gravitational attractive force to provide repulsion, leading to a model of an accelerating universe [12]. One method of determining the expansion of the universe is by means of calculating the Doppler effect of distant objects. In 1929, Hubble discovered, observationally, that distant galaxies in our local group recede away from each other and the receding velocity was found to be proportional to the relative distance of the object [13]. This became known as Hubble's law and is expressed mathematically as

$$u = H_0 d_{phys}, \tag{1.1}$$

where u is the velocity of the receding object, H is the Hubble constant and d_{phys} is the instantaneous physical distance. The subscript "0" indicates that H takes the present day value. Hubble's law can also be derived from a pure mathematical consideration. One can expand the scale factor, $a(t)$, as a power series about the present epoch, t_0, to

obtain

$$\begin{aligned} a(t) &= a(t_0 - (t_0 - t)), \\ &= a(t_0) - (t_0 - t)\dot{a}(t_0) + \frac{1}{2}(t_0 - t)^2\ddot{a}(t_0) - ..., \\ &= a(t_0)[1 - (t_0 - t)H(t_0) - \frac{1}{2}(t_0 - t)^2 q(t_0)H^2(t_0) - ...], \end{aligned} \tag{1.2}$$

where the Hubble parameter and the deceleration parameter are, respectively, given by

$$H(t) = \frac{\dot{a}(t)}{a(t)}, \tag{1.3}$$

$$q(t) = -\frac{\ddot{a}(t)a(t)}{\dot{a}^2(t)}, \tag{1.4}$$

where dots refer to differentiation with respect to cosmic time. The redshift, z, can be written in terms of the 'look-back time', $t - t_0$, as

$$z = \frac{a(t_0)}{a(t)} - 1 = [1 - (t_0 - t)H(t_0) - \frac{1}{2}(t_0 - t)^2 q(t_0)H^2(t_0) - ...]^{-1} - 1, \tag{1.5}$$

and, assuming that $t_0 - t \ll t_0$, (1.5) yields

$$z = (t_0 - t)H(t_0) + \frac{1}{2}(t_0 - t)^2(1 + \frac{1}{2}q_0)H_0^2. \tag{1.6}$$

For the very nearby galaxies the proper physical distance to these galaxies can be approximated as

$$d \approx c(t_0 - t). \tag{1.7}$$

Moreover, from (1.6), $z \approx (t_0 - t)H_0$. In this case, the cosmological redshift can be treated as a Doppler shift due to a recession velocity, u, of the emitting galaxy. One obtains

$$u = cz = H_0 d, \tag{1.8}$$

which yields the Hubble's law as we introduced earlier. Objects moving toward the observer would produce blue-shifted wavelengths while those moving away from the observer would be red-shifted in the spectrum. The redshift, z, of objects moving away from observer can be expressed as

$$1 + z = \frac{\lambda_0}{\lambda}, \tag{1.9}$$

where λ is the wavelength. There is uncertainty about the estimated value of H_0: Freedman et al [14] estimates $H_0 = 72 \pm 8\text{km.s}^{-1}\text{Mpc}^{-1}$, while Riess et al [10] estimates $H_0 = 74.2 \pm 3.6\text{km.s}^{-1}\text{Mpc}^{-1}$, while most recently, it is measured to be $H_0 = 67.4 \pm 1.4\text{km.s}^{-1}\text{Mpc}^{-1}$ by Planck team[1]

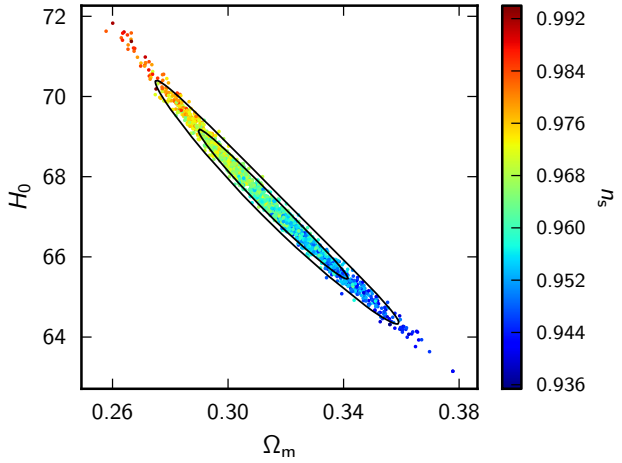

FIGURE 1.1: Constrain The Hubble parameter value using the Planck data, the 1-σ and 2-σ contours exhibit a more tight constraints by implementing joint analysis with different data sets.i.e, Planck+lensing+WP [1].

1.2.1 Distance Measures

Using the instantaneous physical distance to represent the distance term in (1.1) is conceivable, providing that the redshifts are small. In case of high redshifts, the physical distance is no longer appropriate to use. The physical distance d_{phys} is not observable, since observations always refer to events on our past light cone, not our current spatial hypersurface [15]. For this purpose we introduce different distance measures which can be calculated from observable quantities. The luminosity distance belongs to that class of measures, and is defined as:

$$d_L = \sqrt{\frac{L}{4\pi F}}, \tag{1.10}$$

where L is the intrinsic luminosity and F is the measured flux. The angular diameter distance,

$$d_A = \frac{D}{\theta}, \tag{1.11}$$

where D is the proper size of the object and θ its apparent angular size. The proper motion distance,

$$d_M = \frac{u}{\dot{\theta}}, \tag{1.12}$$

where u is the transverse proper velocity and $\dot{\theta}$ the observed angular velocity. These three measures are linked in the following way

$$d_L = (1+z)d_M = (1+z)^2 d_A. \tag{1.13}$$

1.3 Foundations of Relativistic Cosmology

1.3.1 The cosmological Principle

Modern cosmological models are based on the idea that the universe is nearly the same everywhere, a stance sometimes known as the **Copernican Principle** [15]. This principle is related to two more mathematically precise properties that a manifold might have: isotropy and homogeneity. If the universe is **isotropic**, then this means you will see no difference in the space as you look in different directions. When viewed on the largest scales, the universe looks the same to all observers. **Homogeneity** states that the average density of matter is nearly the same in all places in the universe and the universe is fairly smooth on large scales. Observations to date support the idea that the universe is both isotropic and homogeneous. Both facts are linked to what is called the **cosmological principle**. The cosmological principle is derived from the Copernican Principle but has no foundation in any particular physical model or theory, i.e. it cannot be 'proved' in a mathematical sense. However, it has been supported by the analysis of the The Wilkinson Microwave Anisotropy Probe (WMAP) observational data [16], which reveals nearly identical temperature of about 2.725 K of the Cosmic Microwave Background (CMB) radiation coming from different parts of the universe [17]. Consequently, the cosmological principle, which asserts that the universe is homogeneous on large scales [18] is assumed to be valid.

1.3.2 Geometry of Friedmann-Lemaître-Robertson-Walker

The only metric, which can be defined on a given spacetime, that is consistent with the properties discussed above (isotropy and homogeneity) is the so-called Friedmann-Lemaître-Robertson-Walker (FLRW) metric. The FLRW line element, is defined as follows [19],

$$ds^2 = -dt^2 + [a(t)]^2[\frac{dr^2}{1-kr^2} + r^2(d\theta^2 + \sin^2\theta d\phi^2)]. \tag{1.14}$$

The geometry of the spatial part is determined by,

$$d\sigma^2 = a_0^2[\frac{dr^2}{1-kr^2} + r^2(d\theta^2 + \sin^2\theta d\phi^2)], \tag{1.15}$$

where $a_0 = a(t_0)$ and k is the constant spatial curvature. k can take one of the values 1, 0 and -1 which correspond to closed, flat and open geometries respectively. We consider the different possible scenarios for the geometry of the universe emerging from assigning

different values for k.

1.3.2.1 Positive curvature $k = 1$

Setting $k = 1$ in (1.14), leads to a singularity in the coefficient of dr^2 at $r = 1$. In order to resolve this singularity we introduce the following coordinate transformations,

$$r = \sin\chi, \tag{1.16}$$

so that

$$dr = \cos\chi d\chi = (1 - r^2)d\chi, \tag{1.17}$$

and (1.15) becomes

$$d\sigma^2 = a_0^2[d\chi^2 + \sin^2\chi(d\theta^2 + \sin^2\theta d\phi^2)], \tag{1.18}$$

and thus (1.14) takes the form

$$ds^2 = -dt^2 + [a(t)]^2[d\chi^2 + \sin^2\chi(d\theta^2 + \sin^2\theta d\phi^2)]. \tag{1.19}$$

Surfaces of constant times correspond to a spherical, or closed geometry. Thus, two particles with initially parallel velocity vectors eventually converge.

1.3.2.2 Zero curvature $k = 0$

If we consider the following set of spherical coordinates substitutions,

$$\begin{aligned} x &= a_0 r\sin\theta\cos\phi, \\ y &= a_0 r\sin\theta\sin\phi, \\ z &= a_0 r\cos\theta, \end{aligned} \tag{1.20}$$

then (1.15) becomes

$$d\sigma^2 = dx^2 + dy^2 + dz^2, \tag{1.21}$$

and hence the metric (1.14) is

$$ds^2 = -dt^2 + [a(t)]^2[dx^2 + dy^2 + dz^2]. \tag{1.22}$$

The spatial section (1.21) is three-dimensional Ecluidean space.

1.3.2.3 Negative curvature $k = -1$

Introducing a new variable χ,

$$r = \sinh \chi, \tag{1.23}$$

then

$$dr = \cosh \chi d\chi, \tag{1.24}$$

and (1.14) becomes

$$ds^2 = -dt^2 + [a(t)]^2[d\chi^2 + \sinh^2 \chi(d\theta^2 + \sin^2 \theta d\phi^2)]. \tag{1.25}$$

This corresponds to hyperbolic, or open, geometry; two particles with initially parallel velocity vectors eventually diverge.
For the sake of simplicity and because it is strongly supported by observations, we will regard the spacetime as spatially flat, homogeneous and isotropic.

1.3.3 Wely's Postulate

The stress energy tensor, $T^{\mu\nu}$, is a symmetric tensor of 2^{nd} rank. The general form of this tensor can be written as below:

$$T^{\mu\nu} = (\rho + P)u^\mu u^\nu + Pg^{\mu\nu} + [q^\mu u^\nu + q_\nu u^\mu + \pi^{\mu\nu}], \tag{1.26}$$

where ρ is the energy density, P is the pressure,g is the metric tensor,q^μ is the heat flux vector and $\pi^{\mu\nu}$ is the viscous shear tensor. Wely's Postulate states that the particles of the substratum lie in spacetime on a congruence of time-like geodesics diverging from a point in the finite or infinite past [19]. It can be inferred from this postulate that the matter at any point possesses a unique velocity and thus treating the substratum as a perfect fluid is a good approximation. For this purpose, we make the following simplifications

$$q^\mu = \pi^{\nu\mu} = 0. \tag{1.27}$$

The perfect fluid will be specified by an energy density ρ and isotropic pressure P in its rest frame. The energy-momentum tensor of such a fluid is then given by

$$T^{\mu\nu} = (\rho + P)u^\mu u^\nu + Pg^{\mu\nu}. \tag{1.28}$$

The last equation can be written with lower indices as

$$T_{\mu\nu} = (\rho + P)u_\mu u_\nu + Pg_{\mu\nu}, \tag{1.29}$$

and with one index raised (1.29) becomes

$$T^{\mu}_{\nu} = diag(-\rho, P, P, P), \tag{1.30}$$

where u^{μ} is the fluid four-velocity and $u_{\mu}u^{\mu} = -1$.

1.3.4 General Relativity

No one can deny that the golden age of cosmology began with the introduction of Einstein's general theory of relativity to describe the gravitational interactions on the largest scales. The theory introduced a profound insight to gravitational interactions: gravitational interaction is a manifestation of the curvature of spacetime. To introduce this new approach to understanding gravity, Einstein applied the universality principle. General Relativity theory, the cosmological principle and Wely's postulate together are the three fundamental pillars upon which modern cosmology lie. The differential equations for the scale factor and the matter density follow from Einstein's field equations given by

$$G_{\mu\nu} = R_{\mu\nu} - \frac{1}{2}g_{\mu\nu} = 8\pi G T_{\mu\nu}, \tag{1.31}$$

where $G_{\mu\nu}$ is the Einstein tensor and $R_{\mu\nu}$ is the Ricci tensor [20]. The Ricci tensor is derived by contracting the Riemann tensor. The Riemann tensor is defined as:

$$R^{\mu}_{\beta\mu\nu} = \Gamma^{\alpha}_{\beta\nu,\mu} - \Gamma^{\alpha}_{\beta\mu,\nu} + \Gamma^{\alpha}_{\sigma\mu}\Gamma^{\sigma}_{\beta\nu} - \Gamma^{\alpha}_{\sigma\nu}\Gamma^{\sigma}_{\beta\mu}, \tag{1.32}$$

the connection, $\Gamma^{\sigma}_{\mu\nu}$, in terms of the metric is :

$$\Gamma^{\sigma}_{\mu\nu} = \frac{1}{2}g^{\sigma\delta}[g_{\delta\mu,\nu} + g_{\delta\nu,\mu} - g_{\mu\nu,\delta}], \tag{1.33}$$

while the Ricci tensor is:

$$R^{\lambda}_{\mu\lambda\nu} = R_{\mu\nu}. \tag{1.34}$$

The trace of the Ricci tensor gives the Ricci scalar:

$$R = R^{\mu}{}_{\mu} = g^{\mu\nu}R_{\mu\nu}. \tag{1.35}$$

The Einstein gravitational field equations, in the presence of a non-zero cosmological constant, are [21]

$$R_{\mu\nu} - \frac{1}{2}g_{\mu\nu}R + \Lambda g_{\mu\nu} = 8\pi G T_{\mu\nu}. \tag{1.36}$$

The trace of (1.36) yields

$$R = 8\pi G T - 4\Lambda. \tag{1.37}$$

The Hubble parameter is related to the scale factor a by

$$H = \frac{\dot{a}}{a}. \tag{1.38}$$

Differentiating the Hubble parameter with respect to time gives

$$\dot{H} = \frac{\ddot{a}a - \dot{a}^2}{a^2} = \frac{\ddot{a}}{a} - H^2. \tag{1.39}$$

Substituting (1.37) in (1.36), and moving the trace term to right hand side, one gets the following equivalent "trace-reversed" form

$$R_{\mu\nu} - \Lambda g_{\mu\nu} = 8\pi G(T_{\mu\nu} - \frac{T}{2} g_{\mu\nu}). \tag{1.40}$$

For a (FLRW) metric (1.14), the non zero components of Ricci tensor are :

$$\begin{aligned} R_{00} &= -3\frac{\ddot{a}}{a}, \\ R_{11} &= \frac{(a\ddot{a} + 2\dot{a}^2 + 2k)}{1 - kr^2}, \\ R_{22} &= (a\ddot{a} + 2\dot{a}^2 + 2k)r^2, \\ R_{33} &= (a\ddot{a} + 2\dot{a}^2 + 2k)r^2 \sin^2\theta. \end{aligned} \tag{1.41}$$

The trace of the energy-momentum tensor (1.29) is:

$$T = T^{\mu}_{\mu} = -\rho + 3P. \tag{1.42}$$

1.3.5 Friedmann's Equations

The $\mu\nu = 00$ component of (1.40) is given by

$$\begin{aligned} R_{00} - \Lambda g_{00} &= 8\pi G(T_{00} - \frac{T}{2} g_{00}), \\ -3\frac{\ddot{a}}{a} + \Lambda &= 8\pi G(\rho + \frac{1}{2}(-\rho + 3P)), \\ -3\frac{\ddot{a}}{a} + \Lambda &= 4\pi G(\rho + 3P). \end{aligned} \tag{1.43}$$

Consequently,

$$\boxed{\frac{\ddot{a}}{a} = -\frac{4}{3}\pi G(\rho + 3P) + \frac{\Lambda}{3}.} \tag{1.44}$$

Because of isotropy, there is only one distinct equation from $\mu\nu = ij$. Thus the component $\mu\nu = 11$ equation gives

$$\begin{aligned} R_{11} - \Lambda g_{11} &= 8\pi G(T_{11} - \frac{T}{2}g_{11}), \\ a\ddot{a} + 2\dot{a}^2 + 2k - \Lambda a^2 &= 8\pi G(a^2 P - \frac{(-\rho + 3P)}{2}a^2), \\ \frac{\ddot{a}}{a} + 2(\frac{\dot{a}}{a})^2 + 2\frac{k}{a^2} &= 4\pi G(\rho - P) + \Lambda. \end{aligned} \tag{1.45}$$

We can use (1.44) to eliminate the second derivative in the last equation, then we have:

$$\boxed{H^2 = \frac{8}{3}\pi G\rho + \frac{\Lambda}{3} - \frac{k}{a^2}.} \tag{1.46}$$

Equations (1.44) and (1.46) together are known as the **Friedmann equations**. The **continuity equation** is obtained from energy-momentum conservation law,

$$\nabla_\mu T^{\mu\nu} = \partial_\mu T^{\mu\nu} + \Gamma^\mu_{\mu\lambda} T^{\lambda\nu} + \Gamma^\nu_{\mu\lambda} T^{\mu\lambda} = 0. \tag{1.47}$$

The former equation has three equivalent components, $\mu = 1, 2, 3$. Considering $\nu = 0$, and taking into consideration that (1.29) is diagonal, then terms of (1.47) are written as

$$\partial_\mu T^{\mu 0} = \partial_0 T^{00} = \dot{\rho}, \tag{1.48}$$

$$\Gamma^\mu_{\mu\nu} T^{\lambda 0} = \Gamma^\mu_{\mu 0} T^{00} = 3\frac{\dot{a}}{a}\rho, \tag{1.49}$$

$$\Gamma^0_{\mu\nu} T^{\mu\lambda} = \Gamma^0_{00} T^{00} + \Gamma^0_{11} T^{11} + \Gamma^0_{22} T^{22} + + \Gamma^0_{33} T^{33} = 3\frac{\dot{a}}{a}P. \tag{1.50}$$

Substituting (1.48), (1.49) and (1.50) in (1.47) gives

$$\boxed{\dot{\rho} + 3\frac{\dot{a}}{a}(\rho + P) = 0,} \tag{1.51}$$

where ρ and P are the total energy density and the pressure of the fluid respectively. Equation (1.44) suggests that the cosmological constant contributes negatively to the pressure term. When there is a vanishing cosmological constant, (1.44) gives

$$\frac{\ddot{a}}{a} = -\frac{4}{3}\pi G(\rho + 3P). \tag{1.52}$$

Therefore, the condition for acceleration is

$$\rho + 3P < 0, \tag{1.53}$$

and hence

$$w = \frac{P}{\rho} < -1/3. \tag{1.54}$$

1.4 Cosmological parameters

For any value of the Hubble parameter H there is a critical value of the energy density such that the spatial geometry is flat ($k = 0$):

$$\rho_{crit} = \frac{3H^2}{8\pi G}. \tag{1.55}$$

The density parameter Ω[1] is defined by

$$\Omega = \frac{\rho}{\rho_{crit}} = \frac{8\pi G}{3H^2}\rho. \tag{1.56}$$

Considering (1.46), and dividing it by H^2 yields

$$1 = \frac{8\pi G}{3H^2}\rho + \frac{\Lambda}{3H^2} - \frac{k}{a^2H^2}, \tag{1.57}$$

with the density parameters of the cosmological constant and the curvature defined respectively as

$$\Omega_\Lambda = \frac{\Lambda}{3H^2}, \tag{1.58}$$

$$\Omega_k = \frac{k}{a^2H^2}, \tag{1.59}$$

we have

$$\Omega_{tot} = \Omega + \Omega_\Lambda, \tag{1.60}$$

$$\Omega_{tot} - 1 = \frac{k}{a^2H^2} = \Omega_k. \tag{1.61}$$

The sign of k is determined by whether Ω_{tot} is greater than, equal to, or less than unity. We have

$$\begin{aligned} \Omega_{tot} > 1 \quad &\equiv \quad \rho > \rho_{crit} \quad \rightarrow \quad k > 0, \\ \Omega_{tot} = 1 \quad &\equiv \quad \rho = \rho_{crit} \quad \rightarrow \quad k = 0, \\ \Omega_{tot} < 1 \quad &\equiv \quad \rho < \rho_{crit} \quad \rightarrow \quad k < 0. \end{aligned}$$

As stated before, throughout this thesis, the universe is assumed to be spatially flat and hence $\Omega_{tot} = 1$. This assumption seems consistent with observations which have shown

[1] $\Omega = \Omega_m + \Omega_r$

that the current state of universe is such that the value of Ω_{tot} is very close to unity [22].

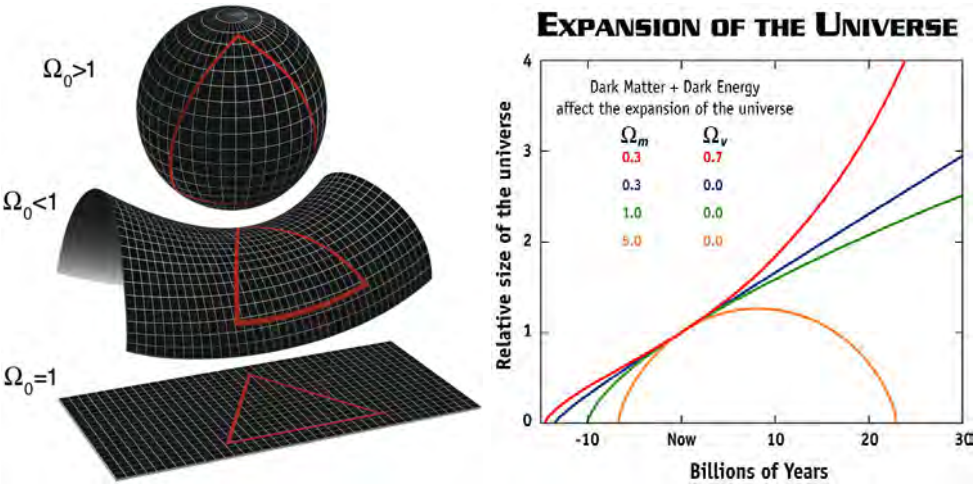

FIGURE 1.2: Left: Depiction of the three possible geometries of the universe.Right: Curvature and expansion history of the universe [2].

1.4.1 The evolution of a universe filled with a perfect fluid

Assuming a universe filled with a barotropic perfect fluid with an equation of state

$$w = P/\rho, \tag{1.62}$$

solving (1.44) and (1.46), with $k = 0$ yields

$$H(t) = \frac{2}{3(1+w)(t-t_0)}. \tag{1.63}$$

Inserting $H(t) = \dot{a}/a$ in (1.63) and integrating gives

$$a(t) \propto (t-t_0)^{\frac{2}{3(1+w)}}. \tag{1.64}$$

Similarly, one can substitute $H(t) = \dot{a}/a$ and $w = P/\rho$ in (1.51). Integrating both sides yields

$$\rho \propto a^{-3(1+w)}. \tag{1.65}$$

The above solution is valid for $w \neq -1$. The solution for the scale factor $a(t)$ represents the dynamics of the universe. Consequently, for a dust-dominated universe with $w = 0$ [23], the solution is

$$a(t) \propto (t - t_0)^{2/3}, \quad \rho \propto a^{-3}. \tag{1.66}$$

For a radiation-dominated universe with $w = 1/3$, the solution is

$$a(t) \propto (t - t_0)^{1/2}, \quad \rho \propto a^{-4}. \tag{1.67}$$

For a matter-dominated universe, $\rho \propto a^{-3}$ is expected as $\rho \propto 1/V$ and $V \propto a^3$, where V is the volume. In the radiation-dominated universe, the energy E is lost as the universe expands as $E \propto 1/a$. The number density, as in the matter-dominated universe, is proportional to $1/a^3$. The dynamical behaviour of the scale factor, in the absence of a cosmological constant, for different epochs of the universe is summarised in Table [1.1]. Subsequently, knowing the evolution of the scale factor $a(t)$ gives an idea about

Cosmological Era	The Evolution of Scale factor	The Equation of State
Dust	$a(t) \propto (t - t_0)^{2/3}$	$w = 0$
Radiation	$a(t) \propto (t - t_0)^{1/2}$	$w = 1/3$
Vacuum energy	$a(t) \propto e^{Ht}$	$w = -1$

TABLE 1.1: Summary for the evolution of the scale factor $a(t)$ for different cosmological eras of the universe.

the energy contents of the universe. Since we are interested in the late-time era of a universe, dominated by dark energy, radiation has been neglected in this thesis.

1.5 Dark matter

1.5.1 Evidences for the existence of dark matter

The first and most robust indication of the existence of dark matter has been inferred from the flattened galactic rotation curves [24] observed by Zwicky [25] during his study of the Coma cluster. Further strong evidence for the existence of dark matter comes from the observations of galaxy rotation curves in spiral galaxies Fig [1.3]. Newtonian dynamics failed to predict the behaviour of the rotation curves in spiral galaxies as they are measured. This suggests the existence of halos of a non-luminous matter around spiral galaxies. It has been reported [1] that only about 4.9% of the universe is the observed ordinary matter such as atoms, while dark matter is believed to make up about 26.8% Fig [1.4]. The rest, presumably, is filled with so-called dark energy whose nature is still unknown.

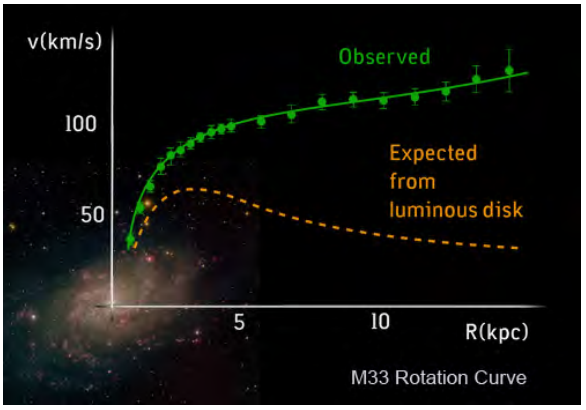

FIGURE 1.3: The green points on the plot correspond to the observed velocities of objects orbiting the M33 galaxy as a function of their distance from the galactic center. The lower curve on the plot (dashed line) shows what the rotational velocity of objects in the M33 galaxy is expected to be based on the luminous matter in the galaxy. Clearly, the green points do not match the dashed line: the rotational velocity of objects outside the galaxy is far faster than the prediction. If, however, there were a large amount of non-luminous matter in the galaxy, objects far from the galactic center would move much faster. The solid green line is the velocity predicted for the orbiting objects if there is dark matter in M33. These rotation curves provide strong indirect evidence for dark matter. Credit: NOAO, AURA, NSF, T.A.Rector.

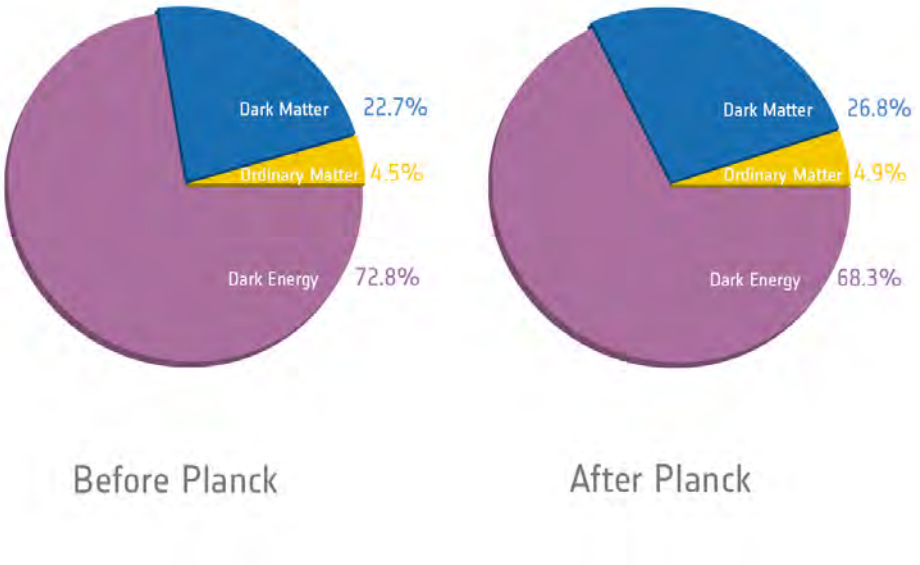

FIGURE 1.4: the so-called the cosmic pie: On the left, showing contents of the universe before WMAP estimations and on the right more recent estimations provided by the analysis of Planck data. Credit: ESA and the Planck Collaboration.

1.5.2 Candidates for dark matter

Dark matter does not interact with normal matter or electromagnetic radiation. It interacts only gravitationally. Therefore, it has not yet been possible to detect dark matter directly. Only the total dark sector energy-momentum tensor is inferred from its combined gravitational effect on visible matter. The search for candidate dark matter particles is still in progress (see e.g. [26]).
The most well-known candidates for dark matter include axions, neutrinos, neutralinos. Dark matter is considered essential in the formation and growth of large scale structures in the universe such as galaxies and clusters of galaxies. Weakly interacting particles, including dark matter and its candidate particles, are collectively classed as Weakly Interacting Massive Particles (WIMPs) [27]. It has been predicted by particle physicists that the dark matter particles must be very massive in order for its properties to be consistent with the structure formation in the universe [28]. There are various classifications of dark matter: one of which is the cold dark matter (CDM) for non-relativistic dark matter which has no significant random motion, and another one is called hot dark matter (HDM) which is relativistic. There is yet another type of dark matter model known as warm dark matter (WDM). The cosmological effects of this model depend both on density and the nature of random motion. The CDM candidates may be some kind of lightest supersymmetric particles or massive primordial black holes while neutrinos may be the possible candidates for HDM. Active experimental efforts have been made to search for neutrinos (see e.g. [29] and the references therein).

1.6 Dark Energy

The latest assessment for the universe energy budget [1] reveals that dark energy dominates with around 68.3% of the total energy. For this reason it is worthwhile to investigate a universe dominated by dark energy. The idea of dark energy, however, is hypothetical since it has never been detected nor created in a laboratory. It has been introduced to explain the accelerated expansion epoch that the universe experiences at the present time. Furthermore, at this stage, it is necessary to include the concept of dark energy in order to account for the vast majority of missing energy in the universe, which otherwise would lead to a "shortfall" of the energy budget of the universe. One of the simplest models for dark energy is the cosmological constant Λ or vacuum energy density, with negative pressure, whose equation of state is given by

$$w_\Lambda = \frac{P_\Lambda}{\rho_\Lambda}, \tag{1.68}$$

where P_Λ is the dark energy pressure and ρ_Λ is the dark energy density. The negative pressure of dark energy distinguishes it from the other components such as baryons and radiations. The disappearance of the original motivation for introducing the cosmological constant did not change its status as a legitimate addition to the gravitational field equations. Alternatively, the cosmological constant is now regarded as a form of dark energy that, possibly, causes the late-time cosmic speed-up.

Indeed, the standard model of cosmology, known as ΛCDM (cold dark matter) model is in good agreement with observational data. However, the model has various problems such as a difference of 10^{121} in order of magnitude between $\rho_\Lambda \approx 10^{-47} GeV^4$ and $\rho_{vac} \approx 10^{74} GeV^4$. This problem is called the cosmological constant problem (for recent review, see e.g. [23, 30]).

The second issue related to the cosmological constant problems is the coincidence between the observed vacuum energy and the current matter density. The best fit values of the cosmological parameters are: $\Omega_{\Lambda 0} = 0.68$ and $\Omega_{M0} = 0.27$, but the relative balance of vacuum and matter changes rapidly as the universe expands:

$$\frac{\Omega_\Lambda}{\Omega_M} \propto a^3. \tag{1.69}$$

As a consequence, at early times the vacuum energy is negligible in comparison to matter and radiation, while at late times matter and radiation are negligible. It has been speculated that if dark energy evolves with time, then the cosmological coincidence problem may be alleviated. One of the simplest scalar field models of time-evolving dark energy is quintessence [31, 32]. Some other models of dark energy are scalar field models such as phantom fields [33], K-essence [34–36], tachyons [37, 38] and Chaplygin gas [39–41].

1.6.1 The dynamics of a universe with a non-vanishing cosmological constant

Earlier in this chapter[2], we included solutions to a flat (FLRW) universe with a zero cosmological constant. A good generalisation of these solutions can be found by investigating the dynamics of a spcetime dominated by cosmological constant (Λ) having a non-trivial value. We will concentrate on deriving the solution of a spatially flat ($\Omega_k = 0$) universe filled with dust only ($\Omega_{r,0} = 0$). In this case, the cosmological field equation becomes [21]

$$\dot{a}^2 = H_0^2[(1 - \Omega_{\Lambda,0})a^{-1} + \Omega_{\Lambda,0}a^2]. \tag{1.70}$$

[2] see Table 1.1

Integrating (1.70) yields

$$t = \frac{1}{H_0}\int_0^a \frac{x dx}{\sqrt{(1-\Omega_{\Lambda,0}) + \Omega_{\Lambda,0} x^4}}. \tag{1.71}$$

In order to evaluate (1.71), we take $y^2 = \frac{x^3|\Omega_{\Lambda,0}|}{1-\Omega_{\Lambda,0}}$. Hence

$$H_0 t = \frac{2}{3\sqrt{\mid \Omega_{\Lambda,0} \mid}} \int_0^{\sqrt{\frac{a^3|\Omega_{\Lambda,0}|}{1-\Omega_{\Lambda,0}}}} \frac{dy}{\sqrt{1 \pm y^2}}, \tag{1.72}$$

where the plus sign in the integrand corresponds to the case $\Omega_{\Lambda,0} > 0$, and the minus sign to $\Omega_{\Lambda,0} < 0$. The integration of (1.72) gives

$$H_0 t = \frac{2}{3\sqrt{\mid \Omega_{\Lambda,0} \mid}} \begin{cases} \sinh^{-1}\left(\sqrt{\frac{a^3|\Omega_{\Lambda,0}|}{1-\Omega_{\Lambda,0}}}\right) & \text{if} \quad \Omega_{\Lambda,0} > 0, \\ \sin^{-1}\left(\sqrt{\frac{a^3|\Omega_{\Lambda,0}|}{1-\Omega_{\Lambda,0}}}\right) & \text{if} \quad \Omega_{\Lambda,0} < 0. \end{cases} \tag{1.73}$$

If the initial dark energy component $\Omega_{\Lambda,0}$ is positive,(Fig [1.5]), then the cosmological force will be repulsive. Specifically for these models, a repulsive force will support an expanding scenario but with an inflection point, at which the expansion rate is changed. If $\Omega_{\Lambda,0}$ is negative, (Fig [1.5]), then the cosmological force will be attractive causing an end to the initial expansion and bringing the model to a collapse usually called " the big crunch".

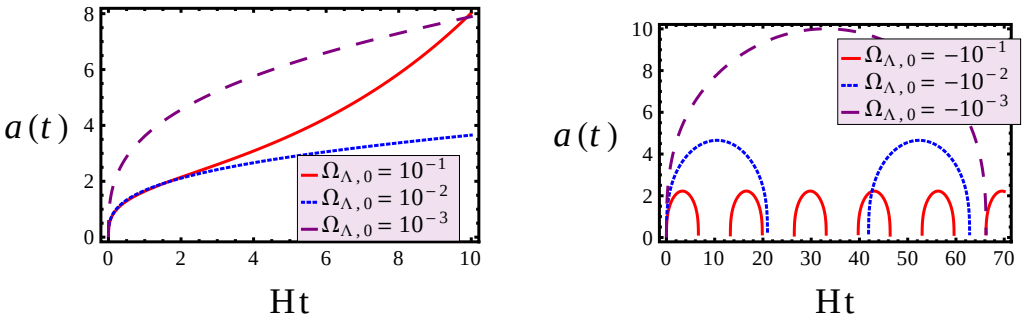

FIGURE 1.5: Left: Expanding models with an inflection point at which the expansion rate is changed. Right: Bouncing evolution of a scale factor for a universe contains a random initial negative dark energy component.

1.7 Shortcomings of the Big Bang Cosmology

1.7.1 Horizon problem

Despite the fact that the early universe was vanishingly small, the rapid expansion precluded causal contact from being established throughout. The Cosmic Microwave Background (CMB) has a perfect black body spectrum. Two photons coming from opposite directions have nearly equal temperatures. Yet these photons come from different regions, that at the time of last scattering were not in causal contact with each other.

Photons travel on null geodesics with $ds^2 = 0 \Rightarrow dr = \frac{dt}{a(t)}$ for a radial path. The

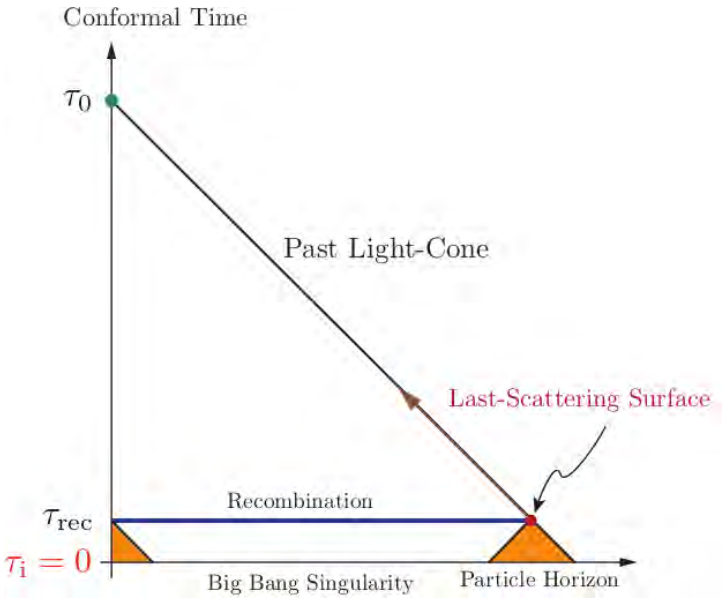

FIGURE 1.6: Conformal diagram for Big Bang cosmology. At the time of recombination there were a lot of photons that never had casual contact among each other and thus there was no time for any thermal equilibrium to took place [3].

particle horizon is the maximum distance a light ray can travel between $t = 0$ and t (and thus gives the size of a causal region).

$$\begin{aligned} R_p &= a(t)\int_0^t \frac{dt'}{a(t')} = a(t)\int_0^a \frac{d(\ln a)}{aH} \\ &= \frac{t}{1-n} \sim H^{-1} \propto \begin{cases} a^{3/2}, & (MD) \\ a^2, & (RD) \end{cases} \end{aligned} \tag{1.74}$$

Where MD stands for matter domination era, while RD stands for radiation domination era. For a more illustrative way of visualising the horizon problem Fig [1.6] we introduce the flat (FLRW) (1.14) in terms of conformal time. Conformal time (τ) relates to cosmic

time by,

$$\tau = \int \frac{t}{a(t)}. \tag{1.75}$$

Thus, for a radial propagation of light the flat (FLRW) becomes

$$ds^2 = a(\tau)^2[-d\tau^2 + d\chi^2] \tag{1.76}$$

Considering that photons travel on null geodesics with ($ds^2 = 0$) gives $d\tau = \pm\sqrt{d\chi^2}$. Thus the evolution of the scale factor $a(\tau)$ is given by

$$a(\tau) = \begin{cases} \tau^2, & (MD) \\ \tau, & (RD) \end{cases} \tag{1.77}$$

Both in radiation- and matter-dominated epochs, there are particle horizons and there exist regions that cannot interact. On the other hand, the cosmic microwave background (CMB) radiation is nearly homogeneous i.e. it has roughly the same temperature distribution in all directions on the sky. These are the regions that cannot have interacted before recombination. Thus, the question arises as to how it was possible to achieve thermal equilibrium if there were no interactions between these regions. This problem is called horizon problem.

1.7.2 Flatness Problem

Consider the Friedmann equation in the form

$$\Omega_{tot} - 1 = \frac{k}{(aH)^2}. \tag{1.78}$$

The comoving Hubble radius $(aH)^{-1}$ grows with time and thus $\Omega_{tot} = 1$ is an unstable fixed point. Indeed

$$\frac{\mid \Omega_{tot} - 1 \mid_{pl}}{\mid \Omega_{tot} - 1 \mid_0} \sim (\frac{a_{pl}}{a_0})^2 \sim (\frac{T_0}{T_{pl}})^2 \sim \mathcal{O}(10^{-64}). \tag{1.79}$$

We adopted an approximation in the first step by assuming a radiation dominated universe (valid up until recombination epoch), while in the last step we took $\mid \Omega_{tot} - 1 \mid_0 = \mathcal{O}(1)$. To have a flat universe at present, the value of Ω_{tot} at earlier times need to be extremely fine-tuned.

The value of Ω_{tot} at time $t = 0$ is of the order of unity. Thus it is expected that Ω_{tot} has to be close to unity at earlier times. For example, it is required that, at time $t = t_{nucleo}$ when nucleosynthesis takes place, $\mid \Omega(t_{nucleo}) \mid < \mathcal{O}(10^{-16})$. This alongside

$\mid \Omega(t_{pl}) \mid < \mathcal{O}(10^{-64})$ are highly fine-tuned conditions and are unlikely. Without these fine-tuned conditions the universe would either collapse too soon, or expand too quickly before large scale structures start forming.

1.7.3 The monopole problem

If the universe can be extrapolated back in time to high temperatures, it is likely that it went through a series of phase transitions during its evolution. There are the electroweak and quantum chromodynamics (QCD) phase transitions, and possibly other ones at (much) higher scales, such as grand unified theory (GUT) phase transition(s). Depending on the symmetry broken in the phase transition, topological defects (domain walls, cosmic strings, monopoles or textures) may form. Monopoles are heavy point-like objects, which behave like ordinary matter. If produced in the early universe, the energy density in monopoles decreases slower than the radiation background, and comes to dominate the energy density in the universe early on (it "overcloses" the universe), in conflict with observations.

1.8 Inflation

In principle, it is possible to tune initial conditions in the big bang cosmology so that our current universe emerges. But the amount of tuning is enormous. Inflation — the idea that the early universe went through a period of rapid accelerated expansion — solves the previous problems (Horizon problem, Monopole problem,... etc). Flatness and isotropy are no longer initial value problems, but rather they emerge dynamically; the monopole problem is addressed as well. We define inflation to be any epoch where $\ddot{a} > 0$ .i.e. an accelerated expansion. We can rewrite this in several different ways

$$INFLATION \Longleftrightarrow \ddot{a} > 0 \Longleftrightarrow \frac{d(aH)^{-1}}{dt} < 0 \Longleftrightarrow (\rho + 3P) < 0. \tag{1.80}$$

The middle definition reveals how the accelerated expansion reverses the behaviour of the co-moving Hubble radius, it will decrease instead of increase. The growing co-moving Hubble radius was the root of both the flatness and the horizon problem. To get inflation the strong energy condition has to be broken. For extensive discussions on the inflationary cosmology see [3, 42–49] .

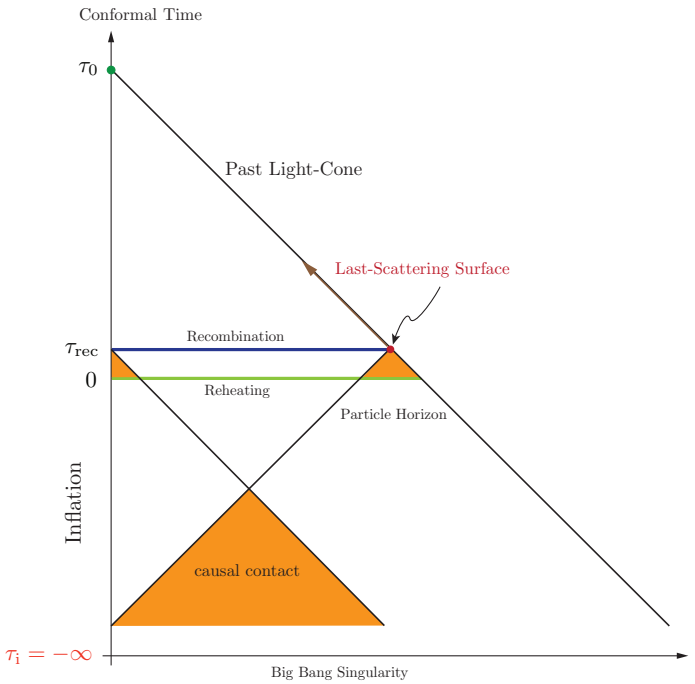

FIGURE 1.7: Conformal diagram of inflationary cosmology. Inflation extends conformal time to negative values! The end of inflation creates an " apparent " Big Bang at $\tau = 0$. There is, however, no singularity at $\tau = 0$ and the light cones intersect at an earlier time if inflation lasts for at least 60 e-folds [3].

1.8.1 The horizon problem revisited

The horizon problem in big bang cosmology stems from the fact that the particle horizon $R_p \sim H^{-1}$ increases faster than a physical length scale $\lambda \propto a$ with time. Thus extrapolating back a scale that is now inside the horizon $\lambda < R_H$, it was outside at earlier times. The inflation scenario solves the problem by providing a long phase in which λ decreases faster than the horizon and the Hubble distance $(aH)^{-1}$, which enters the particle horizon, decreases. The ratio

$$\frac{R_p}{\lambda} \propto \int_0^a \frac{d\ln(a)}{(aH)}, \tag{1.81}$$

decreases with time during inflation, since $(aH)^{-1}$ decreases.

1.8.2 The flatness problem revisited

Inflation solves the flatness problem more or less by definition (so that at least any classical, as opposed to quantum, solution of the problem will fall under the umbrella of

the inflationary definition) [28]. The Freedman equation during inflation gives

$$\Omega_{tot} - 1 = \frac{k^2}{(aH^2)^2} \propto e^{-2N} \to 0, \tag{1.82}$$

since

$$\frac{\mid \Omega_{tot} - 1 \mid_{t_f}}{\mid \Omega_{tot} - 1 \mid_{t_i}} = (\frac{a_i}{a_f})^2 = e^{-2N}, \tag{1.83}$$

this requires $N \gtrsim 60 - 70$; inflation predicts $\Omega_0^{tot} = 1$.

1.8.3 The monopole problem revisited

If inflation takes place after the phase transition during which monopoles form, the monopole density is mitigated by inflation to insignificant size:

$$n_{mp} \propto \frac{N_{mp}}{a^3} \to 0. \tag{1.84}$$

1.9 Scalar Field Dynamics

The great advantage of employing a scalar field is that it has the same quantum number as the vacuum, and thus can mimic a vacuum like state. Consider the action for a scalar

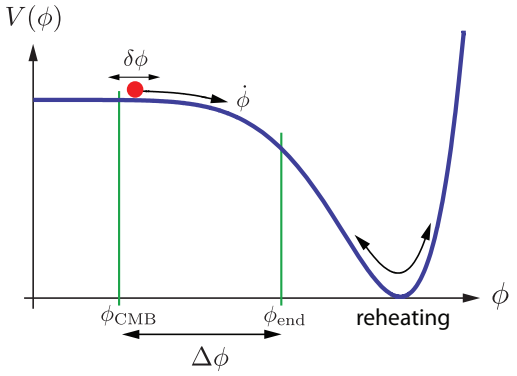

FIGURE 1.8: Example of an inflation potential. CMB fluctuations are created by quantum fluctuations $\delta\phi$ about 60 e-folds before the end of inflation. At reheating, the energy density of the inflaton is converted into radiation [3].

field ϕ, which we will call the inflation field,

$$S = \int d^4\sqrt{-g}[\frac{R}{2} + \mathcal{L}_\phi], \tag{1.85}$$

with

$$\mathcal{L}_\phi = \frac{1}{2} g^{\mu\nu}\partial_\mu\phi\partial_\nu\phi - V(\phi). \tag{1.86}$$

The potential $V(\phi)$ describes the self-interactions of the scalar field. The energy-momentum tensor for the scalar field is

$$T^{(\phi)}_{\mu\nu} \equiv -\frac{2}{\sqrt{-g}}\frac{\delta S_\phi}{\delta g^{\mu\nu}} = \partial_\mu\phi\partial_\nu\phi - g_{\mu\nu}\left(\frac{1}{2}\partial^\sigma\phi\partial_\sigma\phi + V(\phi)\right). \tag{1.87}$$

Then the field equation is

$$\frac{\delta S_\phi}{\delta\phi} = \frac{1}{\sqrt{-g}}\partial_\mu(\sqrt{-g}\partial^\mu\phi) + \frac{dV}{d\phi} = 0\ . \tag{1.88}$$

If we assume a flat FLRW metric (1.14) and restrict to the case of a homogeneous field $\phi(t,\mathbf{x}) \equiv \phi(t)$ [3], then the energy-momentum tensor takes the form of a perfect fluid with

$$\rho_\phi = \frac{1}{2}\dot\phi^2 + V(\phi)\,, \tag{1.89}$$

$$p_\phi = \frac{1}{2}\dot\phi^2 - V(\phi)\,. \tag{1.90}$$

The equation of state then reads

$$w_\phi = \frac{p_\phi}{\rho_\phi} = \frac{\frac{1}{2}\dot\phi^2 - V}{\frac{1}{2}\dot\phi^2 + V}. \tag{1.91}$$

For $\frac{1}{2}\dot\phi^2 \ll V(\phi)$, $w_\phi = -1$. If the potential energy $V(\phi)$ dominates over the kinetic energy term $\frac{1}{2}\dot\phi^2$, this leads to an epoch of accelerated expansion. The dynamics of the (homogeneous) scalar field and the FLRW geometry is determined by

$$\ddot\phi + 3H\dot\phi + V_{,\phi} = 0 \qquad \text{and} \qquad H^2 = \frac{1}{3}\left(\frac{1}{2}\dot\phi^2 + V(\phi)\right). \tag{1.92}$$

1.10 Slow-Roll Inflation

The dynamical system given by (1.92) only enables accelerated expansion under specific approximations. These approximations are satisfied in what is known as the slow roll inflation. The slow roll approximation consists of

$$\dot\phi/2 \ll V(\phi) \quad \Rightarrow \quad H^2 = \rho/3 \approx V(\phi)/3, \tag{1.93}$$

$$\ddot\phi \ll 3H\dot\phi \quad \Rightarrow \quad 3H\dot\phi \approx -\frac{dV}{d\phi}. \tag{1.94}$$

The first approximation ensures that H is almost constant $\dot H \ll H^2$, leading to inflation with $a \sim e^{Ht}$. The second approximation guarantees inflation is prolonged. The slow

roll conditions are equivalent to requiring the slow roll parameters

$$\epsilon \equiv \frac{M_{pl}^2}{2}(\frac{V_{,\phi}}{V})^2, \quad \eta \equiv M_{pl}^2 \frac{V_{,\phi\phi}}{V}, \tag{1.95}$$

to be small: $\epsilon, \mid \eta \mid \ll 1$ [44].
Let us define N as the number of e-folds left to the end of inflation,

$$N(\phi) = \ln(\frac{a_f}{a}) = \int_t^{t_f} H dt = H \int_\phi^{\phi_f} \frac{d\phi}{\dot{\phi}} \approx \int_{\phi_f}^{\phi} \frac{V}{V_{,\phi}} d\phi. \tag{1.96}$$

Inflation ends when slow roll is violated, $\epsilon(\phi_f) \approx 1$ or $\eta(\phi_f) \approx 1$.

1.11 Classification of models for inflation

Single field models are typically placed under one of the following broad classes:

- Large Field Models: inflation parameters obey $0 < \eta \leqslant \epsilon$. In these models, the scalar field is perturbed from a stabled minimum by an amount $\Delta\phi \approx M_{pl}$ [3].

- Small-Field Inflation: the field moves over a small (sub-Planckian) distance ($\Delta\phi < M_{pl}$). The inflation parameters obey $\eta < 0 < \epsilon$. The potentials that give rise to such small-field evolutions often arise in mechanisms of spontaneous symmetry breaking, where the field rolls off an unstable equilibrium toward a displaced vacuum [3].

- Hybrid Models: These models are identified by conditions on the second derivative of the potential as well as on the slow roll parameters, $V_{,\phi\phi} > 0$ and $\eta < 0 < \epsilon$.

1.12 Constraints on the inflationary models

The recent Planck data analysis [1] pointed out that the cosmological perturbations in the Cosmic Microwave Background (CMB) radiation are nearly Gaussian and of the adiabatic type. Thus, even if one insists in assuming that these perturbations are to be ascribed to single-field models of inflation [46], the data puts strong restrictions on the inflationary parameter. Planck results disfavour many inflationary models. For instance, the chaotic models ϕ^n with $n \leq 2$ are not consistent with Planck data. In particular, the simplest quadratic chaotic model $m^2\phi^2$ does not fit well with data and

thus has been excluded. Surprisingly, the Planck team reported that there is a very good agreement between the data and the Starobinsky model ($R + R^2$) proposed in [50]. The perfect agreement between the model and the data is due to $\frac{1}{N}$ suppression (N being the number of e-folds till the end of inflation) of r with respect to the prediction for the scalar spectral index n_s [51].

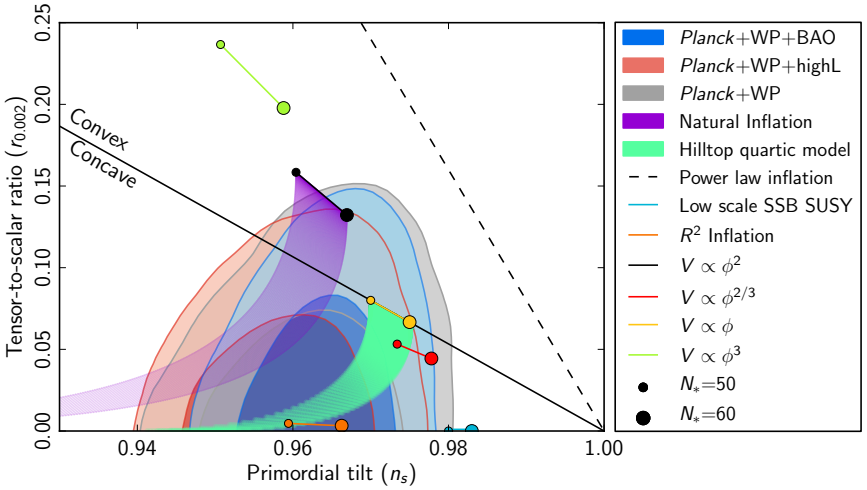

FIGURE 1.9: Marginalizing joint 68% and 95% CL regions for n_s and $r_{0.002}$ from Planck in combination with other data sets compared to the theoretical predictions of selected inflationary models [1].

1.13 Good news for Inflation?!

The BICEP2 Experiment [4, 52] has announced a detection of B-modes of polarization in the cosmic microwave background; see Fig [1.12]. In general, there are two types of polarization patterns having imprints in (CMB). The first type is E-mode and can be caused by density (scalar) perturbations, whilst gravitational wave (tensor) perturbations produce both E- and B-mode polarization. The first type i.e. E-mode was first detected by the DASI experiment [53]. The lensing B-mode spectrum is similar to a smoothed version of the E-mode spectrum but a factor ~ 100 lower in power Fig [1.10]. If the results hold, then they will be the most robust evidence for existence of primordial gravitational waves generated during inflation epoch [50, 54, 55]. This, in turn, would be a conclusive confirmation of the inflation scenario.

The measured B-mode component of the polarization is consistent with a scale invari-

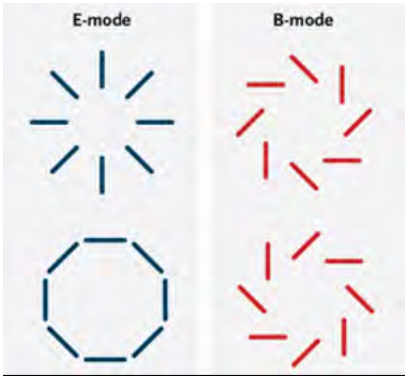

FIGURE 1.10: E-mode polarization patterns look like asterisks or loops, and they don't change when mirror-imaged. B-modes, on the other hand, curl either clockwise or counter-clockwise into spiral patterns. Credit: skyandtelescope.

ant gravitational wave background with a tensor-scalar ratio $r = 0.2$ Fig [1.11], which is little different from the tensor fluctuation as calculated by the Planck team [1].

This new discovery leads to major consequences, the first consequence is binding the energy scale of inflation to be

$$\rho^{\frac{1}{4}} \simeq 2.2(\frac{r}{0.2})^{\frac{1}{4}} 10^{16} GeV, \tag{1.97}$$

i.e. around the Grand Unified Theory (GUT) energy scale [56]. This gives a glimpse of the importance of this discovery in enabling the physics of the universe to be studied at a very high energy scale. The second consequence is that the single field slow roll inflation scenario is favoured by the analysis of the BICEP2 results in contrast to Planck project. Although BICEP2 results are compelling, and if they hold up, they will deepen our understanding of our universe, there are some concerns that the results about the fraction of polarization due to dust have been underestimated. There is a claim that a

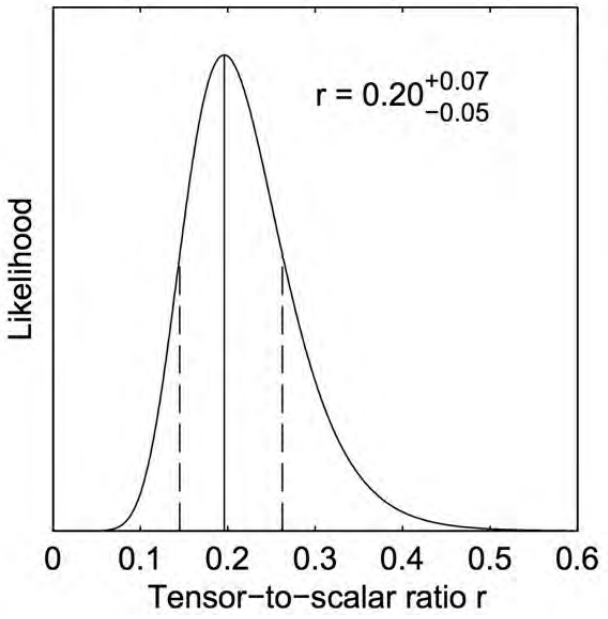

FIGURE 1.11: The constraint on the tensor-to-scalar ratio r.The maximum likelihood and the $\pm 1\sigma$ interval is $r = 0.20^{+0.07}_{-0.05}$, as indicated by the vertical lines [4].

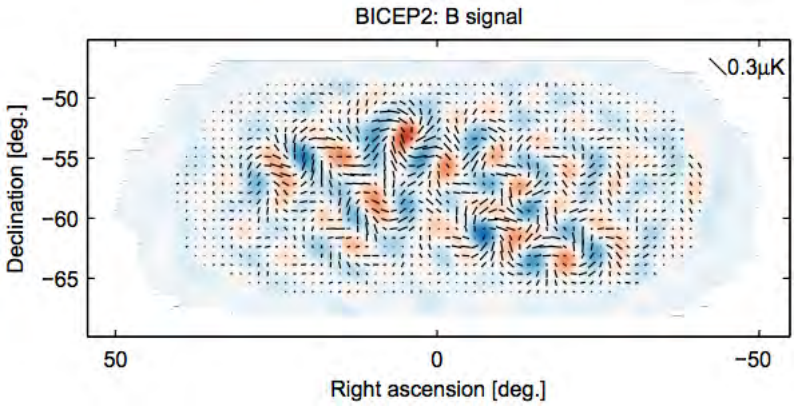

FIGURE 1.12: BICEP2 apodized B-mode maps filtered to $50 < \ell < 120$ [4].

combination of Galactic foregrounds and lensed E-modes[3] could be responsible for the strong signal [57] detected by the BICEP2 team. In a recent study [57] it has been shown that the 100×150 GHz and 150×150 GHz data are consistent with a cosmology with $r = 0.2$ and negligible foregrounds, but also with a cosmology with $r = 0$ and a significant dust polarization signal. In their estimation of the fraction of polarization caused by dust[4], the BICEP2 team relied on a map presented in [58], but a newer version of the map [59] showed that the cosmic infra-red background (CIB) was not corrected for in the first map [60]. Accounting for the (CIB) will increase the polarization fraction from 5% to 8.5%. This in turn increases the dust polarization power spectrum by a factor

[3]Gravitational lensing can generate B-modes by lensing E-modes.
[4]The team assumed the fraction of polarization due to dust in the field to equal 5%.

of 3 [60]. Therefore, the strong signal detected by the BICEP2 team, could possibly, be ascribed to dust and not to a primordial gravitational waves. We can see that the BICEP2 results are not yet confirmed[5], so we should be careful in either accepting or rejecting these results.

1.13.1 The debate continues

Although the latest map of interstellar dust, which has been released by the Planck team [61], did not conclude that BICEP2 results are entirely incorrect, it certainly lowered the chances that the signal detected by the team can be ascribed to real primordial gravitational waves. The analysis of the latest dust map reveals that BICEP2 team significantly underestimated the dust polarization in the region around the South Pole Fig [1.13]. Based on Planck's team latest dust map, a joint project between BICEP2 and Planck's teams has been established. The project aims to re-analyse BICEP2 data and give the final word about the residual signal after subtracting the dust. The map shows that the dust cannot be ignored in any patch in the sky even in the South Pole. More importantly, the dust map serves as a guide to astronomers as it indicates precisely where the forthcoming telescope projects aiming to study the gravitational waves, CMB must be established.

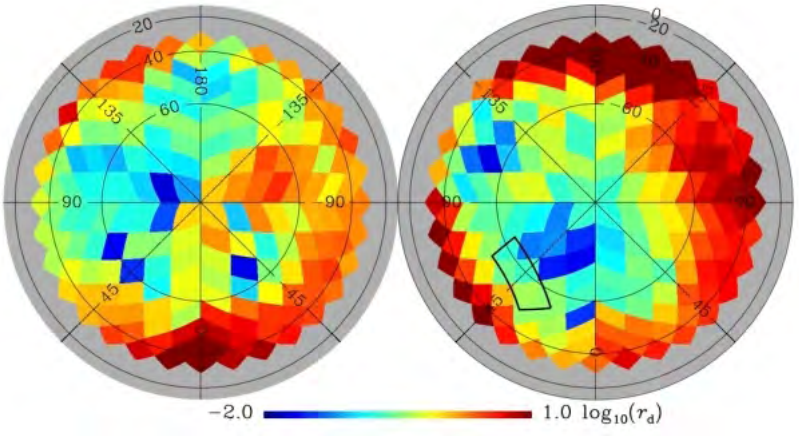

FIGURE 1.13: Planck's full-sky map grades regions of lower (blue) and higher (red) interstellar dust — and shows that the patch observed by the BICEP2 telescope (rectangle) was not among the least dusty. The left panel shows the northern Galactic hemisphere and the right panel shows the southern one.

[5] At the time of writing this manuscript the final dust maps of Planck project have not been published yet. When the final maps are released in October 2014, they might put an end to this controversy.

1.14 Concluding Remarks

This chapter has been dedicated to demonstrating the fundamental pillars upon which modern cosmology is established. The Big Bang cosmology with a cosmological constant i.e. the ΛCDM model successfully accounts for most of the observations up to now. However the model has some problems such as the monopole problem, the horizon problem and the flatness problem,..., etc. Assuming an epoch of rapid accelerated expansion leads to resolving most of these problems. Moreover, we introduced a brief review of the latest outputs of both Planck and BICEP2 projects. The Planck (2013) results came first and put tight constraints on the inflationary models thus excluding some of these models. Although BICEP2 (2014) results concerning the detection of primordial gravitational waves were considered to be one of the biggest achievements in modern cosmology, the results did not hold up according to some research groups. These groups claimed that the BICEP2 team data analysis results are fallacious and the signal extracted by the BICEP2 team is due to polarized dust. In the next chapter we will survey a number of modified theories of gravity and will reveal how we can recast the late accelerated expansion of the universe within them, without invoking a cosmological constant in the field equations.

Chapter 2

Extended Theories of Gravity

2.1 The quest for Extended Theories of Gravity

Although the merits of the theory of General Relativity (GR) are undisputed, our understanding of the universe through (GR) is still far from complete. Indeed, the Standard Big Bang model of the universe [62] is one of the most successful cosmological models since it agrees with various observations and explains many cosmological phenomena. However, the model suffers from a variety of problems such as the flatness problem, the horizon problem, the monopole problem,..., etc [1] [54]. The ΛCDM model problems inspired the growing thought that the standard cosmological model based on (GR) and the Standard Model of particle physics is inadequate to describe the universe at extreme regimes. Moreover, the absence of a complete and self-consistent quantum theory of gravitation has a crucial role in prompting the efforts to modify (GR). One of the various alternatives which has been introduced is Extended Theories of Gravity (ETG). The underlying idea in (ETG) is extending (GR) by adding higher order curvature invariants and minimally or non-minimally coupled scalar fields into the dynamics emerging from some effective quantum gravity action [63].

2.2 The Fundamental Physics motivation

From a pure physical perspective, there are two reasons that motivated the search for a new theory of gravity, or modifying (GR). The first motivation is the obvious inconsistency between (GR) and Mach's principle. According to Mach's principle the local inertial frame is determined by the average motion of distant astronomical objects [63].

[1] For a comprehensive discussion on the origin of these problems and how inflation scenario has resolved them, one goes back to section (1.7) and section (1.8).

Therefore, the gravitational coupling could be scale-dependent and could be related to some scalar field. As a consequence, the concepts of "inertia" and the Equivalence Principle have to be revised [64].

The second motivation has appeared in the context of introducing a quantized version of (GR) or what we call a quantum theory of gravity. Actually, the new terms in " Einstein-Hilbert action" emerge as a natural result of the interactions among quantum scalar fields and background geometry or gravitational self-interactions. More recently, it was shown that the corrective terms are unavoidable in order to obtain the effective action of Quantum Gravity at scales closer to the Planck scale [65].

2.3 The Cosmology motivation

In this section, we investigate the cosmological motivations for (ETG) in more detail. The recent observations of light-curves of supernovae type Ia [10, 11, 66], and independently from measurements of the Baryon acoustic oscillations, Cosmic Microwave Background anisotropies [22, 67], Large Scale Structure formation [68–70] and weak lensing [71], have excluded the possibility that the universe is modelled by an Einstein-de Sitter solution. Furthermore, the observations favoured the possibility that the present universe is experiencing an epoch of accelerated expansion. The first attempt to resolve late time cosmic speed-up was by constructing the concordance model (ΛCDM) in which a negative pressure cosmic fluid called dark energy is responsible for the current cosmic speed-up. However, the ΛCDM model has a fine tuning problem: a significant difference in magnitudes ($\mathcal{O}(10^{121})$) between the cosmological constant and the vacuum energy density value predicted by particle physics. A more general concept of dark energy has been proposed, that is quintessence: a hypothetical fifth fundamental force which, unlike the cosmological constant (Λ), is of a dynamical form. It takes the form of a scalar field (ϕ), which strongly couples to matter. Although (ϕCDM) managed to accomplish a good correlation with observations, the values of the dark energy and dark matter densities remain comparable at the present epoch which means that the new model suffers from the same coincidence problem as well. In the early time, the scalar field ϕ mimics and tracks the matter behaviour in contrast to the late time situation, the dynamical dark energy stops tracking the matter and dominates it. In a parallel way, lots of efforts have been done to address the dark energy problem in the context of (ETG). Most of these efforts attempt to reveal the potential geometrical origin of dark energy.

2.4 $f(R)$ theories of gravity

That class of modified gravity theories, firstly, was proposed by Buchdahl [72], $f(R)$ theories gained more popularity after further developments by Starobinsky [50] and later, following the realization of the discrepancy between theory and observation [73–88]. Although the principle on which all the modified theories of gravity have been established, namely generalizing the (E-H) action, remains the same, the techniques that have been adopted to accomplish that goal vary from one theory to another. Analogously, $f(R)$ theory takes the same path of generalizing (E-H) action,

$$\mathcal{A}_{EH} = \frac{1}{2\kappa^2}\int d^4x\sqrt{-g}R, \tag{2.1}$$

to become a general function of R

$$\mathcal{A} = \frac{1}{2\kappa^2}\int \mathrm{d}^4x\sqrt{-g}\,f(R) + \int \mathrm{d}^4x\mathcal{L}_M(g_{\mu\nu},\Psi_M)\,, \tag{2.2}$$

where $\kappa^2 = 8\pi G$, g is the determinant of the metric $g_{\mu\nu}$, and $\mathcal{L}_M$ is a matter Lagrangian that depends on $g_{\mu\nu}$ and matter fields Ψ_M. The Ricci scalar R is defined by $R = g^{\mu\nu}R_{\mu\nu}$, where the Ricci tensor $R_{\mu\nu}$ is

$$R_{\mu\nu} = R^{\alpha}{}_{\mu\alpha\nu} = \partial_\lambda\Gamma^\lambda_{\mu\nu} - \partial_\mu\Gamma^\lambda_{\lambda\nu} + \Gamma^\lambda_{\mu\nu}\Gamma^\rho_{\rho\lambda} - \Gamma^\lambda_{\nu\rho}\Gamma^\rho_{\mu\lambda}\,. \tag{2.3}$$

In the case of the torsionless metric formalism, the connections $\Gamma^\alpha_{\beta\gamma}$ are the usual metric connections defined in terms of the metric tensor $g_{\mu\nu}$, as

$$\Gamma^\alpha_{\beta\gamma} = \frac{1}{2}g^{\alpha\lambda}\left(\frac{\partial g_{\gamma\lambda}}{\partial x^\beta} + \frac{\partial g_{\lambda\beta}}{\partial x^\gamma} - \frac{\partial g_{\beta\gamma}}{\partial x^\lambda}\right). \tag{2.4}$$

This follows from the metricity relation, $\nabla_\lambda g_{\mu\nu} = \partial g_{\mu\nu}/\partial x^\lambda - g_{\rho\nu}\Gamma^\rho_{\mu\lambda} - g_{\mu\rho}\Gamma^\rho_{\nu\lambda} = 0$.

There are many reason to consider the $f(R)$ theory of gravity as a worthwhile candidate among the higher order theories of gravity:

- The flexibility of the function $f(R)$ makes it easy to select and combine different terms that could address the different epochs that the universe evolves over them.
- It has been confirmed that $f(R)$ is unique among the higher order gravity theories that could avoid the fatal Ostrogradski instability [89].
- Even if $f(R)$ is far from being the ultimate theory of gravity, it has helped us to obtain a better insight to General Relativity (GR).

2.5 The metric formalism of $f(R)$

In this section, we derive the field equations for $f(R)$ in the metric formalism. In addition to the metric version, there is also Palatini $f(R)$ gravity [72, 90, 91]. In (GR), there is no difference between the two approaches, and thus the field equations remain independent of the derivation method. Extended Theories of Gravity (ETG) are unlike (GR) because when we generalize the (E-H) action and attempt to work out the $f(R)$ field equations, a substantial difference arises between the two approaches. In the Palatini approach, the metric and the connection are assumed to be independent variables and one varies the action with respect to both [90]. In addition to these two types, we have another approach called "metric-affine" $f(R)$ gravity [90, 91]. The metric-affine approach is the same as the Palatini approach but without imposing that the matter action is independent of the connection. In fact, addressing the cosmological acceleration within the metric-affine gravity is complicated and can be achieved with less effort in simpler theories. There are also other editions of $f(R)$ which have elements of both the metric and the Palatini versions.

2.5.1 Field equations of the metric $f(R)$ in Jordan frame

Applying the variational principle on the $f(R)$ Lagrangian density yields

$$\delta \int d^4x\sqrt{-g}f(R) = 0, \tag{2.5}$$

and we have

$$\begin{aligned}
\delta \int d^4x\sqrt{-g}f(R) &= \int d^4x[\delta(\sqrt{-g}f(R)) + \sqrt{-g}\delta(f(R))] \\
&= \int d^4x\sqrt{-g}[f'(R)R_{\mu\nu} - \frac{1}{2}g_{\mu\nu}f(R)]\delta g^{\mu\nu} \\
&+ \int d^4x\sqrt{-g}f'(R)g^{\mu\nu}\delta R_{\mu\nu},
\end{aligned} \tag{2.6}$$

where the prime denotes differentiation with respect to R. We consider the following substitution

$$\begin{aligned}
g^{\mu\nu}\delta R_{\mu\nu} &= g^{\mu\nu}\partial_\sigma(\delta\Gamma^\sigma_{\mu\nu}) - g^{\mu\sigma}\partial_\sigma(\delta\Gamma^\nu_{\nu\mu}) \\
&\equiv \partial_\sigma W^\sigma,
\end{aligned} \tag{2.7}$$

where

$$W^{\sigma} = g^{\mu\nu}\delta\Gamma^{\sigma}_{\mu\nu} - g^{\mu\sigma}\delta\Gamma^{\nu}\mu\nu. \tag{2.8}$$

We employ (2.7) to rewrite the second integral in (2.6) as follows

$$\int d^4x\sqrt{-g}f'(R)g^{\mu\nu}\delta R_{\mu\nu} = \int d^4x\sqrt{-g}f'(R)\partial_{\sigma}W^{\sigma}, \tag{2.9}$$

integration by parts yields

$$\begin{aligned}\int d^4x\sqrt{-g}f'(R)g^{\mu\nu}\delta R_{\mu\nu} &= \int d^4x\frac{\delta}{\delta x^{\sigma}}[\sqrt{-g}f'(R)W^{\sigma}] \\ &- \int d^4x\partial_{\sigma}[\sqrt{-g}f'(R)]W^{\sigma}.\end{aligned} \tag{2.10}$$

The first integration in (2.10) can be set to zero if we assume that the fields vanish at infinity.

$$\int d^4x\sqrt{-g}f'(R)g^{\mu\nu}\delta R_{\mu\nu} = -\int d^4x\partial_{\sigma}[\sqrt{-g}f'(R)]W^{\sigma}. \tag{2.11}$$

We calculate the term W^{σ} as follows

$$\delta\Gamma^{\sigma}_{\mu\nu} = \delta[\frac{g^{\sigma\alpha}}{2}(\partial_{\mu}g_{\alpha\nu} + \partial_{\nu}g_{\mu\alpha} - \partial_{\alpha}g_{\mu\nu})] \tag{2.12}$$

$$= \frac{g^{\sigma\alpha}}{2}[\partial_{\mu}\delta g_{\alpha\nu} + \partial_{\nu}\delta g_{\mu\alpha} - \partial_{\alpha}\delta g_{\mu\nu})], \tag{2.13}$$

by invoking the fact that we derive these equations in the context of a local inertial frame. Therefore

$$\partial_{\alpha}g_{\mu\nu} = \nabla_{\alpha}g_{\mu\nu} = 0. \tag{2.14}$$

Similarly

$$\delta\Gamma^{\nu}_{\mu\nu} = \frac{1}{2}g^{\nu\alpha}\partial_{\mu}(\delta g_{\nu\alpha}). \tag{2.15}$$

By combining (2.14) and (2.15), we obtain

$$g^{\mu\nu}\delta\Gamma^{\sigma}_{\mu\nu} = \frac{g^{\mu\nu}}{2}[-\partial_{\mu}(g_{\alpha\nu}\delta g^{\alpha\sigma}) - \partial_{\nu}(g_{\alpha\mu}\delta g^{\sigma\alpha}) - g^{\sigma\alpha}\partial_{\alpha}(\delta g_{\mu\nu})] \tag{2.16}$$

$$= \frac{1}{2}\partial^{\sigma}(g_{\mu\nu}\delta g^{\mu\nu}) - \partial^{\mu}(g_{\alpha\mu}\delta g^{\nu\alpha}), \tag{2.17}$$

$$g^{\mu\sigma}\delta\Gamma^{\nu}_{\mu\nu} = -\frac{1}{2}\partial^{\sigma}(g_{\nu\alpha}\delta g^{\nu\alpha}). \tag{2.18}$$

Consequently

$$W^{\sigma} = \partial^{\sigma}(g_{\mu\nu}\delta g^{\mu\nu}) - \partial^{\mu}(g_{\mu\nu}\delta g^{\sigma\nu}). \tag{2.19}$$

Using this equation, we write

$$\begin{aligned}\int d^4x\sqrt{-g}f'(R)g^{\mu\nu}\delta R_{\mu\nu} &= \int d^4x[\sqrt{-g}f'(R)][\partial^\mu(g_{\mu\nu}\delta g^{\sigma\nu}) \\ &- \partial^\sigma(g_{\mu\nu}\delta g^{\mu\nu})].\end{aligned} \tag{2.20}$$

Integrating by parts and setting the total divergence to zero, leads to

$$\begin{aligned}\int d^4x\sqrt{-g}f'(R)g^{\mu\nu}\delta R_{\mu\nu} &= \int d^4x g_{\mu\nu}\partial^\sigma\partial_\sigma[\sqrt{-g}f'(R)]\delta g^{\mu\nu} \\ &- \int d^4x g_{\mu\nu}\partial^\mu\partial_\sigma[\sqrt{-g}f'(R)]\delta g^{\sigma\nu}.\end{aligned} \tag{2.21}$$

The variation of the action is then

$$\begin{aligned}\delta\int d^4x\sqrt{-g}f(R) &= \int d^4x\sqrt{-g}[f'(R)R_{\mu\nu} - \frac{f(R)g_{\mu\nu}}{2}]\delta g^{\mu\nu} \\ &+ \int d^4x[g_{\mu\nu}\partial^\sigma\partial_\sigma(\sqrt{-g}f'(R)) - g_{\sigma\nu}\partial^\mu\partial_\sigma(\sqrt{-g}f'(R))]\delta g^{\mu\nu}.\end{aligned} \tag{2.22}$$

Setting the last equation to zero yields the $f(R)$ vacuum field equations

$$f'(R)R_{\mu\nu} - \frac{f(R)g_{\mu\nu}}{2} = \nabla_\mu\nabla_\nu f'(R) - g_{\mu\nu}\Box f'(R). \tag{2.23}$$

Consequently, the equivalent of the Einstein equation in $f(R)$ gravity reads

$$f'(R)R_{\mu\nu} - \frac{1}{2}f(R)g_{\mu\nu} - (\nabla_\mu\nabla_\nu - g_{\mu\nu}\Box)f'(R) = T_{\mu\nu}. \tag{2.24}$$

An interesting feature of $f(R)$ manifests itself through the trace equation of (2.24)

$$3\,\Box f'(R) + f'(R)R - 2f(R) = \kappa T\,, \tag{2.25}$$

where $T = T_{\mu\nu}g^{\mu\nu}$. The trace equation (2.25) exhibits a differential relation between R and T unlike (GR). In (GR), the relation between R and T was $R = -T$ is an algebraic relation permitting a number of solutions less than that of the previous one related to the metric $f(R)$ gravity.

2.6 Conformal Transformations

Conformal transformations arise when we deal with Extended Theories of Gravity (ETG) as well as GR. The purpose is to perform a conformal rescaling of the spacetime metric $g_{\mu\nu} \to \tilde{g}_{\mu\nu}$. In the Jordan frame the energy momentum tensor is covariantly conserved

and test particle follow geodesics. In the Einstein frame this is not necessarily the case since the energy momentum tensor is not always covariantly conserved. The photon world lines are geodesics in the Jordan frame as well as in the Einstein frame, but the case of massive particles is different: their Jordan frame geodesics are no longer transformed into Einstein frame geodesics, and vice-versa.

If $(M, g_{\mu\nu})$ is a spacetime, the point–dependent rescaling of the metric tensor

$$g_{\mu\nu} \to \tilde{g}_{\mu\nu} = \Omega^2 g_{\mu\nu} \,, \tag{2.26}$$

where $\Omega = \Omega(x)$ is a non vanishing, regular function, is called a *Weyl* or *conformal transformation*. It affects the lengths of time [space]-like intervals and the norm of time [space]-like vectors, but it leaves the light cones unchanged [92]. In the previous section we demonstrated how varying an action like (2.2) with respect to the metric $g_{\mu\nu}$ yields the generalized field equations (2.24) in *Jordan frame*. In this section, we use a conformal transformation [93–96] to derive the $f(R)$ action in *Einstein frame*. From now on, we use the tilde ($\sim$) to refer to the quantities in the Einstein's frame.
The relation between the Ricci scalar (R) and the transformed $(\tilde{R})$ and $(\tilde{g_{\mu\nu}})$ in the two frames is given by

$$R = \Omega^2 \tilde{g}^{\mu\nu} R_{\mu\nu}, \tag{2.27}$$

while

$$\tilde{R} = \tilde{g}^{\mu\nu} \tilde{R}_{\mu\nu}. \tag{2.28}$$

The ultimate relation between the Ricci scalar (R) in the two frames is,

$$R = \Omega^2 (\tilde{R} + 6\tilde{\Box}\omega - 6\tilde{g}^{\mu\nu}\partial_\mu\omega\partial_\nu\omega) \,, \tag{2.29}$$

where

$$\omega \equiv \ln \Omega \,, \qquad \partial_\mu\omega \equiv \frac{\partial\omega}{\partial\tilde{x}^\mu} \,, \qquad \tilde{\Box}\omega \equiv \frac{1}{\sqrt{-\tilde{g}}}\partial_\mu(\sqrt{-\tilde{g}}\,\tilde{g}^{\mu\nu}\partial_\nu\omega) \,. \tag{2.30}$$

We rewrite the action (2.2) in the form

$$\mathcal{A} = \int^4 x\sqrt{-g}\left(\frac{1}{2\kappa^2}FR - U\right) + \int \mathrm{d}^4x\mathcal{L}_M(g_{\mu\nu}, \Psi_M) \,, \tag{2.31}$$

where

$$F = \frac{\partial f}{\partial R} \,, \qquad \text{and} \qquad U = \frac{FR - f}{2\kappa^2} \,. \tag{2.32}$$

Since $g_{\mu\nu}$ is of order 4:

$$det(\Omega^2 g_{\mu\nu}) = \Omega^8 det(g_{\mu\nu}), \tag{2.33}$$

$$\sqrt{-g} = \Omega^{-4}\sqrt{-\tilde{g}}, \tag{2.34}$$

and using (2.29) and (2.34), the action (2.31) is transformed as follows:

$$\mathcal{A} = \int^4 x\sqrt{-\tilde{g}}\left[\frac{1}{2\kappa^2}F\Omega^{-2}(\tilde{R} + 6\tilde{\Box}\omega - 6\tilde{g}^{\mu\nu}\partial_\mu\omega\partial_\nu\omega) - \Omega^{-4}U\right] + \int \mathrm{d}^4x\mathcal{L}_M(\Omega^{-2}\,\tilde{g}_{\mu\nu}, \Psi_M)\,. \tag{2.35}$$

Taking Ω as

$$\Omega^2 = F. \tag{2.36}$$

The conformal transformation then gives

$$g^{\mu\nu} = F\tilde{g}^{\mu\nu}. \tag{2.37}$$

Let us define the potential (V),

$$V = \frac{U}{F^2} = \frac{U}{\Omega^4} = \frac{FR - f}{2\kappa^2F^2}. \tag{2.38}$$

We introduce a new scalar field (ϕ) [75]

$$\kappa\phi \equiv \sqrt{3/2}\ \ln F\,. \tag{2.39}$$

Consequently,

$$\omega = \frac{1}{2}\ln F = \kappa\phi/\sqrt{6}. \tag{2.40}$$

The integral $\int^4 x\sqrt{-\tilde{g}}\,\tilde{\Box}\omega$ vanishes on account of Gauss's theorem. Then the action in the Einstein frame is

$$\mathcal{A}_E = \int^4 x\sqrt{-\tilde{g}}\left[\frac{1}{2\kappa^2}\tilde{R} - \frac{1}{2}\tilde{g}^{\mu\nu}\partial_\mu\phi\partial_\nu\phi - V(\phi)\right] + \int \mathrm{d}^4x\mathcal{L}_M(F^{-1}(\phi)\tilde{g}_{\mu\nu}, \Psi_M)\,. \tag{2.41}$$

Indeed, the action in the Einstein frame (2.41) is equivalent to the action in the Jordan frame (2.2).

2.6.1 Field Equations of Metric $f(R)$ in the Einstein Frame

One can extract the Lagrangian density $\mathcal{L}_\phi$ from (2.41) as

$$\mathcal{L}_\phi = -\frac{1}{2}\tilde{g}^{\mu\nu}\partial_\mu\phi\partial_\nu\phi - V(\phi), \tag{2.42}$$

with the energy-momentum tensor $\tilde{T}^{(\phi)}_{\mu\nu}$:

$$\tilde{T}^{(\phi)}_{\mu\nu} = -\frac{2}{\sqrt{-\tilde{g}}}\frac{\delta(\sqrt{-\tilde{g}}\mathcal{L}_\phi)}{\delta\tilde{g}^{\mu\nu}} = \partial_\mu\phi\partial_\nu\phi - \tilde{g}_{\mu\nu}\left[\frac{1}{2}\tilde{g}^{\alpha\beta}\partial_\alpha\phi\partial_\beta\phi + V(\phi)\right]. \tag{2.43}$$

To derive the generalized field equations in the Einstein frame, one takes the variation of the action (2.41) with respect to the field ϕ:

$$-\partial_\mu\left(\frac{\partial(\sqrt{-\tilde{g}}\mathcal{L}_\phi)}{\partial(\partial_\mu\phi)}\right)+\frac{\partial(\sqrt{-\tilde{g}}\mathcal{L}_\phi)}{\partial\phi}+\frac{\partial\mathcal{L}_M}{\partial\phi}=0\,, \tag{2.44}$$

If we define

$$\tilde{\Box}\phi\equiv\frac{1}{\sqrt{-\tilde{g}}}\partial_\mu(\sqrt{-\tilde{g}}\,\tilde{g}^{\mu\nu}\partial_\nu\phi)\,, \tag{2.45}$$

and then substituting $(\mathcal{L}_\phi)$ into (2.44) gives

$$\tilde{\Box}\phi-V_{,\phi}+\frac{1}{\sqrt{-\tilde{g}}}\frac{\partial\mathcal{L}_M}{\partial\phi}=0. \tag{2.46}$$

The energy-momentum tensor of matter in Einstein frame takes the form:

$$\tilde{T}^{(M)}_{\mu\nu}=-\frac{2}{\sqrt{-\tilde{g}}}\frac{\delta\mathcal{L}_M}{\delta\tilde{g}^{\mu\nu}}=\frac{T^{(M)}_{\mu\nu}}{F}\,. \tag{2.47}$$

In the case of a perfect fluid, the energy-momentum tensor $(\tilde{T}^{\mu(m)}_{\ \ \nu})$ is represented by

$$\tilde{T}^{\mu(m)}_{\ \ \nu}=\mathrm{diag}(-\tilde{\rho}_m,\tilde{P}_m,\tilde{P}_m,\tilde{P}_m)=\mathrm{diag}(-\rho_m/F^2,P_m/F^2,P_m/F^2,P_m/F^2)\,, \tag{2.48}$$

where ρ_m is the mass-energy density and P_m is the hydrostatic pressure of the fluid. One can use the chain rule to find the derivative of $\mathcal{L}_m$ with respect to ϕ,

$$\frac{\partial\mathcal{L}_m}{\partial\phi}=\frac{\delta\mathcal{L}_m}{\delta g^{\mu\nu}}\frac{\partial g^{\mu\nu}}{\partial\phi}. \tag{2.49}$$

Hence,

$$\frac{\partial\mathcal{L}_M}{\partial\phi}=\frac{1}{F(\phi)}\frac{\delta\mathcal{L}_M}{\delta g^{\mu\nu}}\frac{\partial(F(\phi)g^{\mu\nu})}{\partial\phi}=-\sqrt{-g}\,\frac{F_{,\phi}}{2F}\,T^{(M)}_{\mu\nu}g^{\mu\nu}\,. \tag{2.50}$$

Inserting the expression for the energy-momentum tensors (2.47) yields:

$$\frac{\partial\mathcal{L}_M}{\partial\phi}=-\sqrt{-g}\,\frac{F_{,\phi}}{2F}\,T^{(M)}_{\mu\nu}g^{\mu\nu}\,. \tag{2.51}$$

A coupling parameter Q between the matter and the field can be introduced as in [75]

$$Q\equiv-\frac{F_{,\phi}}{2\kappa F}=-\frac{1}{\sqrt{6}}\,. \tag{2.52}$$

Finally,

$$\frac{\partial\mathcal{L}_m}{\partial\phi}=\sqrt{-\tilde{g}}\,\kappa Q\tilde{T}\,, \tag{2.53}$$

where $\tilde{T} = \tilde{g}_{\mu\nu}\tilde{T}^{\mu\nu(m)} = -\rho_m + 3P_m$. Substituting (2.53) into (2.46), we obtain the field equation in the Einstein frame:

$$\tilde{\Box}\phi - V_{,\phi} + \kappa Q\tilde{T} = 0\,. \tag{2.54}$$

2.7 The cosmology of metric $f(R)$ gravity

In this section we discuss the implications of adding non-linear terms to the Ricci scalar in the (E-H) action on the cosmological evolution of the theory. We demonstrate the effective equation of state for metric $f(R)$ in two different parametrizations, although we stress that the observable quantity is the total equation of state, not the effective one. Actually, the parametrization of effective equation of state depends on the way we cast the generalized field equations (2.24). In the first method we have a non-minimal coupling between the matter field and the geometry through the term $1/f'(R)$. The generalized field equations take the form

$$G_{\mu\nu} = R_{\mu\nu} - \frac{1}{2}g_{\mu\nu}R = T^{(eff)}_{\mu\nu} + \frac{T^m_{\mu\nu}}{f'(R)}, \tag{2.55}$$

with

$$T^{(eff)}_{\mu\nu} = \frac{1}{f'(R)}[\frac{f(R) - Rf'(R)}{2}g_{\mu\nu} + (\nabla_\mu\nabla_\nu - g_{\mu\nu}\Box)f'(R)]. \tag{2.56}$$

The field equations can be manipulated to get rid of the non-minimal coupling. By this manipulation, we have a minimal coupling between the matter and the geometry. The generalized field equations in this approach takes the form,

$$G_{\mu\nu} = T^m_{\mu\nu} + \tilde{T}^{(eff)}_{\mu\nu}, \tag{2.57}$$

with

$$\tilde{T}^{(eff)}_{\mu\nu} = \frac{f(R) - Rf'(R)}{2}g_{\mu\nu} + (\nabla_\mu\nabla_\nu - g_{\mu\nu}\Box)f'(R) + (1 - f'(R))G_{\mu\nu}. \tag{2.58}$$

In our study we adopt a flat Friedmann-Lemaître-Robertson-Walker (FLRW) metric to describe a universe filled with a perfect fluid. The field equations of metric $f(R)$ gravity then take the form

- **Raychaudhuri equation:**

$$\begin{aligned} 2\dot{H}+3H^2 &= -\frac{1}{f'}[P^{(m)}+\frac{f-f'R}{2}+2Hf''\dot{R} \\ &+ f'''\dot{R}^2+f''\ddot{R}]; \end{aligned} \tag{2.59}$$

- **Friedmann equation :**

$$3H^2=\frac{1}{f'}[\rho+\frac{Rf'-f}{2}-3Hf''\dot{R}]; \tag{2.60}$$

- **Trace equation:**

$$3\ddot{R}f''=\rho-3P+f'R-2f-9Hf''\dot{R}-3f'''\dot{R}^2, \tag{2.61}$$

- **Energy Conservation equation :** The energy conservation equation for a standard matter takes the form

$$\dot{\rho}=-3H(1+\omega)\rho\ , \tag{2.62}$$

If we combine both the Raychaudhuri equation (5.17) and the Friedmann equation (5.18), we obtain the usual definition of the Ricci scalar in flat (FLRW)

- **Ricci scalar equation:**

$$R=6(\dot{H}+2H^2). \tag{2.63}$$

Cosmic speed-up can be achieved if we guarantee that the right hand side of the acceleration equation remains positive [97]. Equivalently,

$$\frac{\ddot{a}}{a}=\frac{-4\pi G}{3}(\rho_{tot}+3P_{tot}). \tag{2.64}$$

Now we introduce the first parametrization of the effective equation of state in which we begin from the field equations described by (5.66). The curvature density and pressure take the form

$$\rho_{curv}=\frac{1}{f'}[\frac{1}{2}(f-Rf')-3H\dot{R}f''], \tag{2.65}$$

$$P_{curv}=\frac{1}{f'}[2H\dot{R}f''+\ddot{R}f''+\dot{R}^2f'''+\frac{1}{2}(f-Rf')], \tag{2.66}$$

and finally the effective (curvature) EOS becomes

$$w_{curv} = -1 + \frac{\ddot{R}f'' + \dot{R}(\dot{R}f''' - Hf'')}{\frac{1}{2}(f - Rf') - 3H\dot{R}f''}. \tag{2.67}$$

Regarding the second parametrization of the effective equation of state in which we start from (5.67), the curvature energy density, the pressure and the effective EoS have the form

$$\begin{aligned} \rho_{curv} &= 3H^2 - \rho_{total}, \\ &= -3(1-f')(\dot{H}+H^2) + \frac{R-f}{2} - 3H\dot{f}', \\ &= \frac{f(R) - Rf'(R)}{2} - 3H\dot{f}' + 3H^2(1-f'), \end{aligned} \tag{2.68}$$

$$\begin{aligned} P_{curv} &= H^2 - \frac{R}{3} - P_r, \\ &= \ddot{f}' + 2H\dot{f}' + \frac{f(R) - Rf'(R)}{2} + (H^2 - \frac{R}{3})(1-f'), \end{aligned} \tag{2.69}$$

and

$$w_{curv} = \frac{P_{curv}}{\rho_{curv}}. \tag{2.70}$$

2.8 The viability of metric $f(R)$ gravity

2.8.1 Correct cosmological dynamics

Part of the success of the ΛCDM model with an inflationary epoch at the early time is due to expecting the logical successive cosmological epochs over which the universe has evolved. So, according to the ΛCDM model, the universe begins with an intensive accelerated expansion epoch (inflation) followed by a radiation epoch, and then by a matter dominated epoch in which large scale structure (LSS) can grow, followed by the present accelerated expansion era. The transition between these epochs must be smooth. We think that any viable $f(R)$ theory of gravity should identify the same expansion history in the same order.

2.8.2 Ricci Stability in metric $f(R)$

The $f(R)$ model given by $f(R) = R - \frac{\mu^4}{R}$ suffers from Dolgov-Kawasaki instability [98], sometimes referred to Dolgov-Kawasaki by Ricci instability or matter instability. This instability has proven to be sufficient to rule out any model having it. In order to

generalize this study to arbitrary $f(R)$ theories, we follow [99]. The deviations from (GR) can be written as

$$f(R) = R + \epsilon\phi(R), \tag{2.71}$$

where ϵ is a small parameter, and $\phi(R)$ is arranged to be dimensionless. Then the trace equation (2.25) gives

$$\Box R + \frac{\phi'''}{\phi''}\nabla^c R \nabla_c R + (\frac{\epsilon\phi' - 1}{3\epsilon\phi''})R = \frac{\kappa T}{3\epsilon\phi''} + \frac{2\phi}{3\phi''}. \tag{2.72}$$

For a small region of spacetime in the weak field regime and expand locally the metric and Ricci scalar by

$$g_{\mu\nu} = \eta_{\mu\nu} + h_{\mu\nu} \quad R = -\kappa T + R_1, \tag{2.73}$$

where $\eta_{\mu\nu}$ is the Minkoswki metric and $h_{\mu\nu}$ and R_1 are perturbations. Equation (2.73) yields, to first order in R_1,

$$\begin{aligned} \ddot{R_1} - \nabla^2 R_1 - \frac{2\kappa\phi'''}{\phi''}\dot{T}\dot{R_1} + \frac{2\kappa\phi'''}{\phi''}\overrightarrow{\nabla}T.\overrightarrow{\nabla}R1 \\ + \frac{1}{3\phi''}(\frac{1}{\epsilon} - \phi')R1 = \kappa\ddot{T} - \kappa\nabla^2 T - \frac{(\kappa T\phi^2 + 2\phi)}{3\phi''}, \end{aligned} \tag{2.74}$$

where $\overrightarrow{\nabla}$ and ∇^2 are the gradient and Laplacian in Euclidean three-dimensional space, respectively, and overdot denotes differentiation with respect to time. The coefficient of R_1 in the fifth term on the left hand side of (2.74) yields the effective mass squared $m^2 = \frac{1}{2\epsilon\phi''}$. The scalar degree of freedom is stable if $\phi'' = f'' > 0$ and unstable if this effective mass is negative; i.e., if $\phi'' = f'' < 0$. This stability analysis may be physically interpreted in the following: the effective gravitational coupling is $G_{eff} = G/f'(R) > 0$. If $\frac{dG_{eff}}{dR} = \frac{-f''G}{(f')^2} > 0$, then gravity becomes stronger as R increases. Conversely, if $\frac{dG_{eff}}{dR} < 0$ then G_{eff} does not increase as the curvature increases and there is a stability [100].

2.8.3 Weak-field Limit in metric $f(R)$ gravity

The idea is to compute the the parametrized post-Newtonian (PPN) parameter $\gamma = \frac{-\Psi(r)}{\Phi(r)}$ through the PNN expansion of the line element

$$\begin{aligned} ds^2 &= -[1 + 2\Psi(r) - H_0^2 r^2]dt^2 \\ &+ [1 + 2\Phi(r) + H_0^2 r^2]dr^2 + r^2(d\theta^2 + \sin^2\theta d\phi^2), \end{aligned} \tag{2.75}$$

in Schwarzschild coordinates, where $\mid \Psi(r) \mid, \mid \Phi(r) \mid \ll 1$, $H_0 r \ll 1$, and $R(r) = R_0 + R_1$. We make the following assumptions:

- Assumption 1: $f(R)$ is analytical at R_0
- Assumption 2: $mr \ll 1$, where m is the effective mass of the scalar degree of freedom. In other words, Ricci curvature must have a range longer than the size of the solar system [90].
- Assumption 3: The pressure $P \simeq 0$ for the energy-momentum of local star-like objects.

The trace of the corresponding energy-momentum tensor reduces to $T \simeq -\rho$. The trace equation (2.25) reduces to

$$\nabla^2 R_1 - m^2 R_1 = -\frac{\kappa\rho}{3f_0''}, \tag{2.76}$$

where

$$m^2 = \frac{(f_0')^2 - 2f_0 f_0''}{3f_0' f_0''}. \tag{2.77}$$

If $mr \ll 1$, the solution is [90]

$$\Psi(r) \simeq \frac{-\kappa M}{6\pi f_0' r}, \quad \Phi(r) \simeq \frac{\kappa M}{12\pi f_0' r}, \tag{2.78}$$

and hence the parametrized post-Newtonian (PNN) parameter (γ) gives

$$\gamma = \frac{-\Psi(r)}{\Phi(r)} = \frac{1}{2}. \tag{2.79}$$

This is a big violation of the Cassini limit $\mid \gamma - 1 \mid < 2.3 \times 10^{-5}$ [101].

2.8.4 The Cauchy Problem

A viable physical theory must have a predictive power and hence, a well-posed initial value problem is necessary. The Cauchy problem in the context of $f(R)$ gravity was studied in [64, 102]. The initial value problem for metric $f(R)$ gravity is well-posed in "vacuum" and with matter.

2.9 Concluding Remarks

This chapter consisted of an introduction to the Extended Theories of Gravity (ETG) and a more specific subclass; that is, metric $f(R)$ gravity. We included the early motivations for modifying Einstein's theory of gravity. Although we confined our attention to metric $f(R)$ gravity theory, we introduced a version of the theory in the Einstein's frame using a defined conformal transformation. We then introduced the cosmology from the perspective of metric $f(R)$ gravity theory. In a brief sections, We spotted some light on both the viability and the weak field limits of the metric $f(R)$ gravity theories.

Chapter 3

Introduction to Dynamical Systems

In this chapter we study some aspects of dynamical systems theory. Most of the tools which are discussed here will be used in chapter 5. Applying the dynamical systems approach to study modified theories of gravity has proven to be fruitful [103–105]. Among the various merits of the dynamical systems approach is that finding the analytical solutions for the modified cosmological field equations at the equilibrium points is possible. In this thesis, we focus on studying the autonomous systems of the differential equations. We define autonomous systems as the systems in which the time variable does not explicitly appear in the differential equation(s) describing the system.

3.1 Dynamical Systems

Before we started let us briefly explain what is meant by dynamical systems: Dynamical systems can be anything ranging from something as simple as a single pendulum to something as complex as the human brain and the entire universe itself. A mathematical dynamical system has two parts

- a state vector
- a function

The state vector describes the state of some real or hypothetical system, while function (i.e. a rule) tells us, given the current state, what the state of the system will be in the next instant of time. There are two main types of dynamical systems; the first one

is the continuous dynamical systems whose evolution is defined by ordinary differential equations (ODEs) and the other is called time-discrete dynamical systems which are defined by a map or difference equations. In this thesis the systems under investigation are called autonomous systems which fall under the category of continuous dynamical systems. The standard form of a dynamical system is usually expressed as [106],

$$\dot{\mathrm{x}} = \mathrm{f(x)}, \tag{3.1}$$

where x ∈ X i.e. x is an element in state space X ⊂ $\mathbb{R}^n$, and $f : \mathrm{X} \to \mathrm{X}$. The function $\mathrm{f} : \mathbb{R}^n \to \mathbb{R}^n$ is a vector field on $\mathbb{R}^n$ such that

$$\mathrm{f(x)} = (f_1(x), ..., f_n(x)), \tag{3.2}$$

and $\mathrm{x} = (x_1, x_2, ..., x_n)$. These ODEs define the vector fields of the system. At any point x ∈ X and any particular time t, f(x) defines a vector field in $\mathbb{R}^n$. As far as this thesis is concerned, the systems under investigation are finite dimensional and continuous autonomous systems.

Definition 3.1 (Critical point)**.** The autonomous equations $\dot{x} = f(x)$ is said to have a critical point or fixed point at $x = x_0$ if and only if $f(x_0) = 0$.
The stability/instability of a fixed point may be categorised as following: A critical point $(x, y) = (x_0, y_0)$ is stable (also called Lyapunov stable) if all solutions x(t) starting near it stay close to it, and attracting fixed point if it is stable and the solutions approach the critical point for all nearby initial conditions. If the point is unstable then solutions will escape away from it. The stability/instability of the fixed points may also be revealed by means of linearisation.

3.2 Linear Theory of Stability

Let x^* be a fixed point, and let $\eta(t) = x(t) - x^*$ be a small perturbation away from x^*. Differentiation η with respect to time yields

$$\dot{\eta} = \frac{d}{dt}(x - x^*) = \dot{x}, \tag{3.3}$$

since x^* is constant. Thus $\dot{\eta} = \dot{x} = f(x) = f(x^* + \eta)$. Now using Taylor's expansion gives

$$f(x^* + \eta) = f(x^*) + \eta f'(x^*) + \mathcal{O}(\eta^2), \tag{3.4}$$

where $\mathcal{O}(\eta^2)$ denotes quadratically small terms in η. Since $f(x^*) = 0$, as x^* is a fixed point.

$$\dot{\eta} = \eta f'(x^*) + \mathcal{O}(\eta^2). \tag{3.5}$$

Now if $f'(x^*) \neq 0$, the $\mathcal{O}(\eta^2)$ terms are negligible and we may write the approximation

$$\dot{\eta} = \eta f'(x^*). \tag{3.6}$$

This a linear equation in η , and is called the **linearisation about** x^* [5]. In this set-up, the critical point x^* can be deduced as

- stable if $f'(x^*) < 0$,
- unstable if $f'(x^*) > 0$,
- if $f'(x^*) = 0$, the $\mathcal{O}(\eta^2)$ are not negligible and a non-linear analysis is needed to determine stability.

In the above we treated a 1D system. For higher dimensional systems, eigenvalues of the Jacobi matrix of the system evaluated at critical points reveal information regarding critical points stabilities. Given a dynamical system $\dot{x} = f(x,t)$ with a fixed point at $x = x_0$, the system is linearised about its critical point by

$$\mathcal{M} = Df(x_0) = (\frac{\partial f_i}{\partial x_j})_{x=x_0}, \tag{3.7}$$

where the matrix $\mathcal{M}$ is called Jacobi matrix.
For example, a simple 2D autonomous system, may be given by

$$\begin{aligned} \dot{x} &= f(x,y), \\ \dot{y} &= g(x,y). \end{aligned} \tag{3.8}$$

where f and g are functions of x and y, with critical point at ($x = x_0$,$y = y_0$). The Jacobi matrix constructed to linearise the system about its critical point would then be

$$\mathcal{M} = \begin{pmatrix} \partial_x f & \partial_y f \\ \partial_x g & \partial_y g \end{pmatrix}.$$

We refer to the eigenvalues of $\mathcal{M}$ with λ_1 and λ_2. The eigenvalues of this matrix linearised about the critical point in question reveal the stability/instability of that point provided that the point is hyperbolic.

Definition 3.2. Let $x = x_0$ be a fixed point (critical point) of the system $\dot{x} = f(x)$, $x \in \mathbb{R}^n$. Then x_0 is said to be hyperbolic if none of the eigenvalues $Df(x_0)$ have zero real part, and non-hyperbolic otherwise [106].

Linear stability theory valid as long as the point is hyperbolic, otherwise the linear stability fails and therefore alternative techniques such as finding Lyapunov's functions or applying centre manifold theory are required.

Assuming a general 2D system with two eigenvalues λ_1 and λ_2, the possibilities regarding the stability of the critical point with respect to the trace $\tau = \lambda_1 + \lambda_2$ and the determinant $\Delta = \lambda_1 \times \lambda_2$ of the matrix $\mathcal{M}$ are as follows:

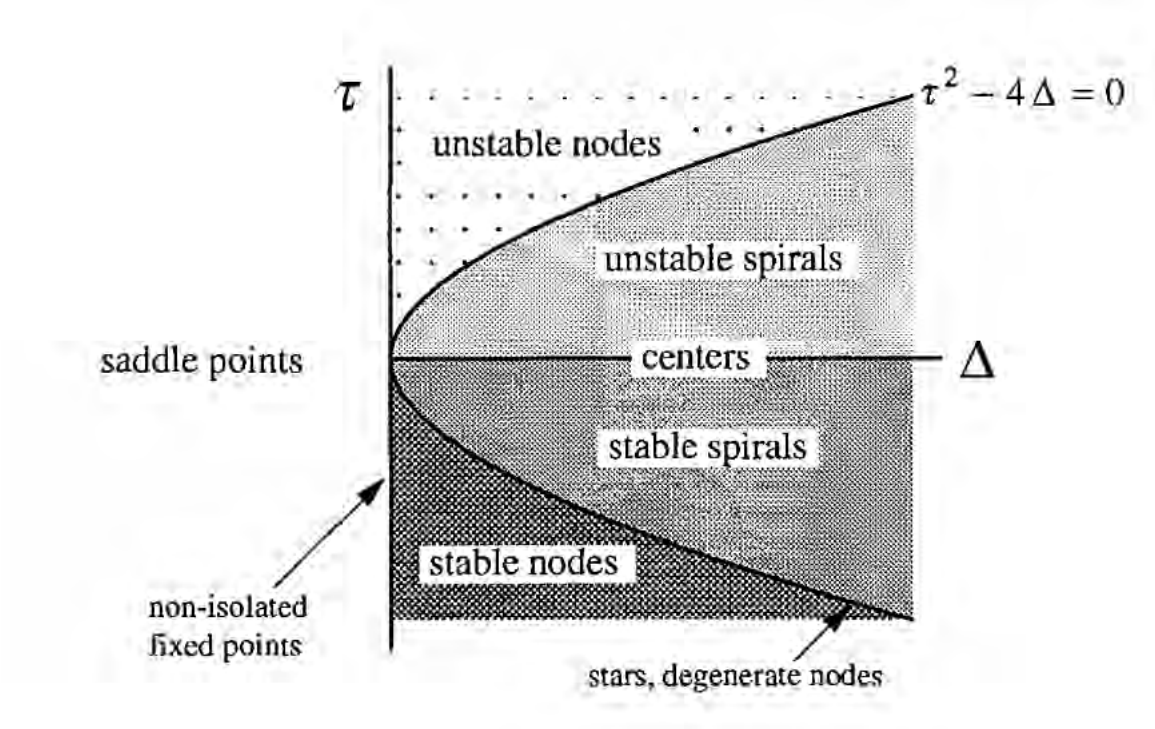

FIGURE 3.1: A depiction to the classifications and the stability of the hyperbolic fixed points [5].

Again, lets point out that all of the information in Fig [3.1] is implied by the following expressions:

$$\lambda_{1,2} = \frac{1}{2}(\tau \pm \sqrt{\tau^2 - 4\Delta}), \quad \Delta = \lambda_1 \times \lambda_2, \quad \tau = \lambda_1 + \lambda_2. \tag{3.9}$$

If $\Delta < 0$, the eigenvalues are real and have opposite signs; hence the fixed point is a **saddle point**.

If $\Delta > 0$, the eigenvalues are either real with the same sign **nodes**, or complex conjugate (**spirals** and **centres**). Nodes satisfy $\tau^2 - 4\Delta > 0$ and spirals satisfy $\tau^2 - 4\Delta < 0$. The parabola $\tau^2 - 4\Delta = 0$ is the border line between nodes and spirals; star nodes and

degenerate nodes live on this parabola.
The stability of the nodes and spirals is determined by τ. When $\tau < 0$, both eigenvalues have negative real parts, and hence the fixed point is stable. Unstable nodes and spirals have $\tau > 0$. Neutrally stable centres live on the borderline $\tau = 0$, where the eigenvalues are purely imaginary. If $\Delta = 0$, at least one of the eigenvalues is zero. Then the origin is an isolated fixed point. In case of $\mathcal{M} = 0$, there is either a whole line of fixed points or a plane of fixed points.

3.3 Lyapunov's Function

Lyapunov's functions, named after the Russian mathematician Aleksandr Mikhailovich Lyapunov, allow us to establish the stability or instability of the system. The advantage of this method is that we do not need to know the actual solution X(t). In addition, this method allows to study the stability of equilibrium points of non-rough systems, for example, in the case when the equilibrium point is a center. Traditionally, Lyapunov's functions have played a key role in control theory, but there has also been some work in which it has been applied in cosmological contexts [107–109].

Definition 3.3 (Lyapunov's function)**.** Consider a system $x = f(x)$ with a fixed point at x^*. Suppose that we can find a Lyapunov function, i.e. a continuously differentiable, real-valued function V(x) with the following properties:

1. $V(x) > 0$ for all $x \neq x^*$, and $V(x^*) = 0$. (We say that V is positive definite.)
2. $\dot{v} < 0$ for all $x \neq x^*$. (All trajectories flow "downhill" toward x^*.)

Unfortunately, there is no systematic way to construct Lyapunov functions. Conjecture is usually required, although sometimes one can work backwards. Thus, if we could not construct a Lyapunov function for a critical point, that does not necessarily imply that such point is unstable.

Theorem 3.4 (lyapunov stability)**.** *let x^* be a critical point of the system $x = f(x)$, where $f : U \to \mathbb{R}^n$ and $U \subset \mathbb{R}^n$ is a domain that contains x^*. If V is a Lyapunov function, then*

1. *If $\dot{V} = \frac{\partial V}{\partial x}$ is negative semi-definite, then $x = x^*$ is a stable fixed point,*
2. *If $\dot{V} = \frac{\partial V}{\partial x}$ is negative definite, then $x = x^*$ is a asymptotically stable fixed point.*

Furthermore, if $\| x \| \to \infty$ and $V(x) \to \infty \ \forall x$, then x_0 is said to be globally stable or globally asymptotically stable, respectively. The intuition is that all trajectories move monotonically down the graph of V(x) toward x_0 Fig [3.2]. The solutions can not get stuck anywhere else because if they did, V would stop changing, but by assumption, $\dot{v} < 0$ everywhere except at x_0.

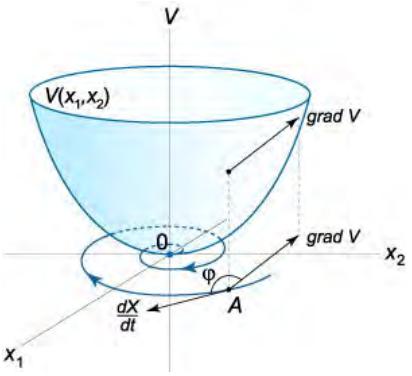

FIGURE 3.2: the trajectories moving toward the fixed point which is the same as origin point [6].

3.3.1 An example of proving the stability of a critical point by finding a corresponding Lyapunov's function

In the following example we investigate the stability of the fixed point $(0, 0)$ of the system,

$$\frac{dx}{dt} = -2x, \quad \frac{dy}{dt} = x - y. \tag{3.10}$$

The system is a linear homogeneous with constant coefficients. We take as a Lyapunov function the quadratic form

$$V(x, y) = ax^2 + by^2, \tag{3.11}$$

where the coefficients a and b are to be determined.
Obviously, the function $V(x, y)$ is positive everywhere except at the origin, where it is zero. We calculate the total derivative of the function $V(x, y)$:

$$\frac{dV}{dt} = \frac{\partial V}{\partial x}\frac{\partial x}{\partial t} + \frac{\partial V}{\partial y}\frac{\partial y}{\partial t} = -2b(\frac{2a}{b}x^2 - xy + y^2). \tag{3.12}$$

The expression in the brackets can be converted to a square of the difference if the following condition is satisfied:

$$\frac{2a}{b} = \frac{1}{4} \quad or \quad 8a = b. \tag{3.13}$$

We can take any suitable combination, for example, we set a = 1, b = 8. Then the derivative becomes

$$\frac{dV}{dt} = -16(\frac{x}{2} - y)^2 < 0. \tag{3.14}$$

Thus, for the given system, there is a Lyapunov function, and its derivative is negative everywhere except at the origin. Hence, the zero solution of the system is asymptotically stable (stable node).

3.4 Centre manifold theory

Centre manifold theory and normal forms are considered as the most applicable methods in the local theory of dynamical systems. Specifically, Centre Manifold Theory allows us to simplify the dynamical systems by reducing their dimensionality. It is also important in the study of bifurcations. Another technique that can also be applied to simplify the dynamical systems is the method of normal forms which eliminates the non-linearity of the system. The eigenspace with corresponding eigenvalues that have zero real parts reveals little information about the system. As a result, where there is a zero eigenvalue resulting from the Jacobi matrix, the corresponding critical point is non-hyperbolic and the structural stability is no longer guaranteed. Thus, it is necessary to investigate further by, for example, applying the centre manifold theory.
In most of our discussion on Centre Manifold Theory, we follow [106].
Let a dynamical system be represented by the vector fields as followings:

$$\begin{aligned} \dot{x} &= Ax + f(x, y), \\ \dot{y} &= By + g(x, y), \quad (x, y) \in \mathbb{R}^c \times \mathbb{R}^s, \end{aligned} \tag{3.15}$$

where

$$\begin{aligned} f(0, 0) &= 0, \quad Df(0, 0) = 0, \\ g(0, 0) &= 0, \quad Dg(0, 0) = 0, \end{aligned} \tag{3.16}$$

are C^r functions.
In the system (3.15), A is a $c \times c$ matrix possessing eigenvalues with zero real parts, while B is an $s \times s$ matrix whose eigenvalues have negative real parts. The aim is to

compute the centre manifold of these vector fields so as to investigate the dynamics of the system.

Definition 3.5 (Centre Manifold)**.** An invariant manifold will be called a centre manifold for (3.15) if it can be locally represented as

$$\mathrm{W}^c = \{(x, y) \in \mathbb{R}^c \times \mathbb{R}^s \mid y = h(x), \mid x \mid < \delta, h(0) = 0, Dh(0) = 0\}, \tag{3.17}$$

for δ sufficiently small. The conditions $h(0) = 0$ and $Dh(0) = 0$ from the definition imply that $\mathrm{W}^c(0)$ is tangent to the eigenspace E^c at the critical point $(x, y) = (0, 0)$. In applying the centre manifold theory, three main theorems [106], each for existence, stability and approximation, have been assumed without proof.

Theorem 3.6 (Existence)**.** *There exist a* C^r *centre manifold for [106]. Its dynamics restricted to the centre manifold is given by*

$$\dot{u} = Au + f(u, h(u)), \quad u \in \mathbb{R}^c \tag{3.18}$$

for u sufficiently small.

Theorem 3.7 (Stability)**.** *Suppose the zero solution of (3.18) is stable (asymptotically stable) (unstable); then the zero solution of (3.18) is also stable (asymptotically stable) (unstable). Furthermore, if (x(t), y(t)) is also a solution of (3.18) with (x(0), y(0)), there exists a solution u(t) of (3.18) such that*

$$x(t) = u(t) + \mathcal{O}(e^{-\gamma t}), \tag{3.19}$$

$$y(t) = h(u(t)) + \mathcal{O}(e^{-\gamma t}), \tag{3.20}$$

as $t \to \infty$*, where* $\gamma > 0$ *is a constant and for sufficiently small* $(x(0), y(0))$*.*

In order to proceed to compute the centre manifold and before stating or considering the third theorem, an equation that $h(x)$ must satisfy, in order that its graph to be a centre manifold for (3.15), needs to be derived. Its explicit derivation is as following. First, by the chain rule, differentiating $y = h(x)$ gives

$$\dot{y} = Dh(x)\dot{x}, \tag{3.21}$$

and is satisfied by any $(\dot{x}, \dot{y})$ coordinates of any point on $\mathrm{W}^c(0)$ since (x, y) coordinates of any point on it must have satisfied $y = h(x)$. Furthermore, $\mathrm{W}^c(0)$ obeys the dynamics generated by the system (3.15).

Substituting

$$\begin{aligned} \dot{x} &= Ax + f(x, h(x)), \\ \dot{y} &= By + g(x, h(x)), \end{aligned} \tag{3.22}$$

into (3.21) gives

$$Dh(x)[Ax + f(x, h(x))] = Bh(x) + g(x, h(x)), \tag{3.23}$$

this is to be re-arranged in a quasilinear partial differential equation $\mathcal{N}$ given by

$$\mathcal{N} \equiv Dh(x)[Ax + f(x, h(x))] - Bh(x) + g(x, h(x)) = 0, \tag{3.24}$$

and must be satisfied by $h(x)$ so as to ensure its graph to be an invariant manifold. Finally the following third and last theorem is assumed in computing the approximate solution of (3.24).

Theorem 3.8 (Approximation)**.** *Let $\phi : \mathbb{R}^c \to \mathbb{R}^s$ be a C^1 mapping with $\phi(0) = D\phi(0) = 0$ such that $\mathcal{N}(\phi(x)) = \mathcal{O}(\mid x \mid^q)$ as $x \to 0$ for some $q > 1$.*
Then

$$\mid h(x) - \phi(x) \mid = \mathcal{O}(\mid x \mid^q) \quad as \quad x \to 0 \tag{3.25}$$

The advantage of this theorem is that one can compute the centre manifold which would return the same degree of accuracy as solving (3.24) but without the need to face the difficulties associated with doing it. The proofs of these theorems can be found in Carr [110].

3.4.1 An example of application of centre manifold theory: a simple two-dimensional case

The following example can be found in [106]. Let's consider a vector field given by the system,

$$\begin{aligned} \dot{x} &= x^2 y - x^5, \\ \dot{y} &= -y + x^2, \quad (x, y) \in \mathbb{R}^2. \end{aligned} \tag{3.26}$$

The system has a fixed point at the origin. Now we investigate how the centre manifold theory will help in determining the stability of that fixed point. The linearisation technique fails because the eigenvalues of (3.26) linearised about $(x, y) = (0, 0)$ are 0 and

-1, in other words the fixed point is not hyperbolic. From Theorem(3.18), there exists a centre manifold for (3.26) which can locally be represented as follows

$$\mathrm{W}^c = \{(x, y) \in \mathbb{R}^c \times \mathbb{R}^s \mid y = h(x), \mid x \mid < \delta, h(0) = 0, Dh(0) = 0\}, \tag{3.27}$$

for δ sufficiently small. We now want to compute $\mathrm{W}^c(0)$. We assume that h(x) to be of the form

$$h(x) = ax^2 + bx^3 + \mathcal{O}(x^4), \tag{3.28}$$

substitute (3.28) into (3.24), which $h(x)$ must satisfy to be a centre manifold. We then equate equal powers of x, and in that way we can compute $h(x)$ to any desire order of accuracy.
From (3.24) the equation for the centre manifold is given by

$$\mathcal{N}(h(x)) = Dh(x)[Ax + f(x, h(x))] - Bh(x) - g(x, h(x)) = 0, \quad (x, y) \in \mathbb{R}^2. \tag{3.29}$$

In this example,

$$\begin{aligned} A &= 0, \\ B &= -1, \\ f(x, y) &= x^2 y - x^5, \\ g(x, y) &= x^2. \end{aligned} \tag{3.30}$$

Substituting (3.28) into (3.29) and using (3.30) gives

$$\begin{aligned} \mathcal{N}(h(x)) &= (2ax + 3bx^2 + ...)(ax^4 + bx^5 - x^5 + ...) \\ &+ ax^2 + bx^3 - x^2 + ... = 0. \end{aligned} \tag{3.31}$$

The coefficients of each power of x must be zero so that (3.31) holds. Then coefficients of each power of x are equated to zero, so that for x^2 and x^3,

$$\begin{aligned} a &= 1, \\ b &= 0, \end{aligned} \tag{3.32}$$

respectively and the higher powers are ignored. Therefore,

$$h(x) = x^2 + \mathcal{O}(x^4). \tag{3.33}$$

Finally, as per theorem (3.18), the dynamics of the system restricted to the centre manifold is obtained to be

$$\dot{x} = x^4 + \mathcal{O}(x^5). \tag{3.34}$$

By studying (3.34), it can be concluded that for x sufficiently small, $x = 0$ is unstable. Therefore, the critical point $(0, 0)$ is unstable.

3.5 Concluding Remarks

This chapter is dedicated to the basics of linear dynamical systems theory, and to introduce techniques which can be used to study the local qualitative behaviour of non linear systems. The linearisation technique can be used to study the local features of hyperbolic equilibrium points of non-linear systems, and the Center Manifold Theorem states that the behaviour near a non hyperbolic fixed point is completely described by the flow on the center manifold at that point. The research presented in Chapter 5 uses the theory outlined in this chapter to study the cosmological dynamics of a fourth order gravity model .i.e, $R \ln R$ and to obtain a qualitative appreciation of the properties of its phase space. In particular, we make use of the Center Manifold Theorem to analyse the local behaviour of the stationary points of the non-linear system which represents the modified cosmological field equations of the model $R \ln R$.

Chapter 4

Dynamical Systems Approach to Cosmology

4.1 Introduction

In the previous chapter, we discussed the theory of dynamical systems and some of its powerful tools. The main purpose of the dynamical systems theory is to model any physical problem in terms of a system of differential equations. Dynamical systems theory is of great importance to cosmology as it helps construct a lucid qualitative understanding to the dynamics of the universe as a whole. Furthermore, analysing the fixed points according to the dynamical systems theory provides us with a better insight to both the history and the present of the universe, as well as to anticipate its fate. The motivation is to rewrite Einstein's field equations for cosmological models in terms of a system of autonomous first-order ODEs, thereby modelling them as a dynamical system in $\mathbb{R}^n$ [111]. Up to now, there has been much progress made in the application of dynamical systems to cosmology, see for example [103–105, 112]. From a dynamical systems perspective, a successful cosmological model should meet the following requirements:

1. There has to be an early time expansion (inflation), an unstable state, thereby it enables the universe to evolve away from that point.

2. An epoch of matter domination is necessary otherwise the universe would not witness any large scale structure formation.

3. A global attractor is needed to resemble the current state of the universe which, according to observational data, is undergoing accelerated expansion and asymptotically approaching de Sitter space.

4.2 Constructing Dynamical Systems approach for Friedmann-Lemaître models

In the following discussion, we closely follow [7]. We adopt a FLRW metric to describe the geometry of the universe, and we assume that the universe is filled with a perfect fluid, with an equation of state $P = w\rho$, where w is the equation of state which admits $-1 \leq w \leq 1$. The field equations become

The Friedmann equation:

$$H^2 = \frac{8\pi G}{3}\rho + \frac{\Lambda}{3} - \frac{k}{a^2}. \tag{4.1}$$

The Raychaudhuri equation:

$$\frac{\ddot{a}}{a} \equiv -qH^2 = -\frac{3w+1}{6}\rho + \frac{1}{3}\Lambda. \tag{4.2}$$

The energy conservation equation:

$$\dot{\rho} = -3H(1+w)\rho. \tag{4.3}$$

Assuming $H \neq 0$, we proceed by defining dimensionless variables according to[1]

$$\Omega_k = \frac{k}{a^2H^2}, \quad \Omega = \frac{\rho}{3H^2}, \quad \Omega_\Lambda = \frac{\Lambda}{3H^2}. \tag{4.4}$$

The density parameter Ω is related to Ω_k and Ω_Λ by

$$\Omega = 1 + \Omega_k - \Omega_\Lambda, \tag{4.5}$$

while the deceleration parameter is given by (4.2)

$$\begin{aligned} q &= \frac{3w+1}{2}\Omega - \Omega_\Lambda, \\ &= \frac{3w+1}{2}(1+\Omega_k) - \frac{3(1+w)}{2}\Omega_\Lambda. \end{aligned} \tag{4.6}$$

The weak energy condition together with $\Lambda \geq 0$ immediately give:

$$0 \leq \Omega, \quad -1 \leq \Omega_k, \quad 0 \leq \Omega_\Lambda. \tag{4.7}$$

[1] In [112], the curvature variable Ω_k was defined with opposite sign.

In addition, for models with non-positive spatial curvature k, these quantities are compact .i.e, the range is contained in a compact interval:

$$0 \leq \Omega \leq 1, \quad -1 \leq \Omega_k \leq 0, \quad 0 \leq \Omega_\Lambda \leq 1. \tag{4.8}$$

Defining a new normalized time variable ($' = \frac{1}{H}\frac{d}{dt}$), we obtain

$$\begin{aligned} \Omega' &= [2q - (3w+1)]\,\Omega, \\ {\Omega_k}' &= 2\Omega_k q, \\ \Omega'_\Lambda &= 2(1+q)\Omega_\Lambda. \end{aligned} \tag{4.9}$$

along with a decoupled differential equation for the Hubble expansion rate:

$$H' = -(1+q))H, \tag{4.10}$$

The H' equation (4.10) can be employed to reduce the dimensionality of the autonomous system, thereby the system becomes two-dimensional instead of three. The new system is written as follows:

$$\begin{aligned} \Omega'_k &= 2\Omega_k(\frac{3w-2}{2}(1+\Omega_k) - \frac{3w}{2}\Omega_\Lambda), \\ \Omega'_\Lambda &= 2\Omega_\Lambda(1 + \frac{3w-2}{2}(1+\Omega_k) - \frac{3w}{2}\Omega_\Lambda). \end{aligned} \tag{4.11}$$

The system (4.11) admits a number of invariant submanifolds such as $\Omega = 0$, $\Omega_\Lambda = 0$ and $\Omega_k = 0$. The finite analysis shows that the fixed points lie at the intersection of these invariant submanifolds. The fixed points alongside their classification and stability are presented below in table [4.1]

Point	Coordinates $(\Omega_k, \Omega_\Lambda, \Omega, q)$	Stability		Solution
		$-1 < w < -1/3$	$-1/3 < w < 1$	
F	$(0,0,1,\frac{3w+1}{2})$	saddle	source	flat Friedmann solution
M	(-1,0,0,0)	source	saddle	Milne solution
ds	(0,1,0,-1)	attractor	attractor	de Sitter solution

TABLE 4.1: Summary of the fixed points and their stability, with the type of solution at each fixed point.

The fixed points in Table [4.1] are produced from a compacatified space with ($\Omega_k \leq 0$). The primary advantage of a dynamical system with compact space is analysing the stability and the behaviour of fixed points at infinity. In order to benefit from compactification for the sector $\Omega_k > 0$, we rewrite the Friedmann's equation (4.1) as follows:

$$\rho = 3H^2 + \frac{3k}{a^2} - \Lambda. \tag{4.12}$$

In the case of positive curvature $k > 0$ models, it is obvious that $D = \sqrt{H^2 + \frac{k}{a^2}}$ is a dominant quantity. Thus D can be used to compactify the space instead of using H. The compact variables in the case of $k = 1$ are:

$$Q = \frac{H}{D}, \quad \tilde{\Omega}_\Lambda = \frac{\Lambda}{3D^2}. \tag{4.13}$$

Analogous to the case ($\Omega_k \leq 0$), we introduce a new time variable defined by ($' = D^{-1}\frac{d}{dt}$), the reduced autonomous system becomes:

$$\begin{aligned} Q' &= \left[1 - \frac{3w}{2}(1 - \tilde{\Omega}_\Lambda)\right](1 - Q^2), \\ \tilde{\Omega}'_\Lambda &= 3w(1 - \tilde{\Omega}_\Lambda)Q\tilde{\Omega}_\Lambda. \end{aligned} \tag{4.14}$$

We apply the usual procedure to extract the fixed points and determine their stability. A full set of fixed points and their types is demonstrated in Table [4.2]. The complete

Point	Coordinates (Q,$\tilde{\Omega}_\Lambda$)	Stability	Solution
${}_+F$	(1,0)	source	Flat Friedmann solution
${}_-F$	(-1,0)	sink	Flat Friedmann solution
${}_+ds$	(1,1)	sink	de Sitter solution
${}_-ds$	(-1,1)	source	de Sitter solution
E	$(0,\frac{3w+1}{3(w+1)})$	saddle	Einstein static solution

TABLE 4.2: Summary for the fixed points identified, along with their corresponding exact solution, and their local stability classification for the compact dynamical systems analysis of FL cosmologies with a cosmological constant. The sign associated with the F and dS points indicate whether it lies within the expanding or contracting sector of the phase space corresponding to positive or negative Q, respectively [7].

image of the dynamical systems of Friedmann models, can be constructed by matching the expanding state space ($\Omega_k > 0$) and the contracting part ($\Omega_k < 0$). The analysis of the state dynamics depends on the value of w. For $w > -1/3$ Fig [4.1], the solutions trajectories have the following behaviour

- Spacetimes with $\Omega_k < 0$, $H > 0$, $\Omega > 0$ and $\Lambda > 0$ evolve from initial big bang singularity (${}_+F$) toward de Sitter point (${}_+ds$).

- Spacetimes with $\Omega_k > 0$ and $H > 0$ are more complicated and depend on the amount of Λ. Spacetimes start out with sufficiently small Λ value are classified

closed Friedmann-Lemaître spacetimes. The solution trajectories enter the contracting state space and recollapse to a 'big crunch' at ($_-F$). If $\Lambda = \Lambda_c = \frac{3w-2}{w}\frac{k}{a_c^2}$, then trajectories evolve towards the Einstein static universe, E.

- The last class of spacetimes is that starting out with large enough Λ. Trajectories of this class evolve towards a de Sitter model and is known as Lemaître models.

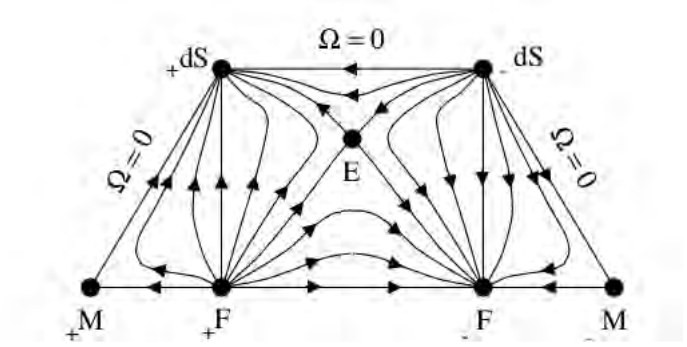

FIGURE 4.1: State space for Friedmann-Lemaître models with $-1/3 < w < -1$. In the $\Omega_k < 0$ regions (triangular), the vertical axis corresponds to Ω_Λ, and the horizontal axis to Ω_k. In the $\Omega_k > 0$ region (rectangular), the vertical axis corresponds to $\tilde{\Omega}_\Lambda$, and the horizontal axis to Q. Subscripts on the equilibrium points refer to the sign of H there [7].

In the case of $w < -1/3$ the fixed point E no longer exists. For $\Omega_k < 0$, all the trajectories are asymptotic to the Milne universe in their past and evolve towards the de Sitter model in their future. For $\Omega_k > 0$, there are only singularity-free contracting and re-expanding models.

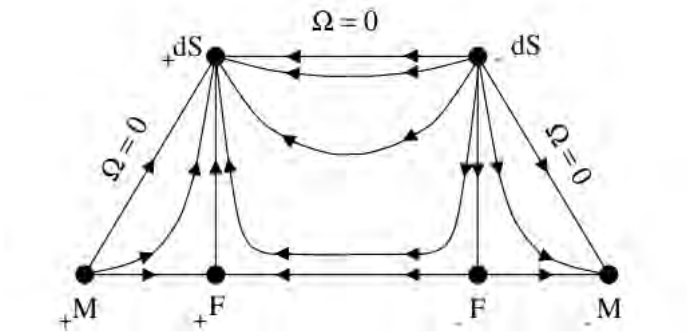

FIGURE 4.2: State space for Friedmann-Lemaître models with $-1 < w < -1/3$. In the $\Omega_k < 0$ regions (triangular), the vertical axis corresponds to Ω_Λ and the horizontal axis to Ω_k. In the $\Omega_k > 0$ region (rectangular), the vertical axis corresponds to $\tilde{\Omega}_\Lambda$ and the horizontal axis to Q. Subscripts on equilibrium points refer to the sign of H there. [7].

4.3 Concluding Remarks

In this chapter, we have reviewed the results of applying dynamical systems approach to the Friedmann-Lemaître models. This study is considered as a corner stone in phase space compactification techniques. Following the same procedures stated in this study, we will establish a parallel study for metric f(R) gravity through studying the phase space dynamics of the logarithmic model $R \ln R$.

Chapter 5

Dynamical Systems Approach to metric $f(R)$ gravity

5.1 Introduction

The first extensive analysis of cosmological models based on f(R) theories of gravity using a dynamical systems approach as proposed in [112] was given in [113]. Several authors have applied a similar approach to other types of Lagrangian [114]. It has also proven to be powerful in theories with non-linear equation of state [115, 116] and brane world models [117–120]. Generally, the modified theories of gravity have complicated effective field equations which makes finding an exact analytical solution very difficult. The dynamical systems approach can therefore be useful in gaining a good idea about the global dynamics of the phase space. In the following sections, we benefit from this approach in depicting the phase space of the $R \ln R$ model, and finding the fixed points which the model autonomous system admits. We, then, proceed by classifying these fixed points and finding the exact solution at each fixed point.

5.2 Introduction to the $R \ln R$ model

Although a presence of a tiny, but non vanishing, cosmological constant supports the possibility of a late time accelerated expansion, it causes a hierarchy problem between Infrared cosmological acceleration scale and ultraviolet Planck scale. In order to give a dynamical origin to the cosmic acceleration, one would need a modified gravity, with new (IR) degrees of freedom, providing that these degrees of freedom are active on cosmological scales, and become suppressed on solar system scales. One such method

to accomplish this type of modified gravity is by applying the idea of re-normalization group [121] from the field of high energy physics. We explain how to do that assuming a classical gravitational coupling which varies with curvature scalar (R) leading to $f(R)$ gravity. In the following discussion, we closely follow [122]. Let us assume that the gravitational constant (G) runs with Ricci scalar (R), by introducing a dimensionless coupling α,

$$8\pi G = \frac{\alpha}{m_{Pl}^2}, \tag{5.1}$$

where m_{Pl}^2 is the Planck mass. Provided there is an autonomous flow of the re-normalization group, a beta function is appropriate to describe the running of the dimensionless coupling α

$$\beta(\alpha) = \mu \frac{d\alpha}{d\mu}, \tag{5.2}$$

where $\mu \equiv \frac{R}{R_0}$, and R_0 is strictly a positive constant parameter. We can integrate the above equation to obtain

$$\int \frac{d\alpha}{\beta(\alpha)} = \int \frac{d\mu}{\mu}. \tag{5.3}$$

If we use (5.1), we can rewrite the Lagrangian density of general relativity $\mathcal{L}_{GR} = \frac{R}{16\pi G}$ in terms of Planck mass, and therefore obtain $f(R)$ gravity with the Lagrangian density

$$\mathcal{L}_{f(R)} = \frac{m_{pl}^2}{2}\frac{R}{2}. \tag{5.4}$$

The power-law corrections to the Einstein-Hilbert action which takes the form

$$f(R) = R[1 + \lambda(\frac{R}{R_0})^n], \tag{5.5}$$

can be generated by an autonomous flow,

$$\beta(\alpha) = n\alpha(\alpha - 1), \tag{5.6}$$

with

$$\alpha \equiv \frac{R}{f(R)} = \frac{1}{1 + \lambda\mu^n}. \tag{5.7}$$

If we make use of (5.2), then the beta function reads

$$\beta = \mu \frac{d}{d\mu}(\frac{1}{1 + \lambda\mu^n}) = -\frac{n\lambda\mu^n}{(1 + \lambda\mu^n)^2}. \tag{5.8}$$

For high-curvature scales, where $\mu \gg 1$, the beta function becomes

$$\beta \approx -\frac{n}{\lambda\mu^n}. \tag{5.9}$$

Hence, a large gap in the beta function corresponds to a large gap in curvature between the Planck scale and the local environment of the Earth [123]. In order to have a big hierarchy curvature we might ignore the linear term in the beta function. Consider a quadratic beta function,

$$\beta = -\alpha^2. \tag{5.10}$$

Inserting this equation in (5.3) and integrating leads to an effective action for gravity with

$$f(R) = \frac{R}{\alpha_0}(1 + \alpha_0 \ln(\frac{R}{R_0})), \tag{5.11}$$

where α_0 is the coupling measured at curvature scale R_0[1]. In this model, the coupling constant runs as

$$\alpha = \frac{\alpha_0}{1 + \alpha_0 \ln(\frac{R}{R_0})}. \tag{5.12}$$

The constant α_0 can be absorbed in the denominator of (5.11) into the definition of the Planck mass m_{Pl} and hence can be rewritten as

$$f(R) = R(1 + \alpha_0 \ln(\frac{R}{R_0})). \tag{5.13}$$

The value of α_0 should be chosen carefully,(meaning that $\alpha_0 \ll 1$), in order to reduce the $f(R)$ into General Relativity at the high curvature scale. In fact, A tiny α_0 generates a heavy mass for the scalar field ϕ [2], causing the potential to evolve very slowly. Conversely, assigning a large value for α_0 yields a small field mass and the fast evolution of ϕ. Consider the first and second derivative of $f(R)$

$$f'(R) = 1 + \alpha_0 + \alpha_0 \ln \frac{R}{R_0}, \tag{5.14}$$

$$f''(R) = \frac{\alpha_0}{R}. \tag{5.15}$$

f' has to be positive to avoid Ghosts; this condition can be satisfied as long as the Ricci scalar is not too much smaller than the de Sitter curvature[3]. Ghosts are fields whose kinetic term has the wrong sign. Such a field, instead of slowing down when it climbs up a potential, is speeding up. Hence the theory will face a serious problem if we seek introducing a quantized version of it. Moreover, f'' has to be positive to avoid

[1] It is better if we think of R_0 as the scale at which the effective action is evaluated.

[2] There is a converse proportionality between α_0 value and the mass of the field; we do not include the governing equations of the scalar field approach since we adopt a different approach. For reviewing these equations one can find them in [122].

[3] de Sitter curvature is given by: $\Lambda = R_0 e^{\frac{-1}{\alpha_0 + 1}}$.

the Dolgov-Kawasaki instability. This can be met easily if we consider the positive Ricci scalar. One has to keep in mind that α_0 is always a positive parameter.

5.3 Constructing a compact phase space

The underlying concept of compact phase space is to define a strictly positive normalization so as to pull the solutions at infinity into a finite volume, which may then be studied conveniently. We begin by introducing a normalized time variable

$$\frac{d}{d\tau} \equiv \frac{1}{D}\frac{d}{dt}. \tag{5.16}$$

Recall that in, section 2.7, the modified cosmological equations are given by:

- **Raychaudhuri equation:**

$$\begin{aligned} 2\dot{H} + 3H^2 &= -\frac{1}{f'}[P^{(m)} + \frac{f - f'R}{2} + 2Hf''\dot{R} \\ &+ f'''\dot{R}^2 + f''\ddot{R}]; \end{aligned} \tag{5.17}$$

- **Friedmann equation :**

$$3H^2 = \frac{1}{f'}[\rho + \frac{Rf' - f}{2} - 3Hf''\dot{R}]; \tag{5.18}$$

- **Trace equation:**

$$3\ddot{R}f'' = \rho - 3P + f'R - 2f - 9Hf''\dot{R} - 3f'''\dot{R}^2, \tag{5.19}$$

- **Energy Conservation equation :** The energy conservation equation for a standard matter takes the form

$$\dot{\rho} = -3H(1 + w)\rho\ , \tag{5.20}$$

If we combine both the Raychaudhuri equation (5.17) and the Friedmann equation (5.18), we obtain the usual definition of the Ricci scalar in flat (FLRW)

- **Ricci scalar equation:**

$$R = 6(\dot{H} + 2H^2). \tag{5.21}$$

The sector $R < 0$ is not of much physical interest therefore we only study the dynamics of the sector $R \geq 0$. We assert the importance of satisfying the no-ghost condition $(f' > 0)$ and $(f'' > 0)$ to avoid the Dolgov-Kawasaki instability. In order to establish the phase space compact, we rewrite Friedmann's equation (5.18) in the following form:

$$D^2 = \frac{3\rho}{f'} + \frac{3}{2}R + \frac{9}{4}(\frac{(\dot{f'})}{f'})^2 \,, \tag{5.22}$$

where

$$D = \sqrt{\left(3H + \frac{3}{2}\frac{(\dot{f'})}{f'}\right)^2 + \frac{3}{2}\frac{f}{f'}} \,. \tag{5.23}$$

We can now define the following set of normalized variables:

$$\begin{aligned} x &= \frac{3}{2}\frac{(\dot{f'})}{f'D}, \qquad y = \frac{3}{2}\frac{f}{f'D^2}, \qquad \Omega_m = \frac{3\rho}{f'D^2}, \\ z &= \frac{3}{2}\frac{R}{D^2}, \qquad Q = \frac{3H}{D} \,. \end{aligned} \tag{5.24}$$

In order to guarantee that the propagation equations for these compact variables will result in a compact dimensionless dynamical system. From Friedmann's equation we obtain the following constraint

$$\Omega_m + z + x^2 = 1 \,,$$

another constraint can be deduced from (5.22)

$$(Q + x)^2 + y = 1. \tag{5.25}$$

The boundaries of this phase space are defined by the above two constraints as follows:

$$\begin{aligned} 0 \;\leq \Omega_m \leq\; 1 \,, \qquad 0 \leq z \leq 1 \,, \qquad -1 \leq x \leq 1 \\ -2 \;\leq Q \leq\; 2, \qquad 0 \leq y \leq 1 \,. \end{aligned} \tag{5.26}$$

5.4 The General Propagation Equations

Differentiating the compact cosmological parameters with respect to τ leads to an autonomous system which is equivalent to the cosmological field equations

$$\begin{aligned}
\frac{dx}{d\tau} &= \frac{1}{6}(2Q^3x + 4x^4 + Q^2(2+4x^2) - 2y - (1+3w)\Omega_m \\
&+ Qx(-2+6x^2+2y-2z+(1+3w)\Omega_m) + x^2(-4+4y-2z(1+\Gamma)+(1+3w)\Omega_m)), \\
\frac{dy}{d\tau} &= \frac{1}{3}(2Q^3y + 4Q^2xy + Qy(6x^2+2y-2z+(1+3w)\Omega_m)) \\
&+ x(4y^2+2\Gamma z + y(-2+4x^2-2(1+\Gamma)z+(1+3w)\Omega_m))), \\
\frac{dz}{d\tau} &= \frac{1}{3}z(2Q^3 + 4Q^2x + Q(6x^2+2y-2z+(1+3w)\Omega_m) \\
&+ x(2\Gamma + 4x^2 + 4y - 2z(1+\Gamma) + (1+3w)\Omega_m)), \\
\frac{dQ}{d\tau} &= \frac{1}{6}(2Q^4 + 4Q^3x + 2z + Q^2(-4+6x^2+2y-2z+(1+3w)\Omega_m) \\
&+ Qx(4x^2+4y-2z(1+\Gamma)+(1+3w)\Omega_m)), \\
\frac{d\Omega_m}{d\tau} &= \frac{1}{3}\Omega_m(2Q^3 + 4Q^2x + Q(-3-3w+6x^2+2y-2z+(1+3w)\Omega_m) \\
&+ x(-2+4x^2+4y-2z(1+\Gamma)+(1+3w)\Omega_m)).
\end{aligned} \tag{5.27}$$

We can use the constraints (5.25) in order to reduce the number of the governing equations to three equations instead of five.

$$\begin{aligned}
\frac{dx}{d\tau} &= \frac{1}{6}(-3-3w+(z-x^4)(1+3w) - 4Q^2(-1+x^2) \\
&- Qx((5+3w)(1-x^2)+3(1+w)z) + x^2(4+6w-(3+2\Gamma+3w)z)), \\
\frac{dz}{d\tau} &= \frac{-z}{3}(4Q^2x + Q((5+3w)x^2+3(1+w)(z-1)) \\
&+ x(-5-2\Gamma-3w+(1+3w)x^2+(3+2\Gamma+3w)z)), \\
\frac{dQ}{d\tau} &= \frac{1}{6}(-4Q^3x + 2z - Q^2(1-3w(5+3w)x^2+3(1+w)z) \\
&- Qx(-5-3w+(1+3w)x^2+(3+2\Gamma+3w)z)),
\end{aligned} \tag{5.28}$$

where $\Gamma = \frac{f'}{Rf''}$. The system is closed as long as Γ can be fully expressed in terms of the dynamical variables. In the case of the logarithmic model $R\ln R$ under study, we specifically have

$$\Gamma \equiv \frac{z}{z-y}. \tag{5.29}$$

The above system (5.28) defines the dynamics of a general $f(R)$ theory for which Γ is invertible in terms of the dynamical variables. Looking at the above system, one can

observe that the system has an invariant sub-manifold $z = 0$. From the definition of the dynamical variable z, $z = 0$ is equivalent to $R = 0$. Consequently we obtain an important result:

For all well defined functions $f(R)$, with $f' > 0$ and $\frac{f'}{Rf''}$ expressed in terms of the dynamical variables defined by (5.24), a FLRW spacetimes with non-negative Ricci scalar continues to be so both in the future and the past. Also an $R = 0$ spacetimes can never undergo a bounce in the future or the past [105].

5.5 The fixed points, stability and exact solutions

The system (5.28) can be simplified further by using the constraints (5.25). This leads to reduction of the system (5.28), namely the system becomes two equations instead of three

$$x' = -\frac{(x^2-1)}{3Q(Q+2x)}(2Q^4+5Q^3x-x^2+x^4+Q^2(-1+x^2)-2Q(x+x^3)), \tag{5.30}$$

$$Q' = \frac{-1}{3(Q+2x)}(-x+2Q^4x+x^5+Q^2x(3+x^2)+Q^3(2+5x^2)-Q(1+x^2+2x^4)). \tag{5.31}$$

5.5.1 The vacuum case

In the vacuum case, we set $\Omega_m = 0$ to emphasize the absence of matter. We shall divide the obtained fixed points into two classes regarding whether the fixed point is analytical or not. In general, when we refer to the fixed points with $(+)$ we mean that it lies in the expanding part of the phase space; consequently if we refer to it with $(-)$ we mean that it exists in the contracting part of the phase space. In what follows we only have one fixed point that lies on the border between the expanding and contracting parts.

5.5.1.1 The class of analytical fixed points

The first class is obtained in a regular way by setting $x' = 0$ and $y' = 0$, and making sure that the denominators in (5.30) are never equal to zero at these points.

$$\begin{aligned}
\mathcal{A}_+ &= (x \to 1, Q \to 1/2),\\
\mathcal{A}_- &= (x \to -1, Q \to -1/2),\\
\mathcal{B}_+ &= (x \to 0, Q \to 1/\sqrt{2}),\\
\mathcal{B}_- &= (x \to 0, Q \to -1/\sqrt{2}).
\end{aligned} \tag{5.32}$$

We notice that the class is independent of the parameters α_0 and R_0.

5.5.1.2 The class of non-analytical fixed points

At these points the denominator of (5.30) equals zero.

$$\begin{aligned} \mathcal{C}_+ &= (x \to 1, Q \to 0), \\ \mathcal{C}_- &= (x \to -1, Q \to 0), \\ \mathcal{D}_+ &= (x \to -1, Q \to 2), \\ \mathcal{D}_- &= (x \to 1, Q \to -2), \\ \mathcal{E} &= (x \to 0, Q \to 0). \end{aligned} \tag{5.33}$$

Considering the nature of the governing equations (5.30), one can easily see that in case of any point with coordinate $Q = 0$, the usual procedure of finding the fixed points fails. Meanwhile, the phase space Fig [5.1] demonstrates that three of the fixed points lay on the line $Q = 0$.
Therefore, the respective stabilities of these points were inferred by inspecting the behaviour of solutions in the neighbourhood of each point [4]. We summarise the fixed points coordinates alongside with classifications and stability in table [5.1].

5.5.1.3 Stability of the fixed points

In the case of fixed points $\mathcal{A}_\pm$, the linearised matrix has both a positive and a negative eigenvalue which is, as we stated before, independent of the model parameters; i.e. it is always a saddle point.
The two fixed points $\mathcal{B}_\pm$ have two independent conjugate complex eigenvalues which means that the two points are **spirals**. The only difference between the two points with respect to stability is that $\mathcal{B}_+$ is stable whilst $\mathcal{B}_-$ is unstable.
In case of the $\mathcal{C}_+$, both eigenvalues are dependent and positive real numbers, and thus the point is a **repeller**.
For $\mathcal{C}_-$, we follow the same analysis of C_+; both of the eigenvalues are dependent and negative real numbers, thus the point is an **attractor**.
The analysis of the two points $\mathcal{D}_\pm$ are typically the same as the points $C_\pm$ with the same classification **repeller/attractor**.
The last point, $\mathcal{E}$, has two eigenvalues opposite in sign, therefore the point is classified as a **saddle**.

[4] Inferring the stability of theses fixed points by means of numerical treatment can be found in Appendix A.

The phase space Fig [5.1] exhibits the nine fixed points: $\mathcal{A}_{\pm}$, $\mathcal{B}_{\pm}$ $\mathcal{C}_{\pm}$, $\mathcal{D}_{\pm}$ and E. Moreover, the figure exhibits line $Q = 0$ as a border between the expanding and contracting solutions. One can see a kind of symmetry on both sides of $Q = 0$ in terms of the number of the fixed points and their types.

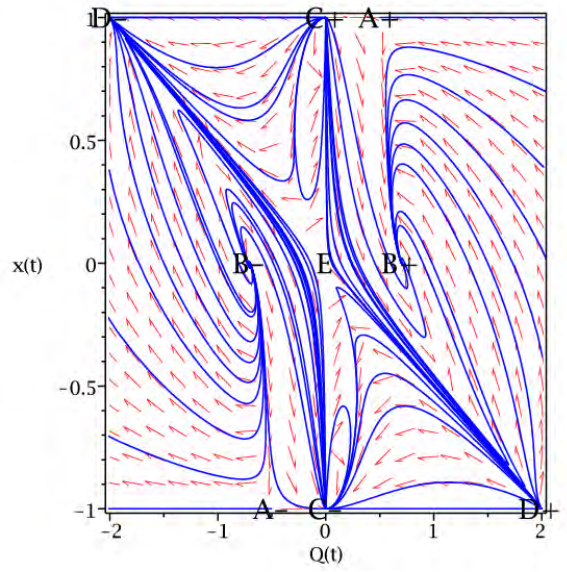

FIGURE 5.1: Vacuum portrait placed on it the 9-fixed points and the orbits between them.

5.5.2 Exact solutions of the scale factor $a(t)$ at the fixed points

Consider (5.21), rearranging the terms gives,

$$\begin{aligned} \dot{H} &= \frac{R}{6} - 2H^2 \\ &= H^2(\frac{R}{6H^2} - 2). \end{aligned} \tag{5.34}$$

We use the definitions of the dynamical variables z and Q and simplifying, we have

$$\begin{aligned} \dot{H} &= H^2(-2 + \frac{z}{Q^2}) \\ &= H^2(-2 + \frac{1-x^2}{Q^2}). \end{aligned} \tag{5.35}$$

From now on we substitute each fixed point coordinates into (5.35) separately; to obtain the solutions at each fixed point. We preview the solution $a(t)$ at $\mathcal{A}_+(1, \frac{1}{2})$,

$$\dot{H} = -2H^2. \tag{5.36}$$

This is a first order ODE in H and t. We adopt the method of separating variables to obtain an exact solution, firstly for the Hubble parameter and then for the scale factor $a(t)$.

$$H = \frac{\dot{a}}{a} = \frac{1}{2t - t_0}, \tag{5.37}$$

The last equation (5.37) is another first order ODE in a and t. The solution can be deduced in the same way as the previous one,

$$a(t) = a_0\sqrt{2t - t_0}. \tag{5.38}$$

The same procedure could have been adopted for the rest of the fixed points, but a singularity arises when we deal with $\mathcal{C}_\pm$ and $\mathcal{E}$ because of the term $\frac{1-x^2}{6Q^2}$. A possible singularity does not occur if we assure[5] that the whole term vanishes; i.e. the numerator reaches zero faster than the denominator. For the points near which the scale factor increases exponentially with time, namely the points $\mathcal{B}\pm$, the points are said to represent **de-Sitter universes**. The evolution of the scale factor $a(t)$ near the other fixed points resolves **radiation-like universes** as the scale factor increases with the square root of the cosmic time.

Although the dynamical systems approach has proved to be efficient in understanding the dynamics of the modified field equations, the approach has some short-comings. One

[5] We include a numerical treatment to this problem in Appendix B.

short-coming is that the dynamical analysis admits some fixed points which correspond to solutions of the dynamical system, but do not satisfy the cosmological equations. In fact, we have that exact situation in our study. Let us consider the fixed points $\mathcal{C}_{\pm}$ and $\mathcal{E}$: these fixed points are true fixed points and admit cosmological solutions, however they do not satisfy the cosmological equations. In many cases, constants of integration, which emerge in families of solutions to the cosmological equations, result in additional constraints which must be satisfied by all physical points of the system. Setting the derivatives of the dynamical variables equal to zero;

$$x' = F(x) = 0, \tag{5.39}$$

implies two consequences,

$$F(x) = 0, \tag{5.40}$$

or

$$x' = 0 \Longrightarrow x = constant \tag{5.41}$$

Solutions to (5.39) may result from solving either the equations (5.40) or (5.41), where the latter now represents a set of constraints imposed on the system [79].
Therefore, the fixed points $\mathcal{C}_{\pm}$ and $\mathcal{E}$, which are being placed on the non-invariant $Q = 0$ submanifold, exemplify solutions for which the scale factor is time independent and thus represent static universes.

Fixed points	Coordinates (x, Q)	Solution $a(t)$	Classifications
$\mathcal{A}\pm$	$(\pm 1, \pm\frac{1}{2})$	$a(t) = a_0(2t - t_0)^{\frac{1}{2}}$	Saddle
$\mathcal{B}\pm$	$(0, \pm\frac{1}{\sqrt{2}})$	$a(t) = a_0 e^{H_0(t-t_0)}$	Stable/Unstable Spirale
$\mathcal{C}\pm$	$(\pm 1, 0)$	$a(t) = a_0(2t - t_0)^{\frac{1}{2}}$	Repeller/Attractor
$\mathcal{D}\pm$	$(\mp 1, \pm 2)$	$a(t) = a_0(2t - t_0)^{\frac{1}{2}}$	Repeller/Attractor
$\mathcal{E}$	$(0, 0)$	$a(t) = a_0$	Saddle

TABLE 5.1: coordinates of the fixed points, solutions and classifications.

5.6 The matter case

In this section we investigate the behaviour of the dynamics in presence of a matter component. The equivalent dynamical equations in this case are

$$\begin{aligned} x' &= \frac{-1}{6(-1+(Q+x)^2+z)}((-1+Q+x)(1+Q+x)(-1+x^2)(-3(1+w) \\ &+ (Q+x)(4Q+x+3wx)) + Q^2(-5-3w(13+9w)x^2))z \\ &+ (-1-3w+3Qx(1+w)+(5+3w)x^2)z^2), \end{aligned} \tag{5.42}$$

$$\begin{aligned} z' &= \frac{z}{3(-1+(Q+x)^2+z)}((-1+Q+x)(1+Q+x)(-3(1+w)Q \\ &+ (-5-3w+4Q^2)x + (5+3w)Qx^2 + (1+3w)x^3 \\ &- (3(1+w)Q(-2+Q^2)) + (-2(5+3w)+(13+9w)Q^2)x \\ &+ 2(7+6w)Qx^2 + 2(2+3w)x^3)z - (3(1+w)Q+(5+3w)x)z^2), \end{aligned} \tag{5.43}$$

$$\begin{aligned} Q' &= \frac{1}{6}(-4xQ^3 + 2z - Q^2(1-3w(5+3w)x^2 + 3z(1+w)) \\ &+ Qx(5+3w-(1+3w)x^2 + z(-3-3w-\frac{2z}{-1+z+(Q+x)^2}))). \end{aligned} \tag{5.44}$$

As a result of the definitions of the compact variables, we find that the only value for w, which of physical interest, is $w=-1$. In order to obtain the system fixed points, we follow the same procedure as in the vacuum case. We set $x'=0$, $z'=0$ and $Q'=0$ then solving for x, z and Q.

$$\begin{aligned} \mathcal{A}_+ &= (x\to 1, z\to 0, Q\to \frac{1}{2}), \\ \mathcal{A}_- &= (x\to -1, z\to 0, Q\to \frac{-1}{2}), \\ \mathcal{B}_+ &= (x\to 0, z\to 1, Q\to \frac{1}{\sqrt{2}}), \\ \mathcal{B}_- &= (x\to 0, z\to 1, Q\to \frac{-1}{\sqrt{2}}), \\ \mathcal{C} &= (x\to \frac{\sqrt{3}\sqrt{1+w}}{\sqrt{1+3w}}, z\to 0, Q\to 0). \end{aligned} \tag{5.45}$$

Intuitively, the fixed points $\mathcal{A}\pm$, $\mathcal{B}\pm$ are independent of the model parameters and the equation of state w. Furthermore, we find that fixed point $\mathcal{C}$ depends on the value of the equation of state w. Therefore we emphasize that the set of fixed points is common for that set of models. Regarding $\mathcal{A}\pm$ and $\mathcal{B}\pm$ two of the eigenvalues are zeros, thus the linear theory of stability fails. Instead, we adopt the Center Manifold Theory in order to classify the stability of these fixed points. The last fixed point, namely, $(0, 0, 0)$ is different because in this case all the eigenvalues are zeros, and hence even the Center Manifold Theory breaks down. Thus, a numerical treatment has been used to find out the stability of this fixed point. Table [5.2] includes the matter fixed points, their stability and the solutions for the scale factor at these fixed points.

Fixed points	Coordinates (x, z, Q)	Solution $a(t)$	Classifications
$\mathcal{A}\pm$	$(\pm 1, 0, \pm\frac{1}{2})$	$a(t) = a_0(2t - t_0)^{\frac{1}{2}}$	Stable/Unstable Saddle node
$\mathcal{B}\pm$	$(0, 1, \pm\frac{1}{\sqrt{2}})$	$a(t) = a_0 e^{H_0(t-t_0)}$	Stable/Unstable Saddle node
$\mathcal{C}$(w = -1)	$(0, 0, 0)$	$a(t) = a_0$	Saddle

TABLE 5.2: The matter case fixed points with their stability and the solutions $a(t)$ which they represents.

5.7 Non-compact phase space analysis of $R \ln R$ model

In the previous section we established a compact analysis of the phase space to study the stability of the fixed points admitted by the autonomous system (5.27). The merit of this analysis is the ability to bring the non-finite equilibrium points into a finite phase space to apply the same procedure in finding the eigenvalues and classify the fixed points. There are, however, some finite fixed points i.e. ($\mathcal{A}_{\pm}$ and $\mathcal{B}_{\pm}$) that did not benefit from the compact analysis. This suggests that a non-compact analysis is helpful in revealing the evolution of the model dynamics between the different fixed points. Moreover, the non-compact analysis, as we shall see in next sections, can be used to study the expansion history of any $f(R)$ model. In order to construct that non-compact analysis, we use the following non-compact coordinates:

$$\tilde{x} = \frac{\dot{f}'}{f'H}, \quad \tilde{y} = \frac{f}{6f'H^2}, \quad \tilde{\upsilon} = \frac{R}{6H^2}, \quad \tilde{w}_m = \frac{\rho_m}{3f'H^2}, \quad h(z) = \frac{H}{H_0}. \tag{5.46}$$

The Friedmann equation (5.18) can be re-expressed to give a constraint equation in terms of the above variables:

$$1 = \tilde{\Omega}_m + \tilde{\upsilon} - \tilde{y} - \tilde{x}. \tag{5.47}$$

We are very interested in investigating the expansion history of metric $f(R)$ exemplified in the logarithmic model $R \ln R$, thus we will differentiate the non-compact variables with respect to redshift (z). Integrating the resultant equations would reveal the expansion history of this model.
Here are the non-compact dynamical equations for a general f(R) model :

$$\frac{d\tilde{x}}{dz} = \frac{1}{1+z}(-2 - \tilde{x} + \tilde{x}^2 + 2\tilde{y} + \tilde{x}\tilde{\upsilon} + (1+3w)\tilde{\Omega}_m), \tag{5.48}$$

$$\frac{d\tilde{y}}{dz} = \frac{1}{1+z}(\Gamma\tilde{\upsilon}\tilde{x} - \tilde{x}\tilde{y} + 4\tilde{y} - 2\tilde{y}\tilde{\upsilon}), \tag{5.49}$$

$$\frac{d\tilde{\upsilon}}{dz} = -\frac{\tilde{\upsilon}}{1+z}(4 + \Gamma\tilde{x} - 2\tilde{\upsilon}), \tag{5.50}$$

$$\frac{d\tilde{\Omega}_m}{dz} = \frac{\tilde{\Omega}_m}{1+z}(-1 + 3w + \tilde{x} + 2\tilde{\upsilon}), \tag{5.51}$$

where the parameter Γ is given by

$$\Gamma = \frac{\tilde{\upsilon}}{\tilde{\upsilon} - \tilde{y}}, \tag{5.52}$$

and the differential equation of renormalized Hubble parameter h takes the form

$$\frac{dh}{dz} = \frac{h}{1+z}(2-\tilde{v}) \tag{5.53}$$

The chapter, however, is concerned with investigating the expansion history of a universe filled with dust, and the gravitational interactions in this universe are described by $f(R) = R(1+\alpha_0 \ln(\frac{R}{R_0}))$. So it is more convenient to introduce a more specific version of the non-compact dynamical equations to account for these concerns

$$\begin{aligned}
\frac{d\tilde{x}}{dz} &= \frac{1}{1+z}(-2-\tilde{x}+\tilde{x}^2+2\tilde{y}+\tilde{x}\tilde{v}+\tilde{\Omega}_m),\\
\frac{d\tilde{y}}{dz} &= \frac{1}{1+z}(-4\tilde{y}+\tilde{x}\tilde{y}+2\tilde{y}\tilde{v}-\frac{\tilde{x}\tilde{v}^2}{\tilde{y}+\tilde{v}}),\\
\frac{d\tilde{v}}{dz} &= -\frac{\tilde{v}}{1+z}(4-2\tilde{v}+\frac{\tilde{x}\tilde{v}}{\tilde{v}-\tilde{y}}),\\
\frac{d\tilde{\Omega}_m}{dz} &= \frac{\tilde{\Omega}_m}{1+z}(-1+\tilde{x}+2\tilde{v}),\\
\frac{dh}{dz} &= \frac{h}{1+z}(2-\tilde{v}).
\end{aligned} \tag{5.54}$$

5.8 Comparing the model ($R(1+\alpha_0 \ln(\frac{R}{R_0}))$) with the standard model ΛCDM

In this section we integrate the system (5.54) in order to calculate the evolution of the key cosmological parameters with redshift (z). In fact, this integration enable us to make precise comparison between the $R\ln R$ model and the ΛCDM model. For the sake of introducing robust results for the expansion history, and suppressing the ghost fields that arise when we use a certain parametrisation for effective equation of state, we calculate both effective and total equations of state using two parametrisations. This technique has proven to be helpful. In the case of the model $R\ln R$ one of the parametrization exhibits ghost fields and singularities in the effective equation of state. These singularities do not exist when we switch to the other parametrization[6].

5.8.1 Initial conditions for $R(1+\alpha_0 \ln(\frac{R}{R_0}))$ at $z_0 = 5$

In order to integrate system (5.54), we need to compute the initial value of each non-compact variable contributed to that system at $z_0 = 5$. We calculate the initial conditions at redshift $z_0 = 5$ as we are primarily interested in studying the late time

[6]For the total EOS (w_{Tot}), difference between the results of the two methods is of order $\mathcal{O}(10^{-8})$.

accelerated expansion. We use the present-day ($z_0 = 0$) values for Ω_m and Ω_Λ,

$$\Omega_{m0} = 0.26, \quad \Omega_{\Lambda 0} = 0.68, \tag{5.55}$$

We use the last equation (5.55) to evaluate the initial values of the normalized Hubble parameter (h_0) and the deceleration parameter (q_0) at $z_0 = 5$,

$$h_0(z_0 = 5) = \sqrt{\Omega_{m0}(1+z_0)^3 + \Omega_{\Lambda 0}} = 7.53923, \tag{5.56}$$

and

$$q_0(z_0 = 5) = \frac{\Omega_{m0}(1+z_0)^3 - 2\Omega_{\Lambda 0}}{2(\Omega_{m0}(1+z_0)^3 + \Omega_{\Lambda 0})} = 0.48205, \tag{5.57}$$

Now we proceed in calculating the initial values of the non-compact dynamical variables as follows

$$\tilde{r}_0 = 6h_0^2(1 - q_0) = 176.64, \tag{5.58}$$

$$\tilde{v}_0 = 1 - q_0 = 0.51794, \tag{5.59}$$

$$\tilde{\Omega}_{m0} = \frac{\Omega_{m0}(1+z_0)^3}{h_0^2(1 + \alpha_0 + \alpha_0 \ln(\tilde{r}_0))} = 0.79235, \tag{5.60}$$

$$\tilde{y}_0 = \frac{\tilde{r}_0(1 + \alpha_0 \ln(\tilde{r}_0))}{6h_0^2(1 + \alpha_0 + \alpha_0 \ln(\tilde{r}_0))} = 0.50133, \tag{5.61}$$

We use the constraint (5.47) to calculate the initial value of $\tilde{x}$,

$$\tilde{x}_0 = \tilde{\Omega}_{m0} + \tilde{v}_0 - \tilde{y}_0 - 1 = -0.19103 \tag{5.62}$$

5.8.2 Hubble parameter $h(z)$

In the ΛCDM model, the dimensionless Hubble parameter (h) as a function of red shift is given by:

$$h(z) = \sqrt{\Omega_{m0}(1+z)^3 + \Omega_{\Lambda 0}}. \tag{5.63}$$

While, the dimensionless Hubble parameter (h) in the $R \ln R$ model can be obtained by integrating , numerically, the system (5.54). The figures below [5.2] show a comparison between the evolution of ($h(z)$) in the two models.

We can observe that there is a good agreement between the evolutionary behaviour of $h(z)$ of the two models over the selected range of redshifts. In general, we found that increasing the value of the parameter α_0 makes the discrepancies between $R \ln R$ and ΛCDM significantly less. At the same time, we should be careful of giving higher values to α_0 because this makes the model suffer several singularities and ghost fields.

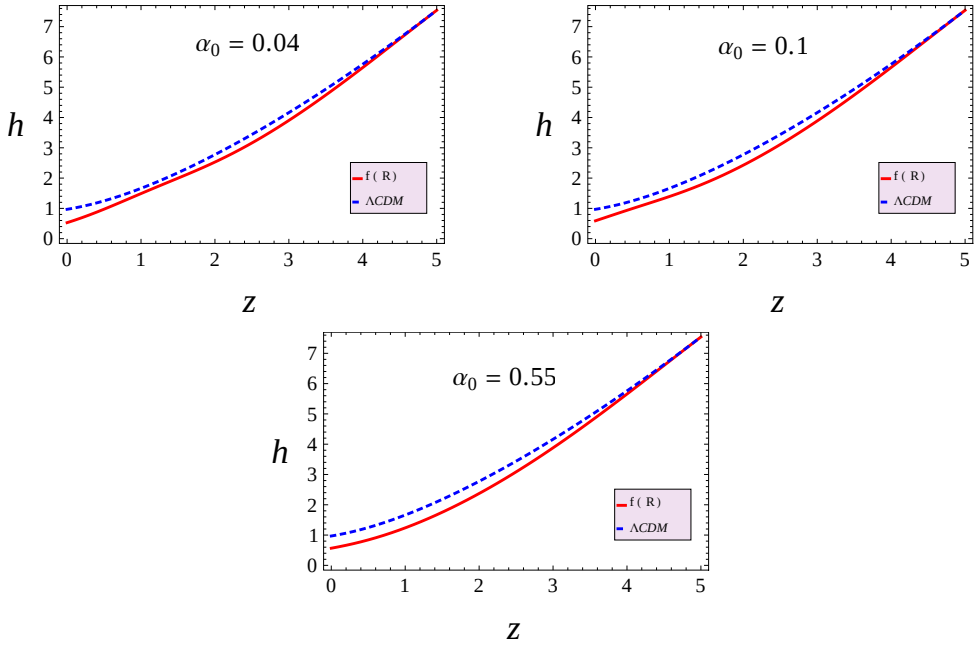

FIGURE 5.2: A comparison between the evolution of normalized Hubble parameter in ΛCDM model and the $f(R)$ gravity $R\ln R$ model.

5.8.3 Deceleration parameter $q(z)$

The deceleration parameter in the ΛCDM model is given by [21]

$$q = \frac{1}{2}\left(\frac{\Omega_{m,0}(1+z)^3 - 2\Omega_{\Lambda,0}}{\Omega_{m,0}(1+z)^3 + \Omega_{\Lambda,0}}\right), \tag{5.64}$$

whilst in the $R\ln R$ model, the deceleration parameter is given by

$$q = 1 - \tilde{v}. \tag{5.65}$$

Fig [5.3] exhibits the evolution of the deceleration parameter in both the $R\ln R$ and the ΛCDM model. Although choosing $\alpha_0 = 0.04$ or 0.1 leads to discrepancies between the two models and makes the $R\ln R$ model gain undesirable behaviour at the present epoch; i.e. the universe decelerating instead of accelerating, assigning $\alpha_0 = 0.55$ makes a major change in the behaviour of the universe in the present epoch and gives the universe the required acceleration.

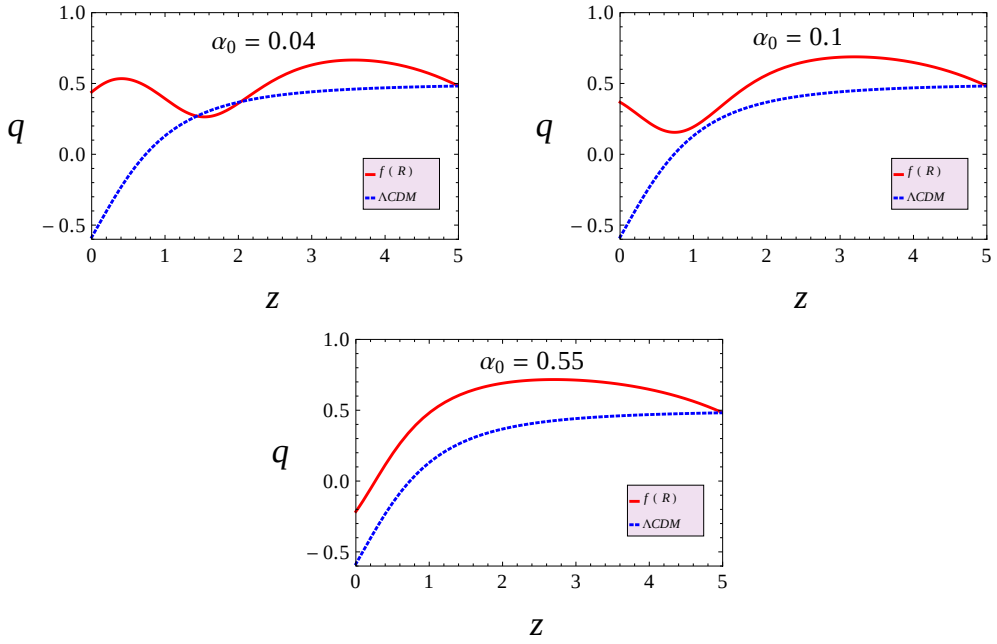

FIGURE 5.3: A comparison between the evolution of deceleration parameter in the ΛCDM model and the $R \ln R$ model.

5.8.4 The Effective Equation of State w_{eff}

We discuss the different parametrizations through which we cast the effective equation of state. We stress that the different expressions for effective equation of state come as a natural result to the way in which we construct the modified field equations. Although there is a debate about which parametrization expresses the real physical state of the system under study, there is no doubt that the total equation of state should be the same as it expresses the physical state of the regime regardless of the way in which the field equations are being formulated. Particularly, for our model we could reveal that the outputs of the two different methods is the same.

5.8.4.1 The first method for obtaining, w_{Eff}

If we set the modified field equation as

$$G_{\mu\nu} = R_{\mu\nu} - \frac{1}{2} g_{\mu\nu} R = T^{(eff)}_{\mu\nu} + \frac{T^{m}_{\mu\nu}}{f'(R)}, \tag{5.66}$$

with

$$T^{(eff)}_{\mu\nu} = \frac{1}{f'(R)} [\frac{f(R) - R f'(R)}{2} g_{\mu\nu} + (\nabla_\mu \nabla_\nu - g_{\mu\nu} \Box) f'(R)], \tag{5.67}$$

then the two Friedmann's equations are

$$H^2 = \frac{1}{3f'}[\rho_m + \frac{1}{2}(f'R - f) - 3H\dot{R}f''], \tag{5.68}$$

$$-\dot{H} = \frac{1}{2f'}[\rho_m + P_m + \ddot{R}f'' + f'''\dot{R}^2 - H\dot{R}f'']. \tag{5.69}$$

In this case, we read off energy density and pressure of the dark-energy component from (5.69) and (5.69) directly

$$\tilde{\rho}_{DE} = \frac{1}{f'}[\frac{1}{2}(f - Rf') - 3H\dot{R}f''], \tag{5.70}$$

$$\tilde{P}_{DE} = \frac{1}{f'}[2H\dot{R}f'' + \ddot{R}f'' + \dot{R}^2 f''' + \frac{1}{2}(f - Rf')]. \tag{5.71}$$

The non-conservation of continuity equation is given by

$$\dot{\tilde{\rho}}_{DE} + 3H(\tilde{\rho}_{DE} + \tilde{P}_{DE}) = \frac{\dot{f}'}{f'^2}\rho_m, \tag{5.72}$$

the last equation can be re-formulated in the following form

$$\dot{\tilde{\rho}}_{DE} + 3H\tilde{\rho}_{DE}(1 + \tilde{w}_{DE} - \frac{\dot{f}'}{3Hf'^2}\rho_m) = 0. \tag{5.73}$$

Consequently, the effective equation of state reads

$$w_{Eff} = \tilde{w}_{DE} - \frac{\dot{f}'}{3Hf'^2}\rho_m. \tag{5.74}$$

The last equation can be reformulated in terms of the non-compact variables (5.46) as follows

$$w_{Eff} = \tilde{w}_{DE} - \frac{\tilde{x}\tilde{\Omega}_m}{3(1 - \tilde{\Omega}_m)}. \tag{5.75}$$

The expressions for $\tilde{\rho}_{DE}$ and $\tilde{P}_{DE}$ [124] are given by

$$\tilde{\rho}_{DE} = 3H^2(1 - \tilde{\Omega}_m), \tag{5.76}$$

and

$$\tilde{P}_{DE} = 3H^2(-1 - \frac{2}{3}(\tilde{v} - 2)), \tag{5.77}$$

in turn, the dark energy equation of state is written as

$$\begin{aligned} \tilde{w}_{DE} &= \frac{\tilde{P}_{DE}}{\tilde{\rho}_{DE}} \\ &= \frac{-1-\frac{2}{3}(\tilde{v}-2)}{1-\tilde{\Omega}_m} \\ &= \frac{1-2\tilde{v}}{3(1-\tilde{\Omega}_m)}. \end{aligned} \tag{5.78}$$

Substituting (5.78) into (5.75), the effective equation of state then takes the form

$$w_{Eff} = \frac{1-2\tilde{v}-\tilde{\Omega}_m\tilde{x}}{3(1-\tilde{\Omega}_m)}. \tag{5.79}$$

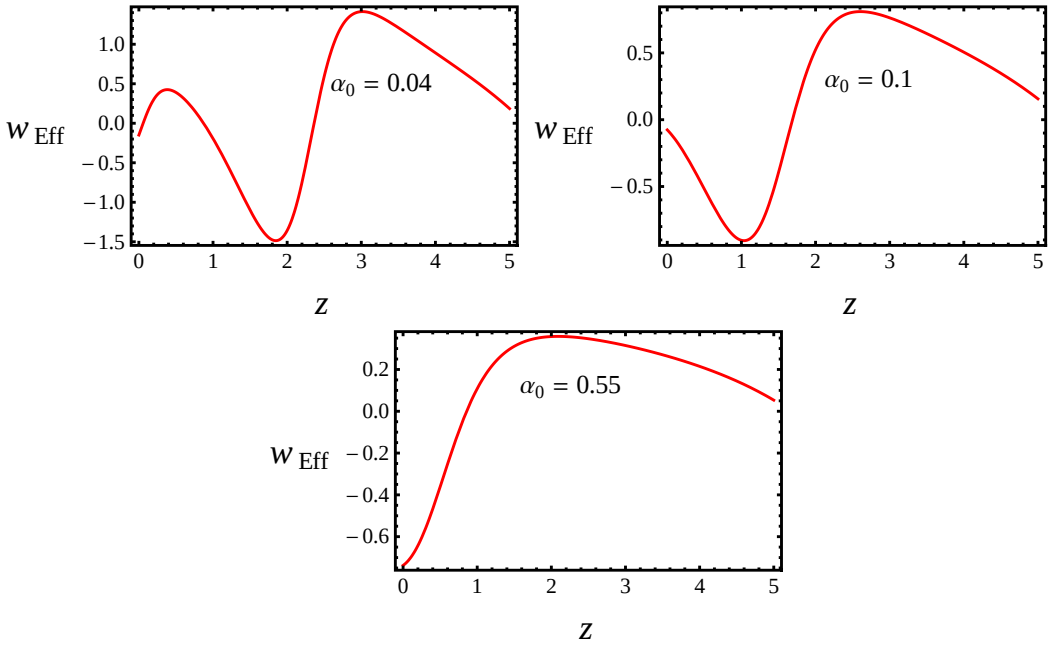

FIGURE 5.4: A comparison between the evolution of the effective equation of state in the model $R \ln R$. The parameter R_0 is always equal to unity

The evolution of the total equation of state w_{Tot} exhibits a negative value at the present epoch ($z = 0$), which is interesting since a negative value of the total equation of state accounts for the present cosmic speed-up.

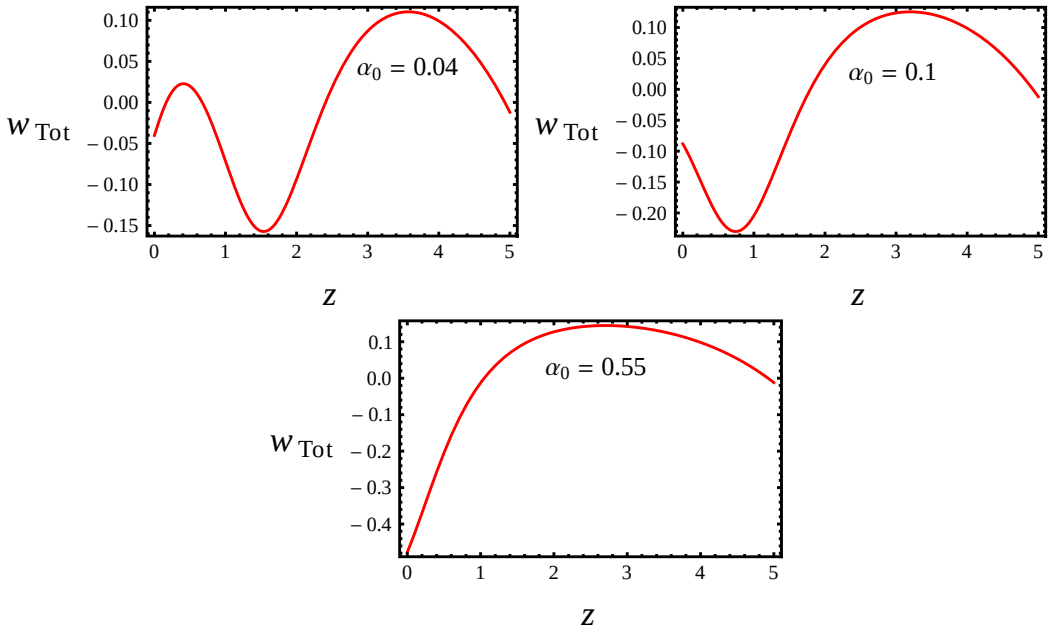

FIGURE 5.5: A comparison between the evolution of the total equation of state in the model $R \ln R$.

5.8.4.2 The second method for obtaining, w_{Eff}

In this approach we manipulate the modified field equations in order to suppress the non-minimal coupling $1/f'(R)$ between the geometry and the matter field.

$$G_{\mu\nu} = T^{m}_{\mu\nu} + \tilde{T}^{(eff)}_{\mu\nu}, \tag{5.80}$$

with

$$\tilde{T}^{(eff)}_{\mu\nu} = \frac{f(R) - Rf'(R)}{2} g_{\mu\nu} + (\nabla_\mu \nabla_\nu - g_{\mu\nu}\Box) f'(R) + (1 - f'(R)) G_{\mu\nu}. \tag{5.81}$$

and

$$\begin{aligned} \rho_{Eff} &= 3H^2 - \rho_{total} \\ &= -3(1 - f')(\dot{H} + H^2) + \frac{R - f}{2} - 3H\dot{f}' \\ &= \frac{f(R) - Rf'(R)}{2} - 3H\dot{f}' + 3H^2(1 - f'), \end{aligned} \tag{5.82}$$

$$\begin{aligned} P_{Eff} &= H^2 - \frac{R}{3} \\ &= \ddot{f}' + 2H\dot{f}' + \frac{f(R) - Rf'(R)}{2} + (H^2 - \frac{R}{3})(1 - f'). \end{aligned} \tag{5.83}$$

Then, the effective equation of state w_{Eff} is obtained by

$$w_{Eff} = \frac{P_{Eff}}{\rho_{Eff}} = \frac{1 - 2\tilde{v}}{3(1 - \Omega_m f')}. \tag{5.84}$$

Finally, the total equation of state gives

$$w_{Tot} = \frac{1 - 2\tilde{v}}{3}. \tag{5.85}$$

Obviously, opting for the parameter $\alpha = 0.55$ gives a desirable behaviour to the total equation of state i.e. it reaches -0.5 at the present epoch. This could possibly explain how the cosmic speed-up could arise as a consequence of modifying the gravity. Although the total equation of state exhibits a good behaviour, one can observe that several singularities appear in Fig [5.6]. These singularities are not recovered even when the value of the parameter α_0 increases. Moreover, the model suffers phantom behaviour, and again this behaviour cannot be recovered by increasing the value of α_0. We conclude that it is better to use the first method in calculating the effective equation of state (5.79);

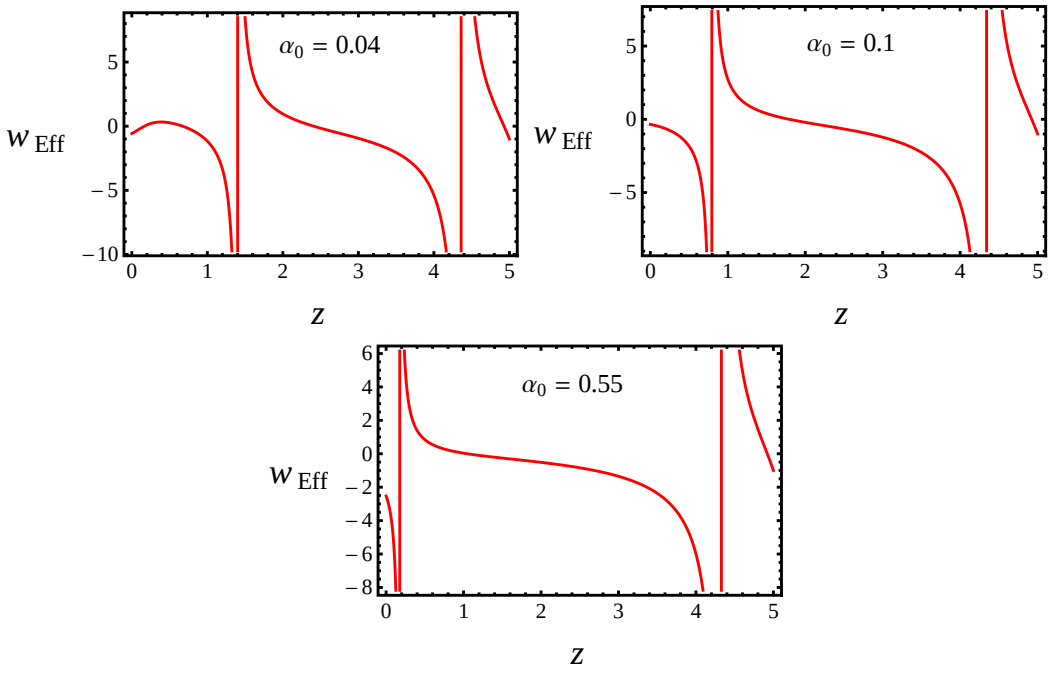

FIGURE 5.6: The evolution of the effective equation of state w_{Eff} for the model $R \ln R$, using the second method.

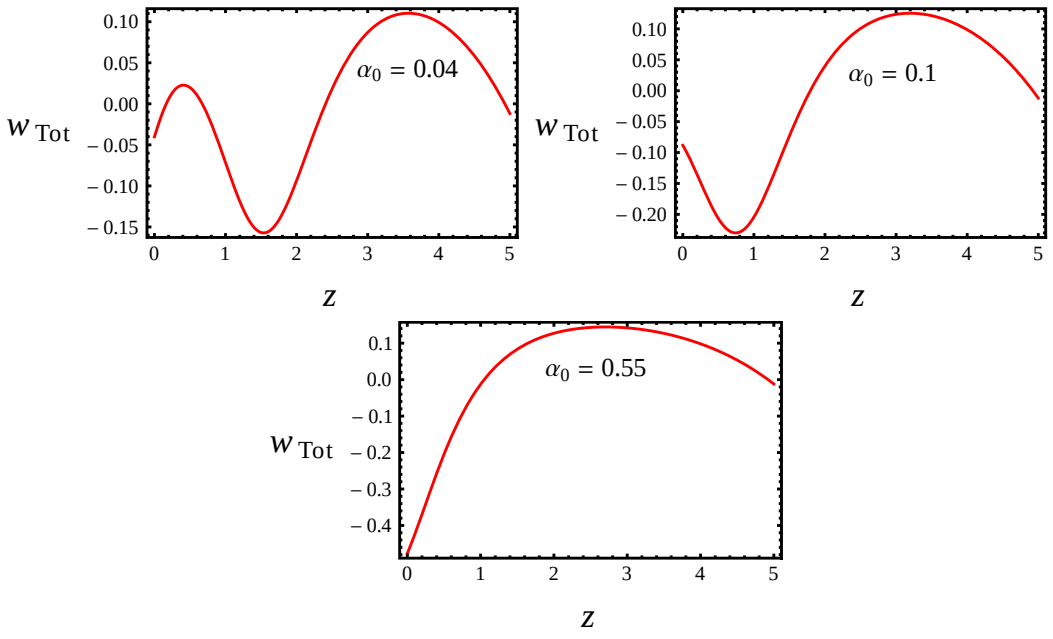

FIGURE 5.7: The evolution of the total equation of state w_{Tot} for the model $R \ln R$, using the second method.

the method cured the model from two very undesirable behaviours i.e. singularities in solutions and phantom behaviour.

5.9 Comparing the model $R(1+\alpha_0 \ln(\frac{R}{R_0}))$ with ΛCDM model at $z_0 = 20$

In this section, we integrate the system (5.54) with initial conditions evaluated at red shift $z_0 = 20$. Our motivation behind this selection to the initial value is seeking the possibility that changing the initial condition might lead to a better results regarding the value of the total equation of state at the present epoch, the thing will reinforcement the cosmic speed-up phenomena. Hereafter, the results of the comparisons between the logarithmic f(R) model and the ΛCDM model

5.9.1 Initial conditions for $R(1 + \alpha_0 \ln(\frac{R}{R_0}))$ with ($R_0 = 1$& $\alpha_0 = 0.04$) at $z_0 = 20$

In order to integrate system (5.54) we need to compute the initial value of each non-compact variable contributed to that system. We use the present day ($z_0 = 0$) values for Ω_m and Ω_Λ

$$\Omega_{m0} = 0.26, \quad \Omega_{\Lambda 0} = 0.68. \tag{5.86}$$

We use the last equation to evaluate the initial values of the normalized Hubble parameter and the deceleration parameter at $z_0 = 20$,

$$h_0(z_0 = 20) = \sqrt{\Omega_{m0}(1 + z_0)^3 + \Omega_{\Lambda 0}} = 49.0769, \tag{5.87}$$

and

$$q_0(z_0 = 20) = \frac{\Omega_{m0}(1 + z_0)^3 - 2\Omega_{\Lambda 0}}{2(\Omega_{m0}(1 + z_0)^3 + \Omega_{\Lambda 0})} = 0.4995775. \tag{5.88}$$

Now we proceed with calculating the initial values of the non-compact dynamical variables, as follows

$$\tilde{r}_0 = 6h_0^2(1 - q_0) = 7231.74, \tag{5.89}$$

$$\tilde{v}_0 = 1 - q_0 = 0.500423, \tag{5.90}$$

$$\tilde{\Omega}_{m0} = \frac{\Omega_{m0}(1 + z_0)^3}{h_0^2(1 + \alpha_0 + \alpha_0 \ln(\tilde{r}_0))} = 0.716413, \tag{5.91}$$

$$\tilde{y}_0 = \frac{\tilde{r}_0(1 + \alpha_0 \ln(\tilde{r}_0))}{6h_0^2(1 + \alpha_0 + \alpha_0 \ln(\tilde{r}_0))} = 0.486079, \tag{5.92}$$

we use the constraint (5.47) to find out the initial value of $\tilde{x}$,

$$\tilde{x}_0 = \tilde{\Omega}_{m0} + \tilde{v}_0 - \tilde{y}_0 - 1 = -0.269243 \tag{5.93}$$

5.9.2 Hubble parameter $h(z)$

In the ΛCDM model, the dimensionless Hubble parameter (h) as a function of red shift is given by:

$$h(z) = \sqrt{\Omega_{m0}(1+z)^3 + \Omega_{\Lambda 0}}. \tag{5.94}$$

While the dimensionless Hubble parameter (h) in the $R \ln R$ model can be obtained once we integrate the system (5.54) numerically. Fig [5.8] below shows a comparison between the evolution the parameter ($h(z)$) in the two models.

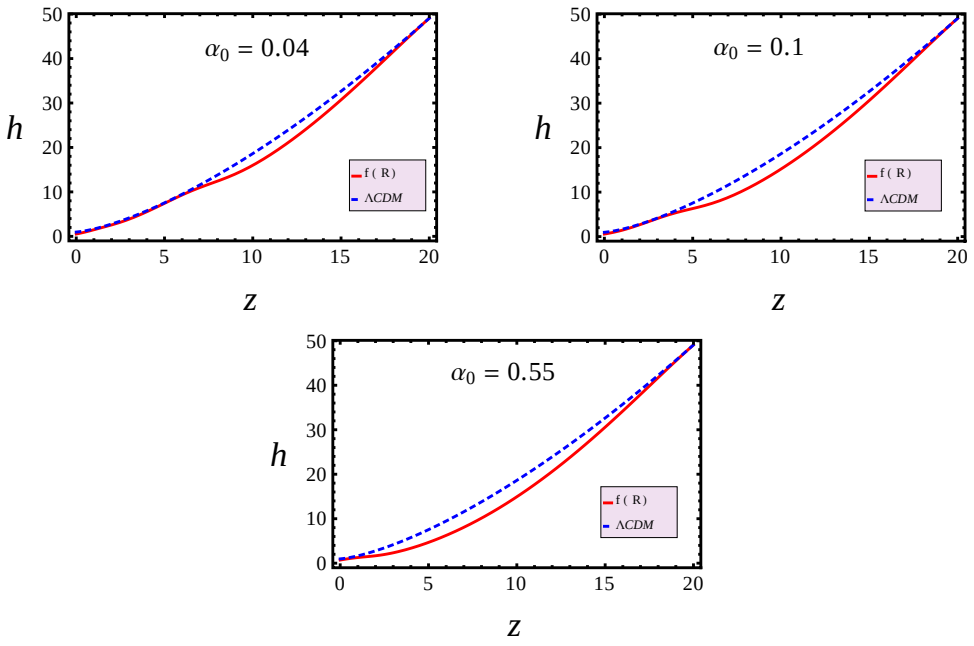

FIGURE 5.8: A comparison between the evolution of normalized Hubble parameter in ΛCDM model and the $f(R)$ gravity $R \ln R$ model.

5.9.3 Deceleration parameter $q(z)$

The deceleration parameter in ΛCDM is proposed as

$$q = \frac{1}{2}\left(\frac{\Omega_{m,0}(1+z)^3 - 2\Omega_{\Lambda,0}}{\Omega_{m,0}(1+z)^3 + \Omega_{\Lambda,0}}\right), \tag{5.95}$$

while in $R \ln R$ model, the deceleration parameter is given by

$$q = 1 - \tilde{v}. \tag{5.96}$$

One can observe that increasing the value of the parameter α_0, makes the behaviour of the deceleration parameter of $f(R)$ closer to the behaviour of ΛCDM model.

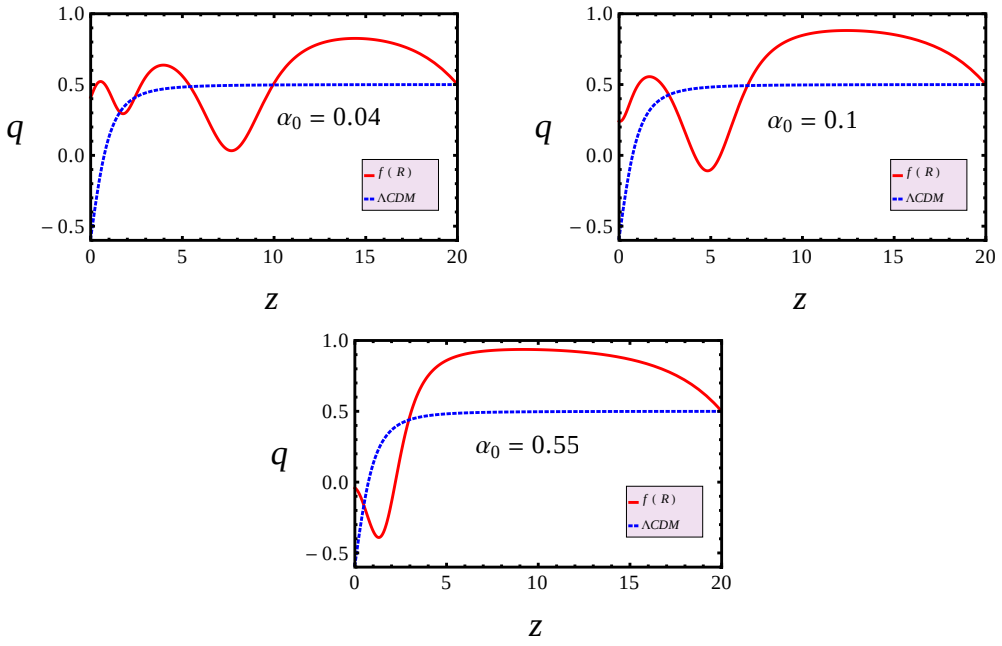

FIGURE 5.9: A comparison between the evolution of deceleration parameter in ΛCDM model and the $f(R)$ gravity $R \ln R$ model.

5.9.4 The total equation of state w_{Tot}

In a previous section, we demonstrated two methods to derive the effective equation of state and as a consequence derived the total equation of state. One of the motivations was clarifying that the total equation of state stays the same regardless of derivation methods. In this subsection, we show that by adjusting the value of the parameter α_0 to be around 0.55, we can attain a good behaviour for the total equation of state. At the present cosmological epoch, the total equation of state reaches $w_{Tot} = -0.36$. Although This value for w_{Tot} meets the critical condition for an accelerated expansion epoch, the value is too far from the constraints implied by the recent observations i.e.$w_{Tot} \approx -1$.

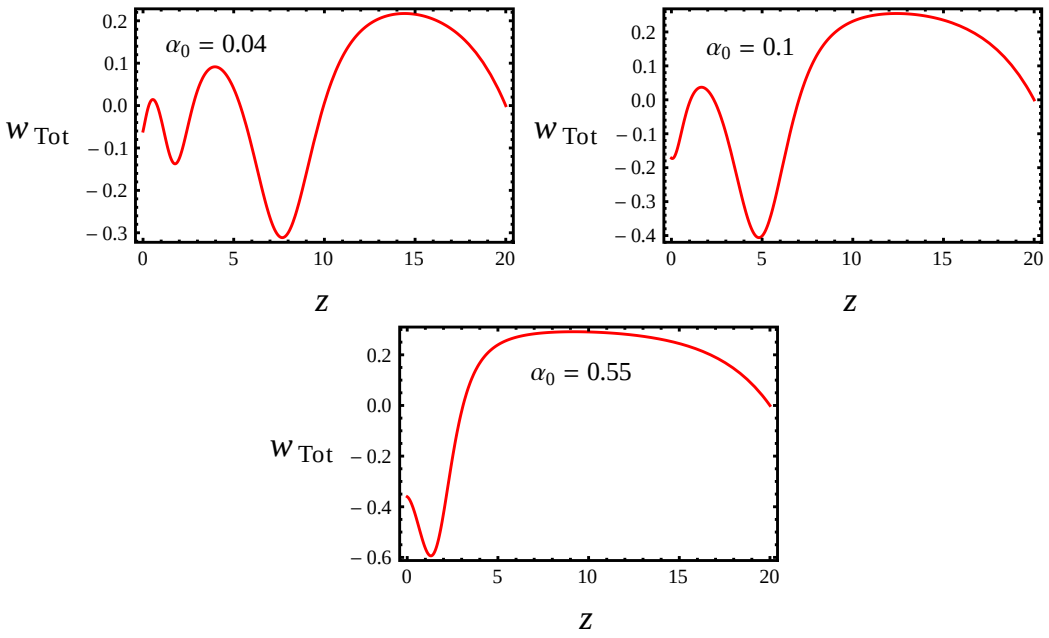

FIGURE 5.10: The evolution of the total equation of state w_{Tot} for the model $R \ln R$, using the second method.

5.10 Concluding Remarks

This chapter has been dedicated to present some new original work on studying the model $R(1 + \alpha_0 \ln(\frac{R}{R_0}))$. Before we started in studying the dynamics of the model, I paved the way by revisiting the calculations in [7]. This paper is considered as one of the most lucid sources in studying the dynamics of the cosmological models. After that, we established a parallel study to the dynamics of the model $R \ln R$. First, we investigated the dynamics of vacuum case and later on the matter case. For both cases we introduced new normalized cosmological parameters, these parameters are very helpful in compacting the phase space and, moreover, help to study the fixed points lying at infinity. A detailed classification of the fixed points and the solution for the scale factor at each of fixed point has been established. Although the compact phase space analysis is advantageous, a non-compact phase space analysis should be constructed to study the expansion history of the model. Consequently, we introduced another set of normalized cosmological variables. The expansion history, then, can be obtained if we integrate the system (5.54). We incorporated the initial conditions of the ΛCDM model in the new non-compact variables in order to obtain the initial conditions of the $R(1 + \alpha_0 \ln(\frac{R}{R_0}))$ model at red shift $z = 5$ and $z = 20$. We calculated the effective equation of state with two methods, and I proved that the total equation of state is the same regardless which method is used. The parameters of the model $R(1 + \alpha_0 \ln(\frac{R}{R_0}))$ need to be fine-tuned in order to have a desirable behaviour.

Chapter 6

Final Remarks

The underlying aim of this thesis was to discuss the application of dynamical systems theory to the field of Extended Theories of Gravity (ETG). The dynamical systems approach has been shown to be very useful in studying (ETG). Due to the high complex nature of this type of theories, it is not easy to gain an understanding of stability and global behaviour of the underlying cosmological models. The dynamical systems approach addresses some of these problems, since it provides one with exact solutions through the determination of equilibrium points and a (qualitative) description of the global dynamics of the system. In this thesis we have adopted this method to study the cosmologies associated with the $R \ln R$ model. A theory with a Lagrangian of the type $R(1 + \alpha_0 \ln(\frac{R}{R_0}))$ first considered in [122], the underlying idea is making use of the effective field theory to resolve the hierarchy problem between the Planck scale and the infra-red cosmological acceleration scale. The study of the model firstly focused on compactifying the phase space to study the fixed points which lay at infinity. In more detail, we identified the analytical fixed points and the non-analytical fixed points, classified their types (repeller, attractor,..., etc), determined their stability, and the exact solutions at every point. Secondly, we investigated the non-compact version of the dynamics, which allowed to have a close look at the expansion history of the model. We, then, established a comparison between the expansion history of the well known ΛCDM model and the $R \ln R$ model. The comparison between the two models revealed that $R \ln R$ model's parameters need to be fine-tuned in order to have a good evolution for the total equation of state, enabling it to account for the current cosmic speed-up. For specific values of the parameter α_0, we obtained a good value for the present day total equation of state which revealed that the accelerated expansion epoch which our universe experiences has a geometrical origin. Although in my study the model's total equation of state has a negative value at the present epoch, the model failed to show the correct cosmological evolution, namely the model did not admit any matter-domination

epoch after the radiation epoch. This was anticipated, since the fixed points have not included any matter-like points. In our probing to this model we employed a flat FLRW metric, so we think it is worthwhile to construct a separate study in which the spatial curvature is considered. Instead of fine-tuning the model parameters, they need to be constrained by the data. The response of the Cosmic Microwave Background power spectrum, the growth of structure and the Newtonian limit, to the general modification of GR must be investigated and confronted with current observations such as the latest CMB data from Planck, BAO and gravitational lensing data to obtain new constraints on the form of f(R).

Appendix A

Stability of the fixed points $\mathcal{C}_{\pm}$,$\mathcal{D}_{\pm}$ and $\mathcal{E}$ in the vacuum case

In chapter 4, we demonstrated a problem which encounters the dynamical phase space analysis: The phase space portrait shows some fixed points $\mathcal{C}_{\pm}$,$\mathcal{D}_{\pm}$ and $\mathcal{E}$, but these fixed points cannot be extracted by the usual mathematical procedure. In order to classify these fixed points, we solved the cosmological equations numerically with initial conditions taken around every fixed point. Fig [??] shows the behaviour of the solution curves in the vicinity of each point.

- For the fixed point $\mathcal{C}_{+}$; if we take the initial conditions to be close to the point, the solution curves, $x(t)$ and $Q(t)$, move forward from the fixed point and approach another fixed point. This suggests that the fixed point is a Repeller.
- The fixed point $\mathcal{C}_{-}$ is different because the solution curves approach the fixed point as the time grows, in other words the fixed point attracts the curves toward it. Clearly, $\mathcal{C}_{-}$ represents an attractor.
- The same argument applies for the the two fixed points $\mathcal{D}_{\pm}$. Their classifications are Repeller and attractor, respectively.
- The last fixed point $\mathcal{E}$ is a saddle as the solution curves do not approach the point neither in the history nor the future.

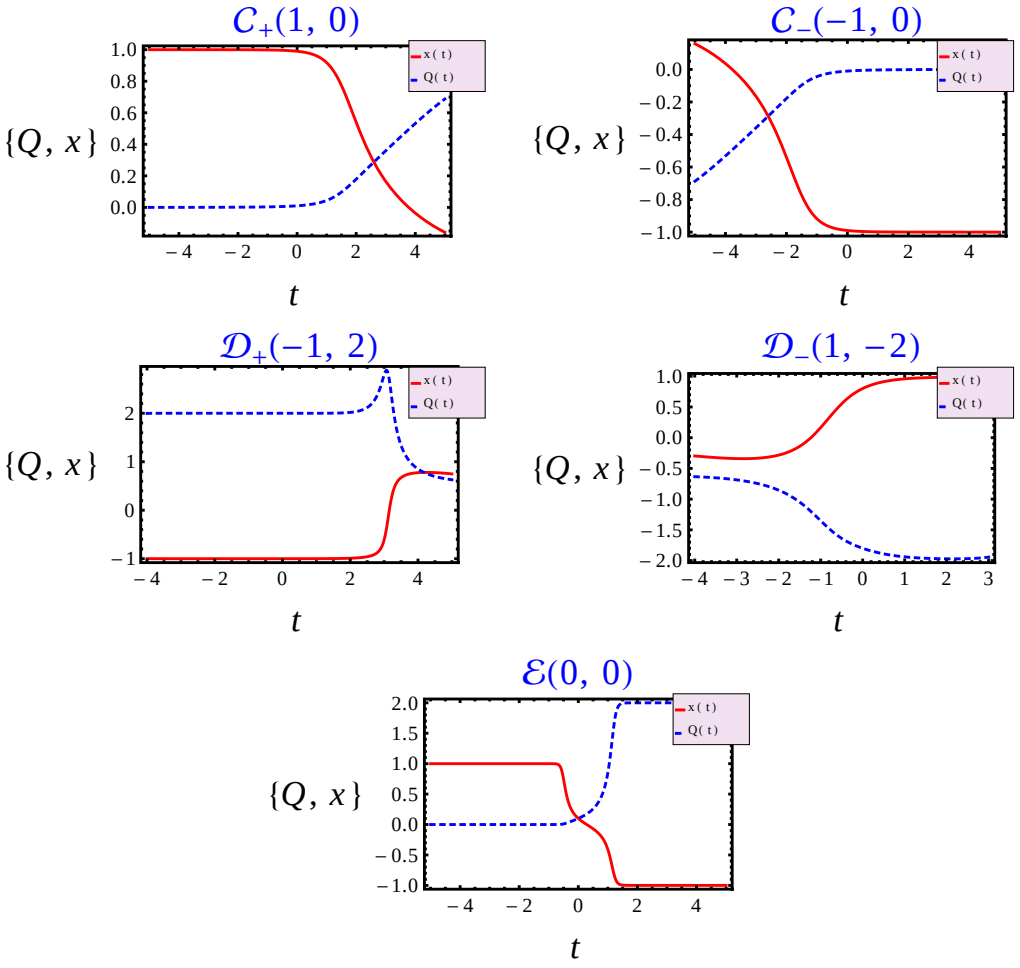

FIGURE A.1: The evolution of the solution of the cosmological equation of the vacuum case around every non-analytic fixed point.

Appendix B

The exact solutions at the fixed points $\mathcal{C}_{\pm}$ and $\mathcal{E}$

In case of the fixed points $\mathcal{C}_{\pm}$ and $\mathcal{E}$, the exact solutions at these fixed points can be regularly derived if we guarantee that the quantity $\frac{1-x^2}{6Q^2}$ vanishes over time at each of the three fixed points.

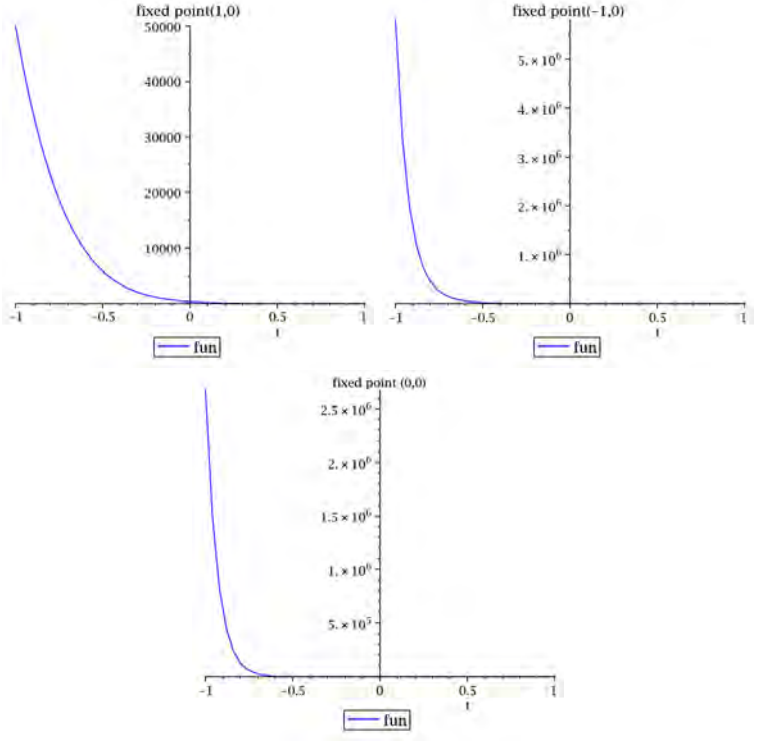

FIGURE B.1: The evolution of the function $\frac{1-x^2}{6Q^2}$ over time. The plots show that this quantity reaches zero at each of the three fixed points.

Bibliography

[1] Planck Collaboration. Planck 2013 results. XXII. Constraints on inflation. page 44, March 2013. URL http://arxiv.org/abs/1303.5082.

[2] Wilkinson Microwave Anisotropy Probe (WMAP). URL http://map.gsfc.nasa.gov/.

[3] Daniel Baumann. TASI Lectures on Inflation. 2009. URL http://inspirehep.net/record/827549/citations?ln=en.

[4] P.A.R. Ade, R.W. Aikin, D. Barkats, S.J. Benton, C.A. Bischoff, J.J. Bock, J.A. Brevik, I. Buder, E. Bullock, C.D. Dowell, L. Duband, J.P. Filippini, S. Fliescher, S.R. Golwala, M. Halpern, M. Hasselfield, S.R. Hildebrandt, G.C. Hilton, V.V. Hristov, K.D. Irwin, K.S. Karkare, J.P. Kaufman, B.G. Keating, S.A. Kernasovskiy, J.M. Kovac, C.L. Kuo, E.M. Leitch, M. Lueker, P. Mason, C.B. Netterfield, H.T. Nguyen, R. O'Brient, R.W. Ogburn, A. Orlando, C. Pryke, C.D. Reintsema, S. Richter, R. Schwarz, C.D. Sheehy, Z.K. Staniszewski, R.V. Sudiwala, G.P. Teply, J.E. Tolan, A.D. Turner, A.G. Vieregg, C.L. Wong, and K.W. Yoon. Detection of ¡span class="aps-inline-formula"¿¡math xmlns="http://www.w3.org/1998/Math/MathML" display="inline"¿¡mi¿B¡/mi¿¡/math¿¡/span¿-Mode Polarization at Degree Angular Scales by BICEP2. *Physical Review Letters*, 112(24):241101, June 2014. ISSN 0031-9007. doi: 10.1103/PhysRevLett.112.241101. URL http://arxiv.org/abs/1403.3985.

[5] Steven Henry Strogatz. *Nonlinear Dynamics and Chaos: With Applications to Physics, Biology, Chemistry, and Engineering*. Westview Press, 1994. ISBN 0738204536. URL http://books.google.co.za/books/about/Nonlinear_Dynamics_and_Chaos.html?id=FIYHiBLWCJMC&pgis=1.

[6] Method of Lyapunov Functions. URL http://www.math24.net/method-of-lyapunov-functions.html.

[7] Martin Goliath and George Ellis. Homogeneous cosmologies with a cosmological constant. *Physical Review D*, 60(2):023502, May 1999. ISSN 0556-2821. doi: 10.1103/PhysRevD.60.023502. URL http://arxiv.org/abs/gr-qc/9811068.

[8] Albert Einstein. Cosmological Considerations in the General Theory of Relativity. *Sitzungsber.Preuss.Akad.Wiss.Berlin (Math.Phys.)*, 1917:142–152, 1917.

[9] George Gamow. *My world line; an informal autobiography*. Viking Press, 1970. URL http://books.google.co.za/books/about/My_world_line_an_informal_autobiography.html?id=KdHvAAAAMAAJ&pgis=1.

[10] Riesset al. Observational Evidence from Supernovae for an Accelerating Universe and a Cosmological Constant. *The Astronomical Journal*, 116(3):1009–1038, September 1998. ISSN 00046256. doi: 10.1086/300499. URL http://arxiv.org/abs/astro-ph/9805201.

[11] S. et al Perlmutter. Measurements of Ω and Λ from 42 HighRedshift Supernovae. *The Astrophysical Journal*, 517(2):565–586, June 1999. ISSN 0004-637X. doi: 10.1086/307221. URL http://iopscience.iop.org/0004-637X/517/2/565/fulltext/.

[12] Andrew Liddle. *An Introduction to Modern Cosmology*. John Wiley & Sons, 2013. ISBN 1118723414. URL http://books.google.com/books?id=t-nbsrjMWK8C&pgis=1.

[13] E. Hubble. A relation between distance and radial velocity among extra-galactic nebulae. *Proceedings of the National Academy of Sciences*, 15(3):168–173, March 1929. ISSN 0027-8424. doi: 10.1073/pnas.15.3.168. URL http://adsabs.harvard.edu/abs/1929PNAS...15..168H.

[14] Wendy L. Freedman, Barry F. Madore, Brad K. Gibson, Laura Ferrarese, Daniel D. Kelson, Shoko Sakai, Jeremy R. Mould, Robert C. Kennicutt, Jr., Holland C. Ford, John A. Graham, John P. Huchra, Shaun M. G. Hughes, Garth D. Illingworth, Lucas M. Macri, and Peter B. Stetson. Final Results from the Hubble Space Telescope Key Project to Measure the Hubble Constant. *The Astrophysical Journal*, 553(1):47–72, May 2001. ISSN 0004-637X. doi: 10.1086/320638. URL http://arxiv.org/abs/astroph/0012376.

[15] Sean M. Carroll, Vikram Duvvuri, Mark Trodden, and Michael S. Turner. Is cosmic speed-up due to new gravitational physics? *Physical Review D*, 70(4):043528, August 2004. ISSN 1550-7998. doi: 10.1103/PhysRevD.70.043528. URL http://link.aps.org/doi/10.1103/PhysRevD.70.043528.

[16] C. L. Bennett, M. Halpern, G. Hinshaw, N. Jarosik, A. Kogut, M. Limon, S. S. Meyer, L. Page, D. N. Spergel, G. S. Tucker, E. Wollack, E. L. Wright, C. Barnes, M. R. Greason, R. S. Hill, E. Komatsu, M. R. Nolta, N. Odegard, H. V. Peiris, L. Verde, and J. L. Weiland. FirstYear Wilkinson Microwave Anisotropy Probe (WMAP) Observations: Preliminary Maps and Basic Results. *The Astrophysical Journal Supplement Series*, 148(1):1–27, September 2003. ISSN 0067-0049. doi: 10.1086/377253. URL http://arxiv.org/abs/astro-ph/0302207.

[17] Ruth Durrer. *The Cosmic Microwave Background [Hardcover]*. Cambridge University Press; 1 edition, 2008. ISBN 0521847044. URL http://www.amazon.com/Cosmic-Microwave-Background-Ruth-Durrer/dp/0521847044.

[18] P. J. E. Peebles. Principles of Physical Cosmology. *Principles of Physical Cosmology by P.J.E. Peebles. Princeton University Press, 1993. ISBN: 978-0-691-01933-8*, -1, 1993. URL http://adsabs.harvard.edu/abs/1993ppc..book.....P.

[19] Ray D'Inverno. *Introducing Einstein's Relativity*. 1992. ISBN 0198596863. URL http://books.google.fr/books/about/Introducing_Einstein_s_Relativity.html?hl=fr&id=yqcT3VICuvMC&pgis=1.

[20] Scott Dodelson. *Modern Cosmology*. Academic Press, 2003. ISBN 0122191412. URL http://books.google.co.za/books/about/Modern_Cosmology.html?id=3oPRxdXJexcC&pgis=1.

[21] M. P. Hobson, G. P. Efstathiou, and A. N. Lasenby. *General Relativity: An Introduction for Physicists*. Cambridge University Press, 2006. ISBN 1139447548. URL http://books.google.co.za/books/about/General_Relativity.html?id=xma1QuTJphYC&pgis=1.

[22] D. N. et al. Spergel. ThreeYear Wilkinson Microwave Anisotropy Probe (WMAP) Observations: Implications for Cosmology. *The Astrophysical Journal Supplement Series*, 170(2):377–408, June 2007. ISSN 0067-0049. doi: 10.1086/513700. URL http://arxiv.org/abs/astroph/0603449.

[23] EDMUND J. COPELAND, M. SAMI, and SHINJI TSUJIKAWA. DYNAMICS OF DARK ENERGY. *International Journal of Modern Physics D*, 15(11):1753–1935, November 2006. ISSN 0218-2718. doi: 10.1142/S021827180600942X. URL http://www.worldscientific.com/doi/abs/10.1142/S021827180600942X.

[24] Gianfranco Bertone, Dan Hooper, and Joseph Silk. Particle dark matter: evidence, candidates and constraints. *Physics Reports*, 405(5-6):279–390, January 2005. ISSN 03701573. doi: 10.1016/j.physrep.2004.08.031. URL http://arxiv.org/abs/hep-ph/0404175.

[25] F. Zwicky. Die Rotverschiebung von extragalaktischen Nebeln. *Helvetica Physica Acta*, 6:110–127, 1933. ISSN 0018-0238. URL http://adsabs.harvard.edu/abs/1933AcHPh...6..110Z.

[26] GRACIELA B. GELMINI. SEARCH FOR DARK MATTER. *International Journal of Modern Physics A*, 23(26):4273–4288, October 2008. ISSN 0217-751X. doi: 10.1142/S0217751X08042729. URL http://arxiv.org/abs/0810.3733.

[27] F. Ruppin, J. Billard, E. Figueroa-Feliciano, and L. Strigari. Complementarity of dark matter detectors in light of the neutrino background. *Physical Review D*, 90 (8):083510, October 2014. ISSN 1550-7998. doi: 10.1103/PhysRevD.90.083510. URL http://link.aps.org/doi/10.1103/PhysRevD.90.083510.

[28] Andrew R. Liddle and David H. Lyth. *Cosmological Inflation and Large-Scale Structure*. Cambridge University Press, 2000. ISBN 0521575982. URL http://books.google.co.za/books/about/Cosmological_Inflation_and_Large_Scale_S.html?id=XmWauPZSovMC&pgis=1.

[29] Peter Niessen and for the AMANDA Collaboration. Recent Results from the AMANDA Experiment. June 2003. URL http://arxiv.org/abs/astro-ph/0306209.

[30] Sean M. Carroll. The Cosmological Constant. *Living Reviews in Relativity*, 4, 2001. ISSN 1433-8351. doi: 10.12942/lrr-2001-1. URL http://relativity.livingreviews.org/Articles/lrr-2001-1/.

[31] Ivaylo Zlatev, Limin Wang, and Paul Steinhardt. Quintessence, Cosmic Coincidence, and the Cosmological Constant. *Physical Review Letters*, 82(5):896–899, February 1999. ISSN 0031-9007. doi: 10.1103/PhysRevLett.82.896. URL http://link.aps.org/doi/10.1103/PhysRevLett.82.896.

[32] Shinji Tsujikawa. Quintessence: A Review. page 20, April 2013. URL http://arxiv.org/abs/1304.1961.

[33] R.R Caldwell. A phantom menace? Cosmological consequences of a dark energy component with super-negative equation of state. *Physics Letters B*, 545(1-2): 23–29, October 2002. ISSN 03702693. doi: 10.1016/S0370-2693(02)02589-3. URL http://arxiv.org/abs/astroph/9908168.

[34] Takeshi Chiba, Takahiro Okabe, and Masahide Yamaguchi. Kinetically driven quintessence. *Physical Review D*, 62(2):023511, June 2000. ISSN 0556-2821. doi: 10.1103/PhysRevD.62.023511. URL http://arxiv.org/abs/astro-ph/9912463.

[35] C. Armendariz-Picon, V. Mukhanov, and Paul Steinhardt. Dynamical Solution to the Problem of a Small Cosmological Constant and Late-Time Cosmic Acceleration. *Physical Review Letters*, 85(21):4438–4441, November 2000. ISSN 0031-9007. doi: 10.1103/PhysRevLett.85.4438. URL http://arxiv.org/abs/astro-ph/0004134.

[36] C. Armendariz-Picon, V. Mukhanov, and Paul Steinhardt. Essentials of k-essence. *Physical Review D*, 63(10):103510, April 2001. ISSN 0556-2821. doi: 10.1103/PhysRevD.63.103510. URL http://arxiv.org/abs/astro-ph/0006373.

[37] T. Padmanabhan. Accelerated expansion of the universe driven by tachyonic matter. *Physical Review D*, 66(2):021301, June 2002. ISSN 0556-2821. doi: 10.1103/PhysRevD.66.021301. URL http://arxiv.org/abs/hep-th/0204150.

[38] T. Padmanabhan and T. Choudhury. Can the clustered dark matter and the smooth dark energy arise from the same scalar field? *Physical Review D*, 66(8):081301, October 2002. ISSN 0556-2821. doi: 10.1103/PhysRevD.66.081301. URL http://arxiv.org/abs/hep-th/0205055.

[39] Alexander Kamenshchik, Ugo Moschella, and Vincent Pasquier. An alternative to quintessence. *Physics Letters B*, 511(2-4):265–268, July 2001. ISSN 03702693. doi: 10.1016/S0370-2693(01)00571-8. URL http://arxiv.org/abs/gr-qc/0103004.

[40] Neven Bilić, Gary B Tupper, and Raoul D Viollier. Unification of dark matter and dark energy: the inhomogeneous Chaplygin gas. *Physics Letters B*, 535(1-4):17–21, May 2002. ISSN 03702693. doi: 10.1016/S0370-2693(02)01716-1. URL http://arxiv.org/abs/astro-ph/0111325.

[41] M. Bento, O. Bertolami, and A. Sen. Generalized Chaplygin gas, accelerated expansion, and dark-energy-matter unification. *Physical Review D*, 66(4):043507, August 2002. ISSN 0556-2821. doi: 10.1103/PhysRevD.66.043507. URL http://arxiv.org/abs/gr-qc/0202064.

[42] Scott Watson. An Exposition on Inflationary Cosmology. April 2000. URL http://arxiv.org/abs/astro-ph/0005003.

[43] Antonio Riotto. Inflation and the Theory of Cosmological Perturbations. page 77, October 2002. URL http://arxiv.org/abs/hep-ph/0210162.

[44] David Langlois. Inflation, quantum fluctuations and cosmological perturbations. page 44, May 2004. URL http://arxiv.org/abs/hep-th/0405053.

[45] Robert H. Brandenberger. Inflationary Cosmology: Progress and Problems. page 43, October 1999. URL http://arxiv.org/abs/hep-ph/9910410.

[46] David H. Lyth and Antonio Riotto. Particle physics models of inflation and the cosmological density perturbation. *Physics Reports*, 314(1-2):1–146, June 1999. ISSN 03701573. doi: 10.1016/S0370-1573(98)00128-8. URL http://arxiv.org/abs/hep-ph/9807278.

[47] Alan H. Guth. Inflation and eternal inflation. *Physics Reports*, 333-334:555–574, August 2000. ISSN 03701573. doi: 10.1016/S0370-1573(00)00037-5. URL http://arxiv.org/abs/astro-ph/0002156.

[48] Andrei Linde, Dmitri Linde, and Arthur Mezhlumian. From the big bang theory to the theory of a stationary universe. *Physical Review D*, 49(4):1783–1826, February 1994. ISSN 0556-2821. doi: 10.1103/PhysRevD.49.1783. URL http://arxiv.org/abs/gr-qc/9306035.

[49] James E. Lidsey, Andrew R. Liddle, Edward W. Kolb, Edmund J. Copeland, Tiago Barreiro, and Mark Abney. Reconstructing the inflaton potential—an overview. *Reviews of Modern Physics*, 69(2):373–410, April 1997. ISSN 0034-6861. doi: 10.1103/RevModPhys.69.373. URL http://arxiv.org/abs/astro-ph/9508078.

[50] A.A. Starobinsky. A new type of isotropic cosmological models without singularity. *Physics Letters B*, 91(1):99–102, March 1980. ISSN 03702693. doi: 10.1016/0370-2693(80)90670-X. URL http://www.sciencedirect.com/science/article/pii/037026938090670X.

[51] Alexandros Kehagias, Azadeh Moradinezhad Dizgah, and Antonio Riotto. Remarks on the Starobinsky model of inflation and its descendants. *Physical Review D*, 89(4):043527, February 2014. ISSN 1550-7998. doi: 10.1103/PhysRevD.89.043527. URL http://arxiv.org/abs/1312.1155.

[52] BICEP2 Collaboration, P. A. R Ade, R. W. Aikin, M. Amiri, D. Barkats, S. J. Benton, C. A. Bischoff, J. J. Bock, J. A. Brevik, I. Buder, E. Bullock, G. Davis, C. D. Dowell, L. Duband, J. P. Filippini, S. Fliescher, S. R. Golwala, M. Halpern, M. Hasselfield, S. R. Hildebrandt, G. C. Hilton, V. V. Hristov, K. D. Irwin, K. S. Karkare, J. P. Kaufman, B. G. Keating, S. A. Kernasovskiy, J. M. Kovac, C. L. Kuo, E. M. Leitch, N. Llombart, M. Lueker, C. B. Netterfield, H. T. Nguyen, R. O'Brient, R. W. Ogburn, A. Orlando, C. Pryke, C. D. Reintsema, S. Richter, R. Schwarz, C. D. Sheehy, Z. K. Staniszewski, K. T. Story, R. V. Sudiwala, G. P. Teply, J. E. Tolan, A. D. Turner, A. G. Vieregg, P. Wilson, C. L. Wong, and K. W. Yoon. BICEP2 II: Experiment and Three-Year Data Set. page 29, March 2014. URL http://arxiv.org/abs/1403.4302.

[53] J M Kovac, E M Leitch, C Pryke, J E Carlstrom, N W Halverson, and W L Holzapfel. Detection of polarization in the cosmic microwave background using

DASI. Degree Angular Scale Interferometer. *Nature*, 420(6917):772–87, January 2002. ISSN 0028-0836. doi: 10.1038/nature01269. URL http://arxiv.org/abs/astro-ph/0209478.

[54] Alan H. Guth. Inflationary universe: A possible solution to the horizon and flatness problems. *Physical Review D*, 23(2):347–356, January 1981. ISSN 0556-2821. doi: 10.1103/PhysRevD.23.347. URL http://link.aps.org/doi/10.1103/PhysRevD.23.347.

[55] A.D. Linde. A new inflationary universe scenario: A possible solution of the horizon, flatness, homogeneity, isotropy and primordial monopole problems. *Physics Letters B*, 108(6):389–393, February 1982. ISSN 03702693. doi: 10.1016/0370-2693(82)91219-9. URL http://adsabs.harvard.edu/abs/1982PhLB..108..389L.

[56] Jerome Martin, Christophe Ringeval, Roberto Trotta, and Vincent Vennin. Compatibility of Planck and BICEP2 in the Light of Inflation. page 25, May 2014. URL http://arxiv.org/abs/1405.7272.

[57] Raphael Flauger, J. Colin Hill, and David N. Spergel. Toward an Understanding of Foreground Emission in the BICEP2 Region. page 11, May 2014. URL http://arxiv.org/abs/1405.7351.

[58] Planck collaboration Bernard and J.-P. Plank results on interstellar dust. URL http://events.asiaa.sinica.edu.tw/meeting/20131118/talk/2013112213_Talk_Jean-PhilippeBernard.pdf.

[59] Planck Collaboration, P. A. R. Ade, N. Aghanim, D. Alina, M. I. R. Alves, C. Armitage-Caplan, M. Arnaud, D. Arzoumanian, M. Ashdown, F. Atrio-Barandela, J. Aumont, C. Baccigalupi, A. J. Banday, R. B. Barreiro, E. Battaner, K. Benabed, A. Benoit-Lévy, J. P. Bernard, M. Bersanelli, P. Bielewicz, J. J. Bock, J. R. Bond, J. Borrill, F. R. Bouchet, F. Boulanger, A. Bracco, C. Burigana, R. C. Butler, J. F. Cardoso, A. Catalano, A. Chamballu, R. R. Chary, H. C. Chiang, P. R. Christensen, S. Colombi, L. P. L. Colombo, C. Combet, F. Couchot, A. Coulais, B. P. Crill, A. Curto, F. Cuttaia, L. Danese, R. D. Davies, R. J. Davis, P. de Bernardis, E. M. de Gouveia Dal Pino, A. de Rosa, G. de Zotti, J. Delabrouille, F. X. Désert, C. Dickinson, J. M. Diego, S. Donzelli, O. Doré, M. Douspis, J. Dunkley, X. Dupac, T. A. Enß lin, H. K. Eriksen, E. Falgarone, K. Ferrière, F. Finelli, O. Forni, M. Frailis, A. A. Fraisse, E. Franceschi, S. Galeotta, K. Ganga, T. Ghosh, M. Giard, Y. Giraud-Héraud, J. González-Nuevo, K. M. Górski, A. Gregorio, A. Gruppuso, V. Guillet, F. K. Hansen, D. L. Harrison, G. Helou, C. Hernández-Monteagudo, S. R. Hildebrandt, E. Hivon,

M. Hobson, W. A. Holmes, A. Hornstrup, K. M. Huffenberger, A. H. Jaffe, T. R. Jaffe, W. C. Jones, M. Juvela, E. Keihänen, R. Keskitalo, T. S. Kisner, R. Kneissl, J. Knoche, M. Kunz, H. Kurki-Suonio, G. Lagache, A. Lähteenmäki, J. M. Lamarre, A. Lasenby, C. R. Lawrence, J. P. Leahy, R. Leonardi, F. Levrier, M. Liguori, P. B. Lilje, M. Linden-Vø rnle, M. López-Caniego, P. M. Lubin, J. F. Macías-Pérez, B. Maffei, A. M. Magalhães, D. Maino, N. Mandolesi, M. Maris, D. J. Marshall, P. G. Martin, E. Martínez-González, S. Masi, S. Matarrese, P. Mazzotta, A. Melchiorri, L. Mendes, A. Mennella, M. Migliaccio, M. A. Miville-Deschênes, A. Moneti, L. Montier, G. Morgante, D. Mortlock, D. Munshi, J. A. Murphy, P. Naselsky, F. Nati, P. Natoli, C. B. Netterfield, F. Noviello, D. Novikov, I. Novikov, C. A. Oxborrow, L. Pagano, F. Pajot, R. Paladini, D. Paoletti, F. Pasian, T. J. Pearson, O. Perdereau, L. Perotto, F. Perrotta, F. Piacentini, M. Piat, D. Pietrobon, S. Plaszczynski, F. Poidevin, E. Pointecouteau, G. Polenta, L. Popa, G. W. Pratt, S. Prunet, J. L. Puget, J. P. Rachen, W. T. Reach, R. Rebolo, M. Reinecke, M. Remazeilles, C. Renault, S. Ricciardi, T. Riller, I. Ristorcelli, G. Rocha, C. Rosset, G. Roudier, J. A. Rubiño Martín, B. Rusholme, M. Sandri, G. Savini, D. Scott, L. D. Spencer, V. Stolyarov, R. Stompor, R. Sudiwala, D. Sutton, A. S. Suur-Uski, J. F. Sygnet, J. A. Tauber, L. Terenzi, L. Toffolatti, M. Tomasi, M. Tristram, M. Tucci, G. Umana, L. Valenziano, J. Valiviita, B. Van Tent, P. Vielva, F. Villa, L. A. Wade, B. D. Wandelt, A. Zacchei, and A. Zonca. Planck intermediate results. XIX. An overview of the polarized thermal emission from Galactic dust. May 2014. URL http://arxiv.org/abs/1405.0871.

[60] Michael J. Mortonson and Uroš Seljak. A joint analysis of Planck and BICEP2 B modes including dust polarization uncertainty. page 12, May 2014. URL http://arxiv.org/abs/1405.5857.

[61] Planck Collaboration, R. Adam, P. A. R. Ade, N. Aghanim, M. Arnaud, J. Aumont, C. Baccigalupi, A. J. Banday, R. B. Barreiro, J. G. Bartlett, N. Bartolo, E. Battaner, K. Benabed, A. Benoit-Lévy, J. P. Bernard, M. Bersanelli, P. Bielewicz, A. Bonaldi, L. Bonavera, J. R. Bond, J. Borrill, F. R. Bouchet, F. Boulanger, A. Bracco, M. Bucher, C. Burigana, R. C. Butler, E. Calabrese, J. F. Cardoso, A. Catalano, A. Challinor, A. Chamballu, R. R. Chary, H. C. Chiang, P. R. Christensen, D. L. Clements, S. Colombi, L. P. L. Colombo, C. Combet, F. Couchot, A. Coulais, A. Curto, F. Cuttaia, L. Danese, R. D. Davies, R. J. Davis, P. de Bernardis, G. de Zotti, J. Delabrouille, J. M. Delouis, F. X. Désert, C. Dickinson, J. M. Diego, K. Dolag, H. Dole, S. Donzelli, O. Doré, M. Douspis, A. Ducout, J. Dunkley, X. Dupac, G. Efstathiou, F. Elsner, T. A. Enß lin, H. K. Eriksen, E. Falgarone, F. Finelli, O. Forni, M. Frailis, A. A. Fraisse, E. Franceschi, A. Frejsel, S. Galeotta, S. Galli, K. Ganga, T. Ghosh, M. Giard, Y. Giraud-Héraud,

E. Gjerlø w, J. González-Nuevo, K. M. Górski, S. Gratton, A. Gregorio, A. Gruppuso, V. Guillet, F. K. Hansen, D. Hanson, D. L. Harrison, G. Helou, S. Henrot-Versillé, C. Hernández-Monteagudo, D. Herranz, E. Hivon, W. A. Holmes, K. M. Huffenberger, G. Hurier, A. H. Jaffe, T. R. Jaffe, J. Jewell, and W. C. Jones. Planck intermediate results. XXX. The angular power spectrum of polarized dust emission at intermediate and high Galactic latitudes. September 2014. URL http://arxiv.org/abs/1409.5738.

[62] Steven Weinberg. *Gravitation and cosmology: principles and applications of the general theory of relativity*. Wiley, 1972. ISBN 0471925675. URL http://books.google.co.za/books/about/Gravitation_and_cosmology_principles_and.html?id=XLbvAAAAMAAJ&pgis=1.

[63] I.L Buchbinder, S Odintsov, and L Shapiro. *Effective Action in Quantum Gravity*. CRC Press, 1992. ISBN 0750301228. URL http://books.google.co.za/books/about/Effective_Action_in_Quantum_Gravity.html?id=NcjI3ydY4e4C&pgis=1.

[64] S. Capozziello and S. Vignolo. The Cauchy problem for f(R)-gravity: an overview. page 14, March 2011. URL http://arxiv.org/abs/1103.2302.

[65] G A Vilkovisky. Effective action in quantum gravity. *Classical and Quantum Gravity*, 9(4):895–903, April 1992. ISSN 0264-9381. doi: 10.1088/0264-9381/9/4/008. URL http://iopscience.iop.org/0264-9381/9/4/008.

[66] J. L. Tonry et al. Cosmological Results from High z Supernovae. *The Astrophysical Journal*, 594(1):1–24, September 2003. ISSN 0004-637X. doi: 10.1086/376865. URL http://arxiv.org/abs/astro-ph/0305008.

[67] D. N. et al Spergel. FirstYear Wilkinson Microwave Anisotropy Probe (WMAP) Observations: Determination of Cosmological Parameters. *The Astrophysical Journal Supplement Series*, 148(1):175–194, September 2003. ISSN 0067-0049. doi: 10.1086/377226. URL http://arxiv.org/abs/astroph/0302209.

[68] Tegmark et al. Cosmological parameters from SDSS and WMAP. *Physical Review D*, 69(10):103501, May 2004. ISSN 1550-7998. doi: 10.1103/PhysRevD.69.103501. URL http://arxiv.org/abs/astro-ph/0310723.

[69] Jaiyul Yoo and Uroš Seljak. Joint analysis of gravitational lensing, clustering, and abundance: Toward the unification of large-scale structure analysis. *Physical Review D*, 86(8):083504, October 2012. ISSN 1550-7998. doi: 10.1103/PhysRevD.86.083504. URL http://link.aps.org/doi/10.1103/PhysRevD.86.083504.

[70] Cole et al. The 2dF Galaxy Redshift Survey: power-spectrum analysis of the final data set and cosmological implications. *Monthly Notices of the Royal Astronomical Society*, 362(2):505–534, September 2005. ISSN 00358711. doi: 10.1111/j.1365-2966.2005.09318.x. URL http://arxiv.org/abs/astro-ph/0501174.

[71] Bhuvnesh Jain and Andy Taylor. Cross-Correlation Tomography: Measuring Dark Energy Evolution with Weak Lensing. *Physical Review Letters*, 91(14):141302, October 2003. ISSN 0031-9007. doi: 10.1103/PhysRevLett.91.141302. URL http://link.aps.org/doi/10.1103/PhysRevLett.91.141302.

[72] H. A. Buchdahl. Non-linear Lagrangians and cosmological theory. *Monthly Notices of the Royal Astronomical Society*, 150:1, 1970. ISSN 0035-8711. URL http://adsabs.harvard.edu/abs/1970MNRAS.150....1B.

[73] Orfeu Bertolami, Tiberiu Harko, and Francisco S. N. Lobo. Extra force in f(R) modified theories of gravity. *Physical Review D*, 75(10):104016, May 2007. ISSN 1550-7998. doi: 10.1103/PhysRevD.75.104016. URL http://link.aps.org/doi/10.1103/PhysRevD.75.104016.

[74] F. Briscese, E. Elizalde, S. Nojiri, and S.D. Odintsov. Phantom scalar dark energy as modified gravity: Understanding the origin of the Big Rip singularity. *Physics Letters B*, 646(2-3):105–111, March 2007. ISSN 03702693. doi: 10.1016/j.physletb.2007.01.013. URL http://www.sciencedirect.com/science/article/pii/S0370269307000925.

[75] Antonio De Felice and Shinji Tsujikawa. f(R) Theories. *Living Reviews in Relativity*, 13, 2010. ISSN 1433-8351. doi: 10.12942/lrr-2010-3. URL http://relativity.livingreviews.org/Articles/lrr-2010-3/.

[76] Shant Baghram, Marzieh Farhang, and Sohrab Rahvar. Modified gravity with f(R)=sqrt[R^{2}-R_{0}^{2}]. *Physical Review D*, 75(4):044024, February 2007. ISSN 1550-7998. doi: 10.1103/PhysRevD.75.044024. URL http://link.aps.org/doi/10.1103/PhysRevD.75.044024.

[77] D. Bazeia, B. Carneiro da Cunha, R. Menezes, and A.Yu. Petrov. Perturbative aspects and conformal solutions of gravity. *Physics Letters B*, 649(5-6):445–453, June 2007. ISSN 03702693. doi: 10.1016/j.physletb.2007.04.040. URL http://www.sciencedirect.com/science/article/pii/S0370269307005163.

[78] S Capozziello, V F Cardone, and A Troisi. Dark energy and dark matter as curvature effects? *Journal of Cosmology and Astroparticle Physics*, 2006(08):001–001, August 2006. ISSN 1475-7516. doi: 10.1088/1475-7516/2006/08/001. URL http://stacks.iop.org/1475-7516/2006/i=08/a=001.

[79] S. Carloni, P. K. S. Dunsby, and A. Troisi. Evolution of density perturbations in f(R) gravity. *Physical Review D*, 77(2):024024, January 2008. ISSN 1550-7998. doi: 10.1103/PhysRevD.77.024024. URL http://link.aps.org/doi/10.1103/PhysRevD.77.024024.

[80] Sean Carroll, Antonio De Felice, Vikram Duvvuri, Damien Easson, Mark Trodden, and Michael Turner. Cosmology of generalized modified gravity models. *Physical Review D*, 71(6):063513, March 2005. ISSN 1550-7998. doi: 10.1103/PhysRevD.71.063513. URL http://link.aps.org/doi/10.1103/PhysRevD.71.063513.

[81] G. Magnano, M. Ferraris, and M. Francaviglia. Nonlinear gravitational Lagrangians. *General Relativity and Gravitation*, 19(5):465–479, May 1987. ISSN 0001-7701. doi: 10.1007/BF00760651. URL http://link.springer.com/10.1007/BF00760651.

[82] Ignacio Navarro and Karel Van Acoleyen. f (R) actions, cosmic acceleration and local tests of gravity. *Journal of Cosmology and Astroparticle Physics*, 2007(02): 022–022, February 2007. ISSN 1475-7516. doi: 10.1088/1475-7516/2007/02/022. URL http://stacks.iop.org/1475-7516/2007/i=02/a=022.

[83] Shin'ichi Nojiri. Modified f(R) gravity consistent with realistic cosmology: From a matter dominated epoch to a dark energy universe. *Physical Review D*, 74(8): 086005, October 2006. ISSN 1550-7998. doi: 10.1103/PhysRevD.74.086005. URL http://link.aps.org/doi/10.1103/PhysRevD.74.086005.

[84] Gonzalo J. Olmo. Limit to general relativity in f(R) theories of gravity. *Physical Review D*, 75(2):023511, January 2007. ISSN 1550-7998. doi: 10.1103/PhysRevD.75.023511. URL http://link.aps.org/doi/10.1103/PhysRevD.75.023511.

[85] A J Bustelo and D E Barraco. Hydrostatic equilibrium equation and Newtonian limit of the singular f (R) gravity. *Classical and Quantum Gravity*, 24(9):2333–2342, May 2007. ISSN 0264-9381. doi: 10.1088/0264-9381/24/9/011. URL http://stacks.iop.org/0264-9381/24/i=9/a=011.

[86] Leszek M Sokołowski. Metric gravity theories and cosmology: I. Physical interpretation and viability. *Classical and Quantum Gravity*, 24(13):3391–3411, July 2007. ISSN 0264-9381. doi: 10.1088/0264-9381/24/13/015. URL http://stacks.iop.org/0264-9381/24/i=13/a=015.

[87] Tonguç Rador. Gravities à la Brans–Dicke. *Physics Letters B*, 652(5-6):228–232, September 2007. ISSN 03702693. doi: 10.1016/j.physletb.2007.07.034. URL http://www.sciencedirect.com/science/article/pii/S0370269307008817.

[88] Anthony W. Brookfield, Carsten van de Bruck, and Lisa M. H. Hall. Viability of f(R) theories with additional powers of curvature. *Physical Review D*, 74(6): 064028, September 2006. ISSN 1550-7998. doi: 10.1103/PhysRevD.74.064028. URL http://link.aps.org/doi/10.1103/PhysRevD.74.064028.

[89] R. P. Woodard. The Invisible Universe: Dark Matter and Dark Energy. 720:30, January 2007. doi: 10.1007/978-3-540-71013-4. URL http://arxiv.org/abs/astro-ph/0601672.

[90] Thomas P Sotiriou and Valerio Faraoni. f (R) theories of gravity. 210.

[91] Timothy Clifton, Pedro G. Ferreira, Antonio Padilla, and Constantinos Skordis. Modified Gravity and Cosmology. page 312, June 2011. URL http://arxiv.org/abs/1106.2476.

[92] Valerio Faraoni, Edgard Gunzig, and Pasquale Nardone. Conformal transformations in classical gravitational theories and in cosmology. page 54, November 1998. URL http://arxiv.org/abs/gr-qc/9811047.

[93] Kei-ichi Maeda. Towards the Einstein-Hilbert action via conformal transformation. *Physical Review D*, 39(10):3159–3162, May 1989. ISSN 0556-2821. doi: 10.1103/PhysRevD.39.3159. URL http://link.aps.org/doi/10.1103/PhysRevD.39.3159.

[94] Guido Magnano and Leszek M. Sokołowski. Physical equivalence between nonlinear gravity theories and a general-relativistic self-gravitating scalar field. *Physical Review D*, 50(8):5039–5059, October 1994. ISSN 0556-2821. doi: 10.1103/PhysRevD.50.5039. URL http://link.aps.org/doi/10.1103/PhysRevD.50.5039.

[95] David Wands. Extended gravity theories and the Einstein–Hilbert action. *Classical and Quantum Gravity*, 11(1):269–279, January 1994. ISSN 0264-9381. doi: 10.1088/0264-9381/11/1/025. URL http://arxiv.org/abs/gr-qc/9307034.

[96] Robert M. Wald. *General Relativity*. University of Chicago Press, 2010. ISBN 0226870375. URL http://books.google.co.za/books/about/General_Relativity.html?id=9S-hzg6-moYC&pgis=1.

[97] V. Faraoni S. Capozziello, M. De Laurentis. A bird's eye view of f(R)-gravity. *Gr-qc*, 2009.

[98] A. D. Dolgov and M. Kawasaki. Can modified gravity explain accelerated cosmic expansion? page 4, July 2003. URL http://arxiv.org/abs/astro-ph/0307285.

[99] Valerio Faraoni. Matter instability in modified gravity. *Phys. Rev. D*, 74:104017, Nov 2006. doi: 10.1103/PhysRevD.74.104017. URL http://link.aps.org/doi/10.1103/PhysRevD.74.104017.

[100] Valerio Faraoni. de sitter space and the equivalence between $f(r)$ and scalar-tensor gravity. *Phys. Rev. D*, 75:067302, Mar 2007. doi: 10.1103/PhysRevD.75.067302. URL http://link.aps.org/doi/10.1103/PhysRevD.75.067302.

[101] B Bertotti, L Iess, and P Tortora. A test of general relativity using radio links with the Cassini spacecraft. *Nature*, 425(6956):374–6, September 2003. ISSN 1476-4687. doi: 10.1038/nature01997. URL http://dx.doi.org/10.1038/nature01997.

[102] Nicolas Lanahan-Tremblay and Valerio Faraoni. The Cauchy problem of f (R) gravity. *Classical and Quantum Gravity*, 24(22):5667–5679, November 2007. ISSN 0264-9381. doi: 10.1088/0264-9381/24/22/024. URL http://stacks.iop.org/0264-9381/24/i=22/a=024.

[103] S. Carloni, A. Troisi, and P. K. S. Dunsby. Some remarks on the dynamical systems approach to fourth order gravity. *General Relativity and Gravitation*, 41 (8):1757–1776, January 2009. ISSN 0001-7701. doi: 10.1007/s10714-008-0747-9. URL http://arxiv.org/abs/0706.0452.

[104] S. Capozziello, M. De Laurentis, and V. Faraoni. A bird's eye view of f(R)-gravity. page 28, September 2009. URL http://arxiv.org/abs/0909.4672.

[105] Mohamed Abdelwahab, Rituparno Goswami, and Peter K. S. Dunsby. Cosmological dynamics of fourth order gravity: A compact view. page 8, November 2011. URL http://arxiv.org/abs/1111.0171.

[106] Stephen Wiggins. *Introduction to Applied Nonlinear Dynamical Systems and Chaos*. Springer, 2003. ISBN 0387001778. URL http://books.google.co.za/books/about/Introduction_to_Applied_Nonlinear_Dynami.html?id=RSI4RGdwnU4C&pgis=1.

[107] L P Chimento and A S Jakubi. Cosmological solutions of the Einstein equations with a causal viscous fluid. *Classical and Quantum Gravity*, 10(10):2047–2058, October 1993. ISSN 0264-9381. doi: 10.1088/0264-9381/10/10/011. URL http://iopscience.iop.org/0264-9381/10/10/011.

[108] Luis P Chimento and Alejandro S Jakubi. Dissipative cosmological solutions. *Classical and Quantum Gravity*, 14(7):1811–1820, July 1997. ISSN 0264-9381. doi: 10.1088/0264-9381/14/7/016. URL http://iopscience.iop.org/0264-9381/14/7/016.

[109] Y Kitada and K Maeda. Cosmic no-hair theorem in homogeneous spacetimes. I. Bianchi models. *Classical and Quantum Gravity*, 10(4):703–734, April 1993. ISSN 0264-9381. doi: 10.1088/0264-9381/10/4/008. URL http://iopscience.iop.org/0264-9381/10/4/008.

[110] Jack Carr. *Applications of Centre Manifold Theory, Volume 35*. Springer-Verlag, 1981. ISBN 0387905774. URL http://books.google.co.za/books/about/Applications_of_Centre_Manifold_Theory.html?id=93BdN7btysoC&pgis=1.

[111] Luca Amendola and Shinji Tsujikawa. *Dark Energy: Theory and Observations*. Cambridge University Press, 2010. ISBN 0521516005. URL http://books.google.co.za/books/about/Dark_Energy.html?id=U0HTngEACAAJ&pgis=1.

[112] G. F. R. Ellis J. Wainwright. *Dynamical Systems in Cosmology*. Cambridge University Press, 2005. ISBN 0521673526. URL http://books.google.co.za/books/about/Dynamical_Systems_in_Cosmology.html?id=FVSuSepCE2UC&pgis=1.

[113] S Carloni, P K S Dunsby, S Capozziello, and A Troisi. Cosmological dynamics of R n gravity. *Classical and Quantum Gravity*, 22(22):4839–4868, November 2005. ISSN 0264-9381. doi: 10.1088/0264-9381/22/22/011. URL http://arxiv.org/abs/gr-qc/0410046.

[114] John Barrow and Sigbjø rn Hervik. Evolution of universes in quadratic theories of gravity. *Physical Review D*, 74(12):124017, December 2006. ISSN 1550-7998. doi: 10.1103/PhysRevD.74.124017. URL http://link.aps.org/doi/10.1103/PhysRevD.74.124017.

[115] Kishore Ananda and Marco Bruni. Cosmological dynamics and dark energy with a quadratic equation of state: Anisotropic models, large-scale perturbations, and cosmological singularities. *Physical Review D*, 74(2):023524, July 2006. ISSN 1550-7998. doi: 10.1103/PhysRevD.74.023524. URL http://link.aps.org/doi/10.1103/PhysRevD.74.023524.

[116] Kishore Ananda and Marco Bruni. Cosmological dynamics and dark energy with a nonlinear equation of state: A quadratic model. *Physical Review D*, 74(2):023523, July 2006. ISSN 1550-7998. doi: 10.1103/PhysRevD.74.023523. URL http://arxiv.org/abs/astro-ph/0512224.

[117] Peter Dunsby, Naureen Goheer, Marco Bruni, and Alan Coley. Are braneworlds born isotropic? *Physical Review D*, 69(10):101303, May 2004. ISSN 1550-7998. doi: 10.1103/PhysRevD.69.101303. URL http://arxiv.org/abs/hep-th/0312174.

[118] A A Coley. No chaos in brane-world cosmology. *Classical and Quantum Gravity*, 19(8):L45–L56, April 2002. ISSN 0264-9381. doi: 10.1088/0264-9381/19/8/102. URL http://arxiv.org/abs/hep-th/0110117.

[119] Antonio Campos and Carlos Sopuerta. Evolution of cosmological models in the brane-world scenario. *Physical Review D*, 63(10):104012, April 2001. ISSN 0556-2821. doi: 10.1103/PhysRevD.63.104012. URL http://arxiv.org/abs/hep-th/0101060.

[120] Antonio Campos and Carlos Sopuerta. Bulk effects in the cosmological dynamics of brane-world scenarios. *Physical Review D*, 64(10):104011, October 2001. ISSN 0556-2821. doi: 10.1103/PhysRevD.64.104011. URL http://arxiv.org/abs/hep-th/0105100.

[121] Kenneth Wilson. The renormalization group and critical phenomena. *Reviews of Modern Physics*, 55(3):583–600, July 1983. ISSN 0034-6861. doi: 10.1103/RevModPhys.55.583. URL http://link.aps.org/doi/10.1103/RevModPhys.55.583.

[122] Jun-Qi Guo and Andrei V. Frolov. Cosmological dynamics in f(R) gravity. page 17, May 2013. URL http://arxiv.org/abs/1305.7290.

[123] Andrei V. Frolov and Jun-Qi Guo. Small Cosmological Constant from Running Gravitational Coupling. page 8, January 2011. URL http://arxiv.org/abs/1101.4995.

[124] Hyung Won Lee, Kyoung Yee Kim, and Yun Soo Myung. Future cosmological evolution in $f(R)$ gravity using two equations of state parameters. page 23, June 2011. URL http://arxiv.org/abs/1106.2865.